

VERMONT YANKEE  
CYCLE 11  
CORE PERFORMANCE ANALYSIS

April 1984

Major Contributors:

D. C. Albright	D. M. Kapitx
B. G. Baharynejad	J. Pappas
K. J. Burns	K. E. St. John
J. T. Cronin	M. A. Sironen
D. P. Heinrichs	R. A. Woehlke

Approved by:

R. J. Cacciapouti  
R. J. Cacciapouti, Manager  
Reactor Physics Group

4/12/84  
(Date)

Approved by:

P. A. Bergeron  
P. A. Bergeron, Manager  
Transient Analysis Group

4/12/84  
(Date)

Approved by:

S. P. Schultz  
S. P. Schultz, Manager  
Nuclear Evaluations and Support Group

4/12/84  
(Date)

Approved by:

A. Husain  
A. Husain, Manager  
LOCA Group

4/12/84  
(Date)

Approved by:

B. C. Slifer  
B. C. Slifer, Director  
Nuclear Engineering Department

4/12/84  
(Date)

# DISCLAIMER OF RESPONSIBILITY

This document was prepared by Yankee Atomic Electric Company for its own use and on behalf of Vermont Yankee Nuclear Power Corporation. This document is believed to be completely true and accurate to the best of our knowledge and information. It is authorized for use specifically by Yankee Atomic Electric Company, Vermont Yankee Nuclear Power Corporation and/or the appropriate subdivisions within the Nuclear Regulatory Commission only.

With regard to any unauthorized use whatsoever, Yankee Atomic Electric Company, Vermont Yankee Nuclear Power Corporation and their officers, directors, agents and employees assume no liability nor make any warranty or representation with respect to the contents of this document or to its accuracy or completeness.

# ABSTRACT

This report presents design information and calculational results pertinent to the operation of Cycle 11 of the Vermont Yankee Nuclear Power Station. These include the fuel design and core loading pattern descriptions; calculated reactor power distributions, exposure distributions, shutdown capability and reactivity functions; and the results of safety analyses performed to justify plant operation throughout the cycle.

## TABLE OF CONTENTS

	<u>Page</u>
DISCLAIMER.....	ii
ABSTRACT.....	iii
TABLE OF CONTENTS.....	iv
LIST OF FIGURES.....	vi
LIST OF TABLES.....	viii
ACKNOWLEDGEMENTS.....	ix
1.0 INTRODUCTION.....	1
2.0 RECENT REACTOR OPERATING HISTORY.....	2
2.1 Operating History of the Current Cycle.....	2
2.2 Operating History of Past Applicable Cycles.....	2
3.0 RELOAD CORE DESIGN DESCRIPTION.....	6
3.1 Core Fuel Loading.....	6
3.2 Design Reference Core Loading Pattern.....	6
3.3 Assembly Exposure Distribution.....	6
4.0 FUEL MECHANICAL AND THERMAL DESIGN.....	9
4.1 Mechanical Design.....	9
4.2 Thermal Design.....	9
4.3 Operating Experience.....	10
5.0 NUCLEAR DESIGN.....	15
5.1 Core Power Distributions.....	15
5.1.1 Haling Power Distribution.....	15
5.1.2 Rodded Depletion Power Distribution.....	15
5.2 Core Exposure Distributions.....	16
5.3 Cold Core Reactivity and Shutdown Margin.....	16
5.4 Standby Liquid Control System Shutdown Capability.....	17
6.0 THERMAL-HYDRAULIC DESIGN.....	26
6.1 Steady-State Thermal Hydraulics.....	26
6.2 Reactor Limits Determination.....	26



TABLE OF CONTENTS  
(Continued)

	<u>Page</u>
7.0 ACCIDENT ANALYSIS.....	28
7.1 Core Wide Transient Analysis.....	28
7.1.1 Methodology.....	28
7.1.2 Initial Conditions and Assumptions.....	29
7.1.3 Reactivity Functions.....	30
7.1.4 Transients Analyzed.....	32
7.2 Core Wide Transient Analysis Results.....	32
7.2.1 Turbine Trip Without Bypass Transient.....	32
7.2.2 Generator Load Rejection Without Bypass Transient.....	33
7.2.3 Loss of Feedwater Heating Transient.....	33
7.3 Overpressurization Analysis Results.....	34
7.4 Local Rod Withdrawal Error Transient Results.....	34
7.5 Misloaded Bundle Error Analysis Results.....	37
7.5.1 Rotated Bundle Error.....	37
7.5.2 Mislocated Bundle Error.....	38
7.6 Control Rod Drop Accident Results.....	39
7.7 Stability Analysis Results.....	40
8.0 STARTUP PROGRAM.....	82
9.0 LOSS-OF-COOLANT ACCIDENT ANALYSIS.....	83
APPENDIX A CALCULATED CYCLE DEPENDENT LIMITS.....	84
REFERENCES.....	87

## LIST OF FIGURES

<u>Number</u>	<u>Title</u>	<u>Page</u>
3.2.1	VY Cycle 11 Design Reference Loading Pattern, Lower Right Quadrant	8
4.2.1	VY Cycle 11 Core Average Gap Conductance versus Cycle Exposure	13
4.2.2	VY Hot Channel Gap Conductance for P8X8R versus Exposure	14
5.1.1	VY Cycle 11 Haling Depletion, EOFPL Bundle Average Relative Powers	19
5.1.2	VY Cycle 11 Core Average Axial Power Distribution Taken from the Haling Calculation to EOFPL	20
5.1.3	VY Cycle 11 Rodded Depletion - ARO at EOFPL Bundle Average Relative Powers	21
5.1.4	VY Cycle 11 Core Average Axial Power Distribution, Rodded Depletion - ARO at EOFPL	22
5.2.1	VY Cycle 11 Haling Depletion, EOFPL Bundle Average Exposures	23
5.2.2	VY Cycle 11 Rodded Depletion, EOFPL Bundle Average Exposures	24
5.3.1	VY Cycle 11 Cold Shutdown Delta K in Percent versus Cycle Exposure	25
7.1.1	Flow Chart for the Calculation of $\Delta$ CPR Using the RETRAN/TCPYA01 Codes	46
7.1.2	Inserted Rod Worth and Rod Position versus Time From Initial Rod Movement at EOFPL11, "Measured" Scram Time	47
7.1.3	Inserted Rod Worth and Rod Position versus Time From Initial Rod Movement at EOFPL11-1000 MWD/ST, "Measured" Scram Time	48
7.1.4	Inserted Rod Worth and Rod Position versus Time From Initial Rod Movement at EOFPL11-2000 MWD/ST, "Measured" Scram Time	49
7.1.5	Inserted Rod Worth and Rod Position versus Time From Initial Rod Movement at EOFPL11, "67B" Scram Time	50
7.1.6	Inserted Rod Worth and Rod Position versus Time From Initial Rod Movement at EOFPL11-1000 MWD/ST, "67B" Scram Time	51
7.1.7	Inserted Rod Worth and Rod Position versus Time From Initial Rod Movement at EOFPL11-2000 MWD/ST, "67B" Scram Time	52

## LIST OF FIGURES

<u>Number</u>	<u>Title</u>	<u>Page</u>
7.2.1	Turbine Trip Without Bypass, EOFPL11 Transient Response versus Time, "Measured" Scram Time	53
7.2.2	Turbine Trip Without Bypass, EOFPL11-1000 MWD/ST Transient Response versus Time, "Measured" Scram Time	56
7.2.3	Turbine Trip Without Bypass, EOFPL11-2000 MWD/ST Transient Response versus Time, "Measured" Scram Time	59
7.2.4	Generator Load Rejection Without Bypass, EOFPL11 Transient Response versus Time, "Measured" Scram Time	62
7.2.5	Generator Load Rejection Without Bypass, EOFPL11-1000 MWD/ST Transient Response versus Time, "Measured" Scram Time	65
7.2.6	Generator Load Rejection Without Bypass, EOFPL11-2000 MWD/ST Transient Response versus Time, "Measured" Scram Time	68
7.2.7	Loss of 100°F Feedwater Heating, EOFPL11-2000 MWD/ST (Limiting Case) Transient Response versus Time	71
7.3.1	MSIV Closure, Flux Scram, EOFPL11 Transient Response versus Time, "Measured" Scram Time	73
7.4.1	Reactor Initial Conditions for the VY Cycle 11 Rod Withdrawal Error Case 1	76
7.4.2	Reactor Initial Conditions for the VY Cycle 11 Rod Withdrawal Error Case 2	77
7.4.3	VY Cycle 11 RWE Case 1 - Setpoint Intercepts Determined by the A+C Channel	78
7.4.4	VY Cycle 11 RWE Case 1 - Setpoint Intercepts Determined by the B+D Channel	79
7.6.1	First Four Rod Arrays Pulled in the A Sequences	80
7.6.2	First Four Rod Arrays Pulled in the B Sequences	80
7.7.1	VY Cycle 11 Reactor Core Decay Ratio versus Power	81

## LIST OF TABLES

<u>Number</u>	<u>Title</u>	<u>Page</u>
2.1.1	VY Cycle 10 Operating Highlights	3
2.2.1	VY Cycle 9 Operating Highlights	4
2.2.2	VY Cycle 8 Operating Highlights	5
3.1.1	VY Cycle 11 Fuel Bundle Types and Numbers	7
3.3.1	Design Basis VY Cycle 10 and Cycle 11 Exposures	7
4.1.1	Nominal Fuel Mechanical Design Parameters	11
4.2.1	Gap Conductance Values Used in VY Cycle 11 Transient Analyses	12
5.3.1	VY Cycle 11 K-Effective Values and Shutdown Margin Calculation	18
5.4.1	VY Cycle 11 Standby Liquid Control System Shutdown Capability	18
7.1.1	VY Cycle 11 Summary of System Transient Model Initial Conditions for Core Wide Transient Analyses	41
7.1.2	VY Cycle 11 Transient Analysis Reactivity Coefficients at Selected Conditions	42
7.2.1	VY Cycle 11 Core Wide Transient Analysis Results	43
7.3.1	VY Cycle 11 Overpressurization Analysis Results	44
7.4.1	VY Cycle 11 Rod Withdrawal Error Transient Summary With Limiting Instrument Failure	44
7.5.1	VY Cycle 11 Rotated Bundle Analysis Results	44
7.6.1	Control Rod Drop Analysis - Rod Array Pull Order	45
7.6.2	VY Cycle 11 Control Rod Drop Analysis Results	45
7.7.1	VY Cycle 11 Stability Analysis Results	45
A.1	Vermont Yankee Nuclear Power Station Limiting Cycle 11 MCPR Results	85
A.2	Vermont Yankee Nuclear Power Station Technical Specification MCPR Operating Limits	86

#### ACKNOWLEDGEMENTS

The authors and principal contributors would like to acknowledge the contributions to this work by W. J. Waterman, S. B. Bowman, and the YAEC Word Processing Center. Their assistance in preparing figures and text for this document is recognized and greatly appreciated.



## 1.0 INTRODUCTION

This report provides information to support the operation of the Vermont Yankee Nuclear Power Station through the forthcoming Cycle 11. In this report, Cycle 11 will frequently be referred to as the Reload Cycle. The preceding Cycle 10 will frequently be referred to as the Current Cycle. The refueling between the two will involve the discharge of 104 irradiated fuel bundles and the insertion of 104 new fuel bundles. The resultant core will consist of 104 new fuel bundles and 264 irradiated fuel bundles. Some of the irradiated fuel was present in the reactor in Cycles 8 and 9, as well as the Current Cycle. These cycles will frequently be referred to as Past Cycles.

This report contains descriptions and analyses results pertaining to the mechanical, thermal-hydraulic, physics, and safety aspects of the Reload Cycle (Cycle 11).

The cycle-dependent operating limits calculated for the Reload Cycle are bounded by the Vermont Yankee Plant Technical Specifications. Both are given in Appendix A.

## 2.0 RECENT REACTOR OPERATING HISTORY

### 2.1 Operating History of the Current Cycle

The currently operating cycle is Cycle 10. During the Current Cycle, the reactor has operated smoothly at, or near, full power with the exception of normal maintenance, sequence exchanges, and a few scrams. The operating history highlights and control rod sequence exchange schedule of the Current Cycle are found on Table 2.1.1.

### 2.2 Operating History of Past Applicable Cycles

The irradiated fuel in the Reload Cycle includes some fuel bundles initially inserted in Cycles 8 and 9. These Past Cycles operated smoothly at, or near, full power with the exception of normal maintenance, sequence exchanges, a few scrams, and coastdown to the end of cycle. The highlights of the Past Cycles are found in Tables 2.2.1 and 2.2.2. The Past Cycles are described in detail in References 1 and 2.

TABLE 2.1.1

VY CYCLE 10 OPERATING HIGHLIGHTS

Beginning of Cycle Date	June 17, 1983
End of Cycle Date	June 15, 1984*
Weight of Uranium As-Loaded (Short Tons)	74.13
Beginning of Cycle Core Average Exposure (MWD/ST)	10463.
End of Full Power Core Average Exposure (MWD/ST)	17188.*
End of Cycle Core Average Exposure (MWD/ST)	17963.*
Number of Fresh Assemblies	108
Number of Irradiated Assemblies	260

## Control Rod Sequence Exchange Schedule:

<u>Date</u>	<u>Sequence</u>	
	<u>From</u>	<u>To</u>
August 13, 1983	A1-1	B2-1
October 1, 1983	B2-1	A2-1
November 5, 1983	A2-1	B1-1
December 17, 1983	B1-1	A1-2
January 24, 1984	A1-2	B2-2
March 3, 1984	B2-2	A2-2
April 14, 1984*	A2-2	B1-2

---

\* Projected Dates and Exposures.

TABLE 2.2.1

VY CYCLE 9 OPERATING HIGHLIGHTS

Beginning of Cycle Date	December 1, 1981
End of Cycle Date	March 5, 1983
Weight of Uranium As-Loaded (Short Tons)	74.15
Beginning of Cycle Core Average Exposure (MWD/ST)	9192.
End of Full Power Core Average Exposure (MWD/ST)	16595.
End of Cycle Core Average Exposure (MWD/ST)	18137.
Capacity Factor While Operating (%)	90.9
Number of Fresh Assemblies	120
Number of Irradiated Assemblies	248

## Control Rod Sequence Exchange Schedule:

<u>Date</u>	<u>Sequence</u>	
	<u>From</u>	<u>To</u>
January 28, 1982	A1-1	B2-1
March 13, 1982	B2-1	A2-1
April 24, 1982	A2-1	B1-1
June 10, 1982	B1-1	A1-2
July 24, 1982	A1-2	B2-2
September 11, 1982	B2-2	A2-2
October 30, 1982	A2-2	B1-2

TABLE 2.2.2

VY CYCLE 8 OPERATING HIGHLIGHTS

Beginning of Cycle Date	December 23, 1980
End of Cycle Date	October 16, 1981
Weight of Uranium As-Loaded (Short Tons)	74.34
Beginning of Cycle Core Average Exposure (MWD/ST)	10888.
End of Full Power Core Average Exposure (MWD/ST)	16211.
End of Cycle Core Average Exposure (MWD/ST)	16794.
Capacity Factor While Operating (%)	94.1
Number of Fresh Assemblies	80
Number of Irradiated Assemblies from Cycle 7	276
Number of Assemblies Reinserted from the Spent Fuel Pool	12

## Control Rod Sequence Exchange Schedule:

<u>Date</u>	<u>Sequence</u>	
	<u>From</u>	<u>To</u>
March 14, 1981	A1	B2
May 12, 1981	B2	A2
August 1, 1981	A2	B1



### 3.0 RELOAD CORE DESIGN DESCRIPTION

#### 3.1 Core Fuel Loading

The Reload Cycle core will consist of both new and irradiated assemblies. All the assemblies have bypass flow holes drilled in the lower tie plate. Table 3.1.1 characterizes the core by fuel type, batch size, and first cycle loaded. A description of the fuel is found in Reference 3.

#### 3.2 Design Reference Core Loading Pattern

The Reload Cycle assembly locations are indicated on the map in Figure 3.2.1. For the sake of legibility only the lower right quadrant is shown. The other quadrants are mirror images with bundles of the same type having nearly identical exposures. The bundles are identified by the reload number in which they were first introduced into the core. If any changes are made to the loading pattern at the time of refueling, they will be checked and verified acceptable under 10CFR50.59. The final loading pattern with specific bundle serial numbers will be supplied with the Startup Test Report.

#### 3.3 Assembly Exposure Distribution

The assumed nominal exposure on the fuel bundles in the Reload Cycle design reference loading pattern is given in Figure 3.2.1. To obtain this exposure distribution, Past Cycles were depleted with the SIMULATE model [4,5] using actual plant operating history. For the Current Cycle, plant operating history was used through August 16, 1983. Beyond this date, the exposure was accumulated using a best-estimate rodged depletion analysis to End of Full Power Life (EOFPL) followed by a projected coastdown to End of Cycle (EOC).

Table 3.3.1 gives the assumed nominal exposure on the Current Cycle and the Beginning of Cycle (BOC) core average exposure that results from the shuffle into the Reload Cycle loading pattern. The Reload Cycle EOFPL core average exposure and cycle capability are provided.

TABLE 3.1.1

VY CYCLE 11 FUEL BUNDLE TYPES AND NUMBERS

	<u>Fuel Designation</u>	<u>Reload Designation</u>	<u>Cycle Loaded</u>	<u>Number</u>	<u>Possible Bundle ID's</u>
<u>IRRADIATED</u>	P8DPB289	R7	8	36	LJPXXX, LJUXXX
	P8DPB289	R8	9	120	LJTXXX, LJZXXX
	P8DPB289	R9	10	108	LY4XXX
<u>NEW</u>	P8DPB289	R10	11	104	LY6XXX, LY7XXX

NOTE: XXX stands for the last three digits of the bundle serial number.

TABLE 3.3.1

DESIGN BASIS VY CYCLE 10 AND CYCLE 11 EXPOSURES

Assumed Current Cycle Core Average Exposure	
End of Cycle 10	17.96 GWD/ST
Assumed Reload Cycle Core Average Exposure	
Beginning of Cycle 11	10.62 GWD/ST
Haling Calculated Core Average Exposure at	
End of Full Power Life, Cycle 11	17.48 GWD/ST
Cycle 11 Exposure Capability	6.96 GWD/ST

VERMONT YANKEE  
CYCLE 11  
BOC BUNDLE AVERAGE EXPOSURES

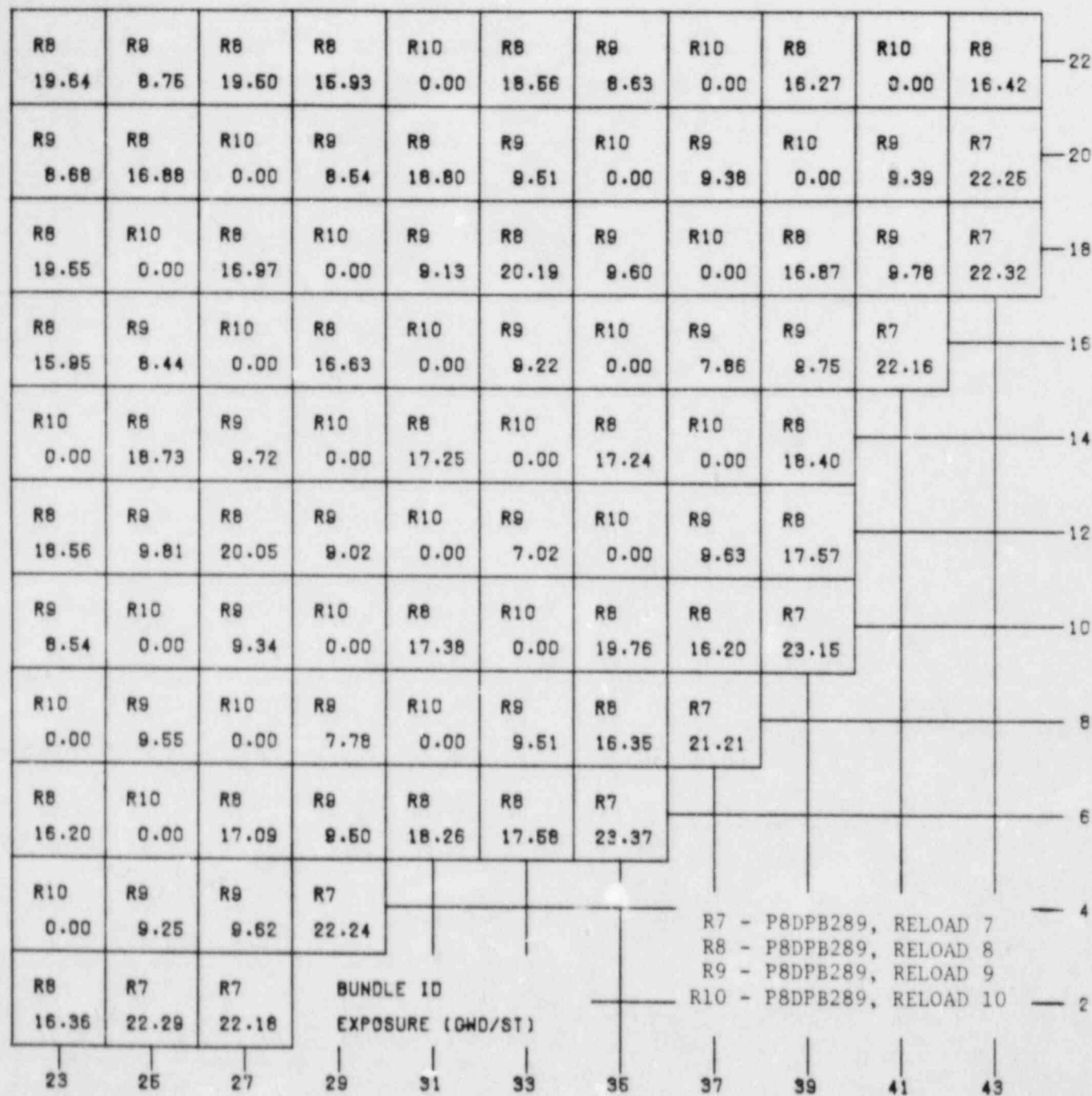


FIGURE 3.2.1

VY CYCLE 11 DESIGN REFERENCE LOADING PATTERN, LOWER RIGHT QUADRANT

## 4.0 FUEL MECHANICAL AND THERMAL DESIGN

### 4.1 Mechanical Design

All fuel to be inserted into the Reload Cycle was fabricated by the General Electric Company (GE). The major mechanical design parameters are given in Table 4.1.1. Detailed descriptions of the fuel rod mechanical design and mechanical design analyses are provided in Reference 3. These design analyses remain valid with respect to the Reload Cycle operation. Mechanical and chemical compatibility of the fuel assemblies with the in-service reactor environment is also addressed in Reference 3.

### 4.2 Thermal Design

The fuel thermal effects calculations were performed using the FROSSTEY computer code [6-8]. The FROSSTEY code calculates pellet-to-clad gap conductance and fuel temperatures from a combination of theoretical and empirical models which include fuel and cladding thermal expansion, fission gas release, pellet swelling, pellet densification, pellet cracking, and fuel and cladding thermal conductivity.

The thermal effects analysis included the calculation of fuel temperatures and fuel cladding gap conductance under nominal core steady state and peak linear heat generation rate conditions. Figure 4.2.1 provides the core average response of gap conductance. These calculations integrate the responses of individual fuel batch average operating histories over the core average exposure range of the Reload Cycle. The gap conductance values are weighted axially by power distributions and radially by volume. The core-wide gap conductance values for the RETRAN system simulations, described in Sections 7.1 through 7.3, are from this data set at the corresponding exposure statepoints.

The gap conductance values input to the hot channel calculations (Section 7.1) were evaluated for the given fuel bundle type as a function of the assembly exposure. The calculation assumed a 1.4 chopped cosine axial power shape with the peak power node running at the MAPLHGR limit defined in Reference 9. Figure 4.2.2 provides the hot channel response of gap

conductance. In Figure 4.2.2, "planar exposure" refers to the exposure of the node running at the MAPLHGR limit. Gap conductance values for the hot channel analysis were extracted from Figure 4.2.2 using the maximum bundle exposure of any MCPR limiting bundle within the exposure interval of interest. The SIMULATE roddeed depletion (Section 5.1.2) provides predictions of both limiting MCPR and the associated bundle exposure for the entire cycle.

Table 4.2.1 provides the core average and hot channel gap conductance values used in the transient analyses (Section 7.1).

Fuel rod local linear heat generation rates at fuel centerline incipient melt and 1% clad plastic strain as a function of local axial segment exposure for the gadolinia concentrations used in Vermont Yankee fuel were previously reported in Reference 10.

#### 4.3 Operating Experience

All irradiated fuel bundles scheduled to be reinserted in the Reload Cycle have operated as expected in Past Cycles of Vermont Yankee. Off-gas measurements in the Current Cycle are at normally low levels indicating that no fuel failures are present.



TABLE 4.1.1

NOMINAL FUEL MECHANICAL DESIGN PARAMETERS

	<u>FUEL TYPE</u> P8X8R
Vendor Designations (Table 3.1.1)	
New	P8DPB289
Irradiated	P8DPB289
Fuel Pellets	
Fuel Material (sintered Pellets)	UO <sub>2</sub>
Initial Enrichment, w/o U-235	2.89
Pellet Density, % theoretical	95.0
Pellet Diameter, inches	0.410
Fuel Rod	
Active Length, inches	150.0
Plenum Length, inches	9.5
Fuel Rod Pitch, inches	0.640
Diametral Gap (cold), inches	0.009
Fill Gas	Helium
Fill Gas Pressure, psig	[See Ref. 3]
Cladding	
Material	Zr-2
Outside Diameter, inches	0.483
Thickness, inches	0.032
Inside Diameter, inches	0.419
Fuel Channel	
Material	Zr-4
Inside Dimension, inches	5.278
Wall Thickness, inches	0.080
Fuel Assembly	
Fuel Rod Array	8x8
Fuel Rods per Assembly	62
Spacer Grid Material	Zr-4

TABLE 4.2.1

GAP CONDUCTANCE VALUES USED IN VY CYCLE 11 TRANSIENT ANALYSES

Cycle Exposure Statepoint	Core Average Gap Conductance	Hot Channel Bundle Exposure	Hot Channel Gap Conductance
<u>(MWD/ST)</u>	<u>(BTU/Hr-Ft<sup>2</sup> - °F)</u>	<u>(MWD/ST)</u>	<u>(BTU/Hr-Ft<sup>2</sup> - °F)</u>
BOC11	755	11240(1)	1490
EOFPL11-2000 MWD/ST	980	6320	1040
EOFPL11-1000 MWD/ST	995	7460	1120
EOFPL11	1010	8720	1250

NOTE

- (1) Between BOC11 and EOFPL11-2000 MWD/ST, the highest exposure limiting hot channel bundle is once-burned.

# VY CYCLE 11 FUEL PERFORMANCE

## CORE AVERAGE GAP CONDUCTANCE

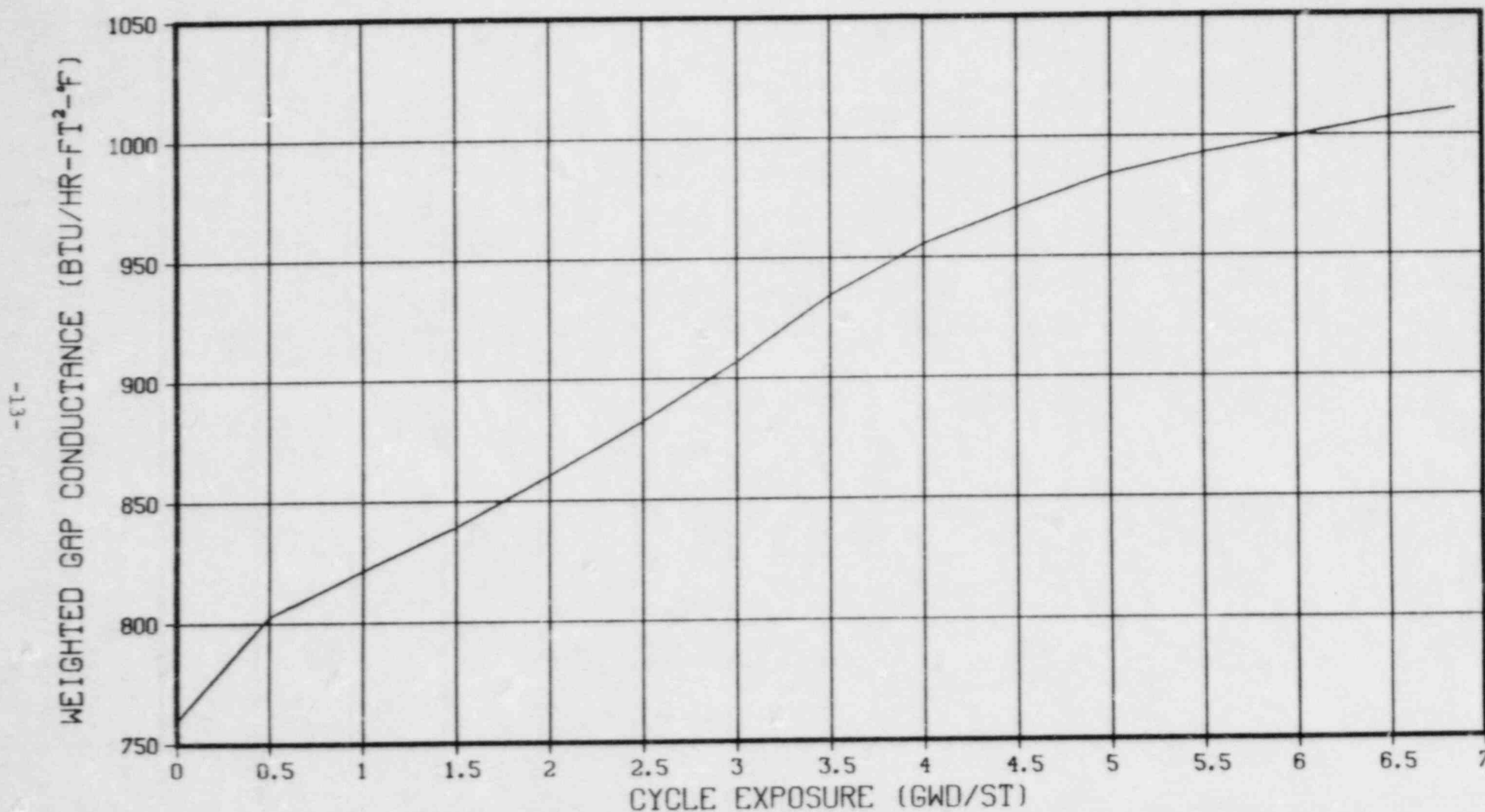


FIGURE 4.2.1

VY CYCLE 11 CORE AVERAGE GAP CONDUCTANCE VERSUS CYCLE EXPOSURE

# VERMONT YANKEE - HOT CHANNEL GAP CONDUCTANCE

P8X8R FUEL -- GAP CONDUCTANCE VS EXPOSURE

1.4 CHOPPED COSINE SPECTRAL POWER SHAPE WITH PEAK AT HAPLHAR

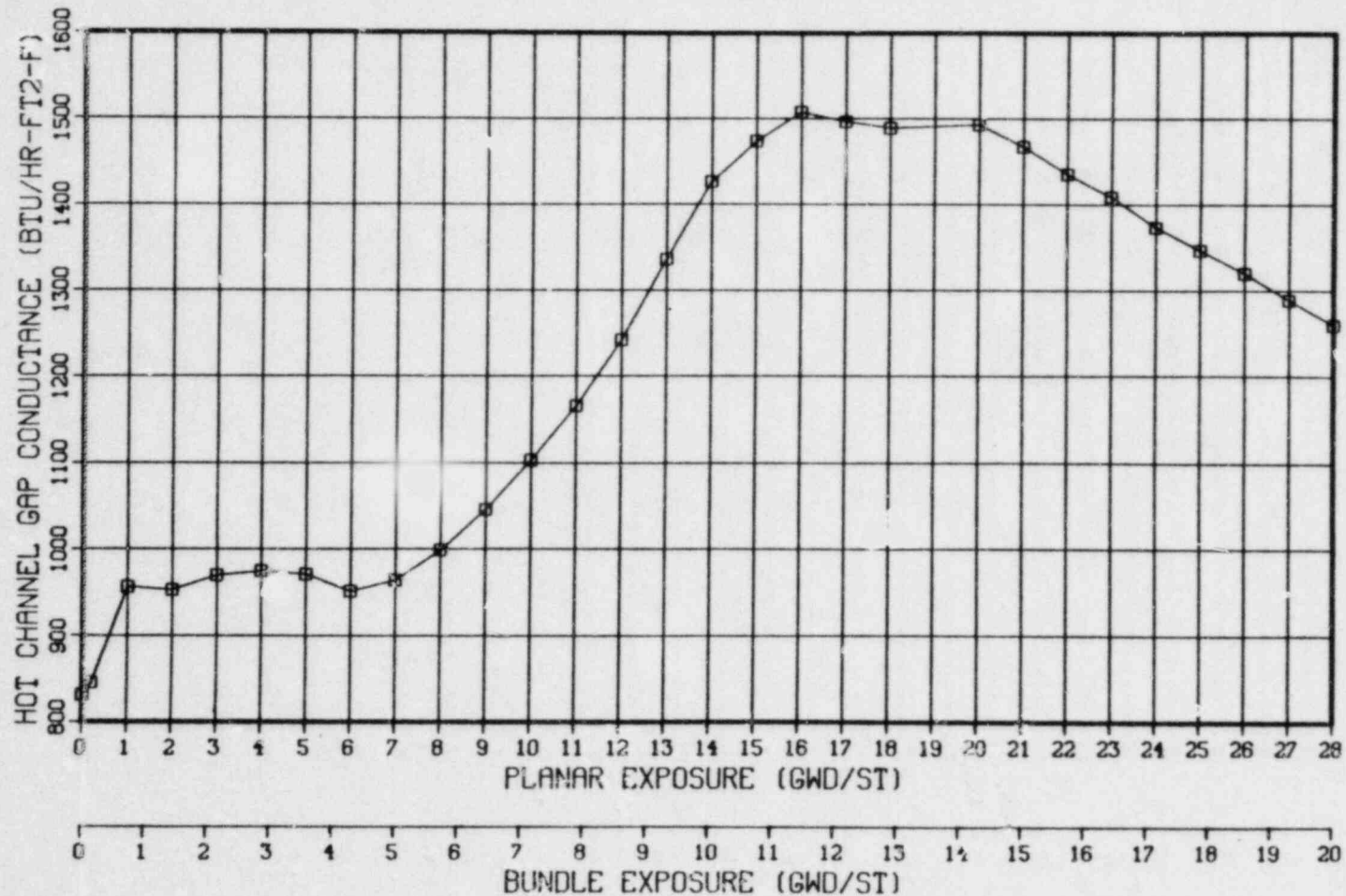


FIGURE 4.2.2

VY HOT CHANNEL GAP CONDUCTANCE FOR P8x8R VERSUS EXPOSURE

## 5.0 NUCLEAR DESIGN

### 5.1 Core Power Distributions

The Reload Cycle was depleted using SIMULATE [4] to give both a roddeed depletion and an All Rods Out (ARO) Haling depletion. The Haling depletion serves as the basis for defining core reactivity characteristics for most transient evaluations. This is primarily because its flat power shape has conservatively weak scram characteristics. The roddeed depletion was used to evaluate the misloaded bundle error and the rod withdrawal error. This is because of the more realistic predictions it makes of initial CPR values. It was also used in the rod drop worth and shutdown margin calculations because it burns the top of the core more realistically than the Haling.

#### 5.1.1 Haling Power Distribution

The Haling power distribution is calculated in the All Rods Out (ARO) condition. The Haling iteration converges on a self-consistent power and exposure shape for the burnup step to EOFPL. In principle, this should provide the overall minimum peaking power shape for the cycle. During the actual cycle, flatter power distributions might occasionally be achieved by shaping with control rods. However, such shaping would leave underburned regions in the core which would peak at another point in time. Figures 5.1.1 and 5.1.2 give the Haling radial and axial average power distributions for the Reload Cycle.

#### 5.1.2 Roddeed Depletion Power Distribution

To generate the roddeed depletion, control rod patterns were developed which gave critical eigenvalues at each point in the cycle and gave peaking similar to the Haling calculation. The resulting patterns were frequently more peaked than the Haling, but were below expected operating limits. However, as stated above, the underburned regions of the core can exhibit peaking in excess of the Haling peaking when pulling ARO at EOFPL. Figures 5.1.3 and 5.1.4 give the ARO at EOFPL power distributions for the Reload Cycle roddeed depletion. Note in Figure 5.1.4 that the average axial power at ARO



for the rodged depletion is more bottom peaked than the Haling (Figure 5.1.2). The rodged depletion would result in better scram characteristics at EOFPL.

## 5.2 Core Exposure Distributions

The Reload Cycle exposures are summarized in Table 3.3.1. Coastdown is not included. The projected BOC radial exposure distribution for the Reload Cycle is given in Figure 3.2.1. The Haling calculation produced the EOFPL radial exposure distribution given in Figure 5.2.1. Since the Haling power shape is constant, it can be held fixed by SIMULATE to give the exposure distributions at various mid-cycle points. BOC, EOFPL-2000 MWD/ST, EOFPL-1000 MWD/ST, and EOFPL exposure distributions were used to develop reactivity input for the core wide transient analyses.

The rodged depletion differs from the Haling during the cycle due to power shaping by the rods. However, rod sequences are swapped frequently and the overall exposure distribution at end of cycle is similar to the Haling. Figure 5.2.2 gives the EOFPL radial exposure distribution for the Reload Cycle rodged depletion.

## 5.3 Cold Core Reactivity and Shutdown Margin

The cold  $K_{eff}$  with ARO and the cold  $K_{eff}$  with All Rods Inserted (ARI) at BOC were calculated using the SIMULATE code [4,5] and are shown in Table 5.3.1.  $K_{eff}$  with ARO minus the cold critical  $K_{eff}$  is the amount of excess core reactivity.  $K_{eff}$  with ARI minus the  $K_{eff}$  with ARO is the worth of all the control rods.

The cold critical eigenvalue  $K_{eff}$  was defined as the average calculated critical eigenvalue minus a 95% confidence level uncertainty. Then all cold results were normalized to make the critical  $K_{eff}$  eigenvalue equal to 1.000.

Technical Specifications [9] state that, for sufficient shutdown margin, the core must be subcritical by at least  $0.2\% \Delta K + R$  (defined below) with the strongest worth control rod withdrawn. Again, using SIMULATE, a

search was made for the strongest worth control rod at various exposures in the cycle. This is necessary because rod worths change with exposure. Then the cold  $K_{eff}$  with the strongest rod out was calculated at BOC and at the end of each control rod sequence. Subtracting each cold  $K_{eff}$  with the strongest rod out from the cold critical  $K_{eff}$  eigenvalue defines the shutdown margin as a function of exposure. Figure 5.3.1 shows the result. Because the local reactivity may increase with exposure, the shutdown margin (SDM) may decrease. To account for this, and other uncertainties, the value  $R$  is calculated.  $R$  is defined as  $R_1$  plus  $R_2$ .  $R_1$  is the difference between the cold  $K_{eff}$  with the strongest rod out at BOC and the maximum cold  $K_{eff}$  with the strongest rod out in the cycle.  $R_2$  is a measurement uncertainty in the demonstration of SDM. It is presently set at .07%  $\Delta K$ . The shutdown margin results are summarized in Table 5.3.1.

#### 5.4 Standby Liquid Control System Shutdown Capability

The shutdown capability of the Standby Liquid Control System (SLCS) is designed to bring the reactor from full power to cold, ARO, xenon free shutdown with at least 5%  $\Delta K$  margin. Using the boron concentration search option in SIMULATE [4], the ppm of boron was adjusted until the  $K_{eff}$  reached the cold critical  $K_{eff}$  minus .05. This case assumed cold, xenon free conditions, with All Rods Out at the most reactive time in the cycle. The criticality search found that the plant would be subcritical by 5%  $\Delta K$  at the worst point in time with less than the 800 ppm of boron required by VY Technical Specifications [9]. Table 5.4.1 lists the amount of boron concentration and the corresponding shutdown capability of the SLCS.

TABLE 5.3.1

VY CYCLE 11  
K<sub>eff</sub> VALUES AND SHUTDOWN MARGIN CALCULATION

BOC K <sub>eff</sub> - Uncontrolled	1.1172
BOC K <sub>eff</sub> - Controlled	.9700
Cold Critical K <sub>eff</sub> Eigenvalue	1.0000
BOC K <sub>eff</sub> - Controlled With Strongest Worth Rod Withdrawn	.9881
Cycle Minimum Shutdown Margin Occurs at BOC With Strongest Worth Rod Withdrawn	1.19% ΔK
R <sub>1</sub> , Maximum Increase in Cold K <sub>eff</sub> With Exposure	.00% ΔK

TABLE 5.4.1

VY CYCLE 11  
STANDBY LIQUID CONTROL SYSTEM SHUTDOWN CAPABILITY

<u>ppm of Boron</u>	<u>Shutdown Margin</u>
680	.050 ΔK
800	.073 ΔK

VERMONT YANKEE  
CYCLE 11 HALING DEPLETION  
EOFPL BUNDLE AVERAGE RELATIVE POWERS

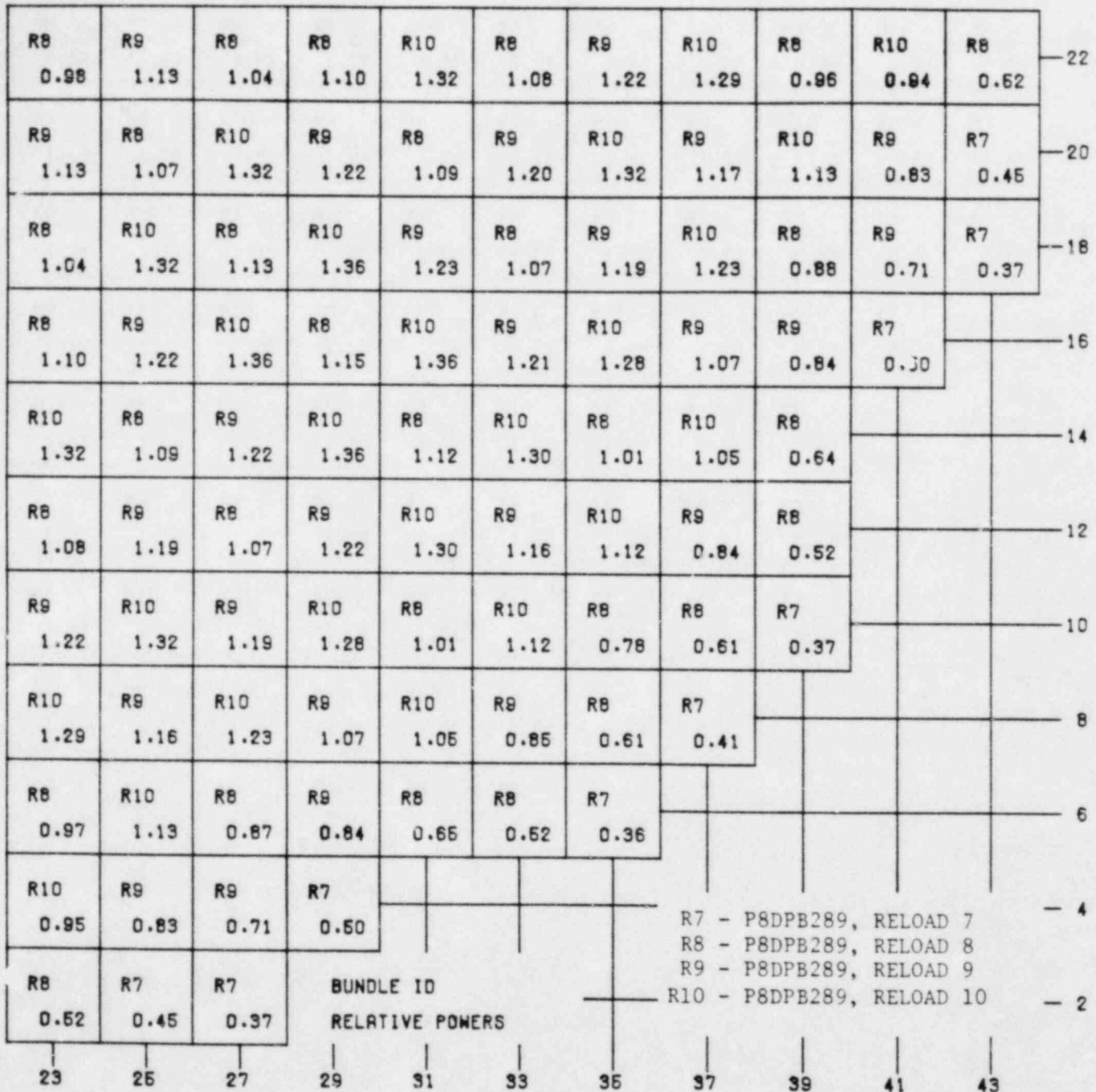


FIGURE 5.1.1

VY CYCLE 11 HALING DEPLETION, EOFPL BUNDLE AVERAGE RELATIVE POWERS

VY CYCLE 11 CORE AVERAGE AXIAL POWER DISTRIBUTION  
TAKEN FROM THE HALING CALCULATION TO EOFPL

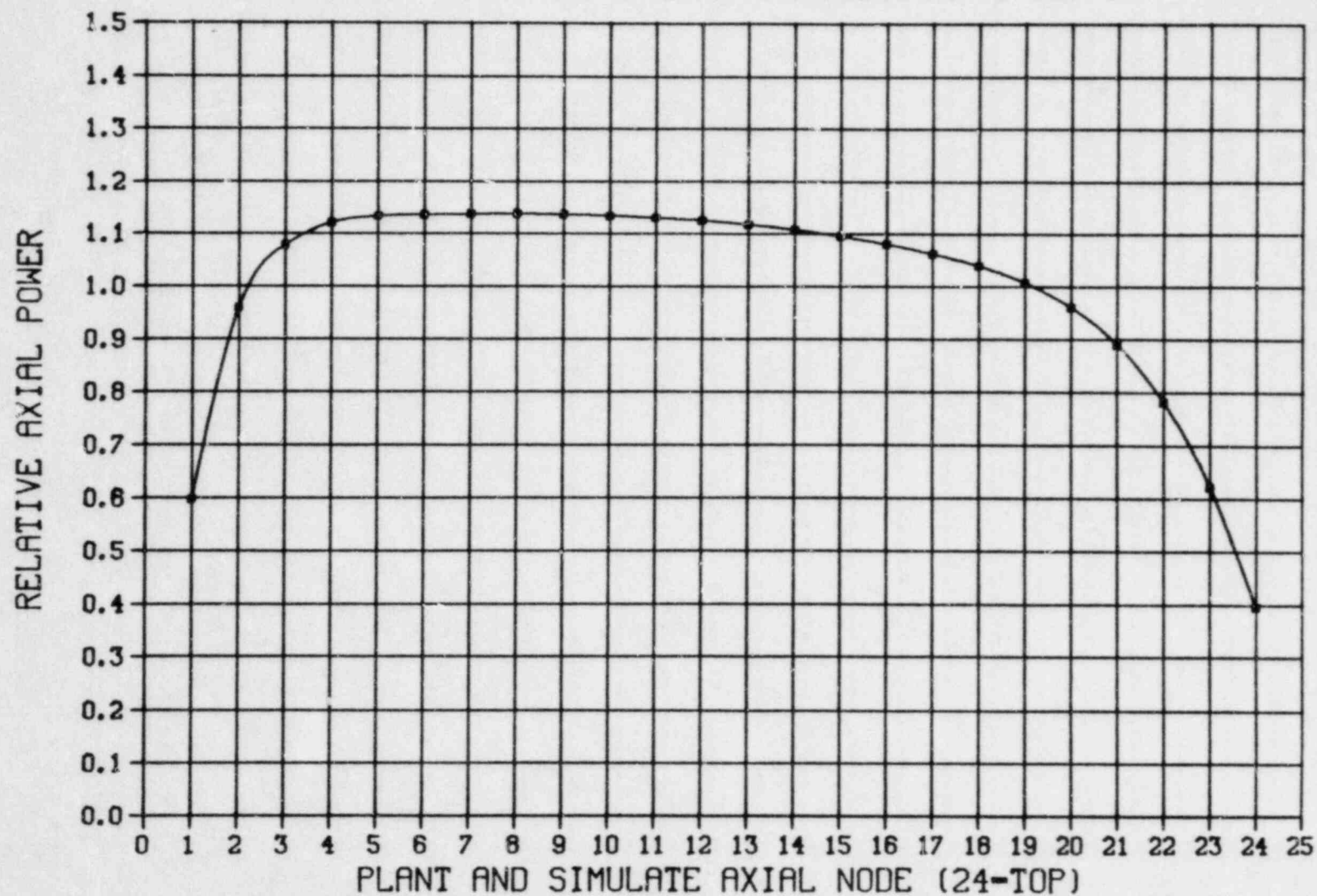


FIGURE 5.1.2

VY CYCLE 11 CORE AVERAGE AXIAL POWER DISTRIBUTION TAKEN FROM THE HALING CALCULATION TO EOFPL



VERMONT YANKEE  
CYCLE 11 RODDED DEPLETION  
EOFPL BUNDLE AVERAGE RELATIVE POWERS

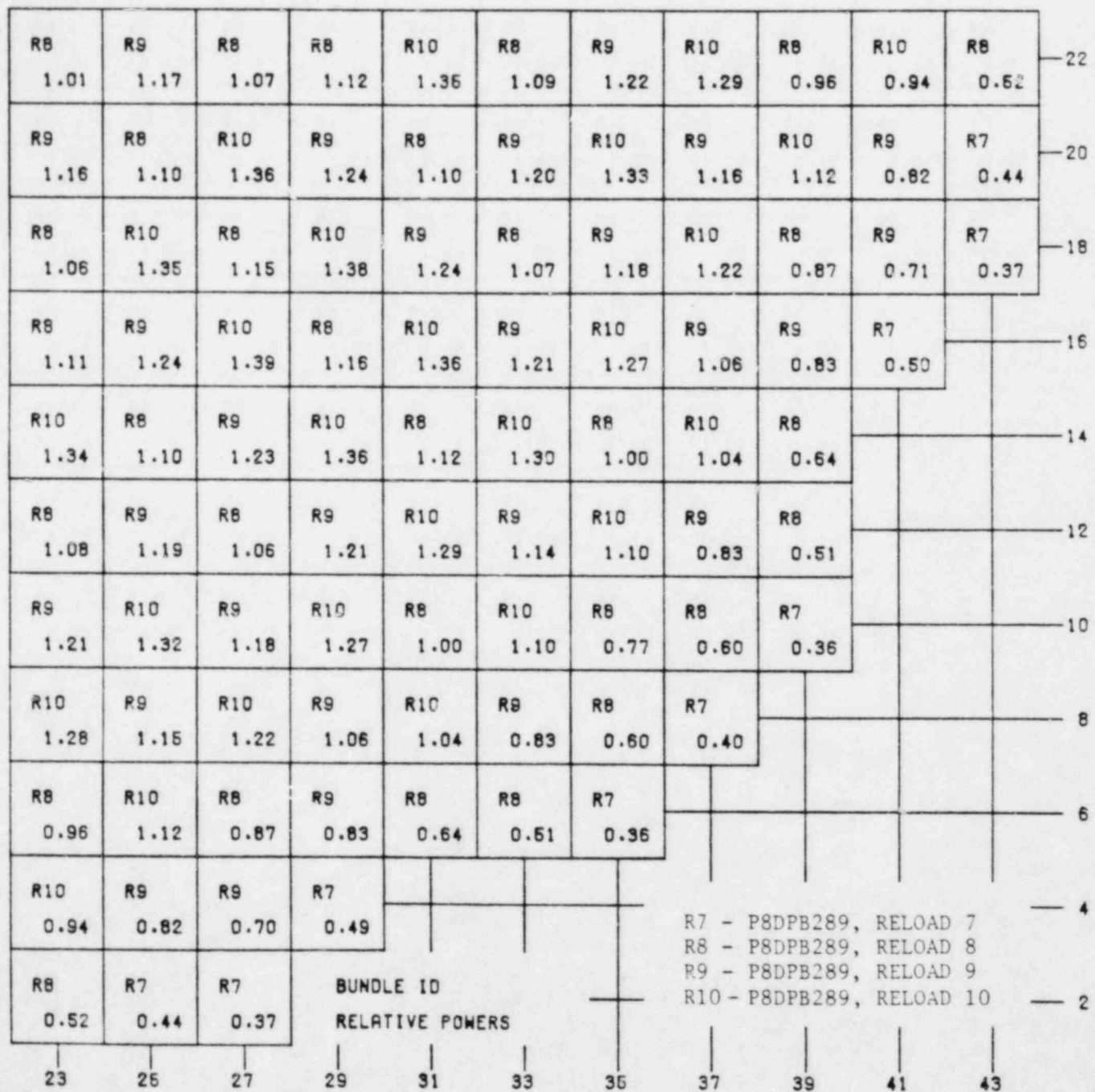


FIGURE 5.1.3

VY CYCLE 11 RODDED DEPLETION-ARO AT EOFPL BUNDLE AVERAGE RELATIVE POWERS

VY CYCLE 11 CORE AVERAGE AXIAL POWER DISTRIBUTION  
 RODDED DEPLETION -- ALL RODS OUT AT EOFPL

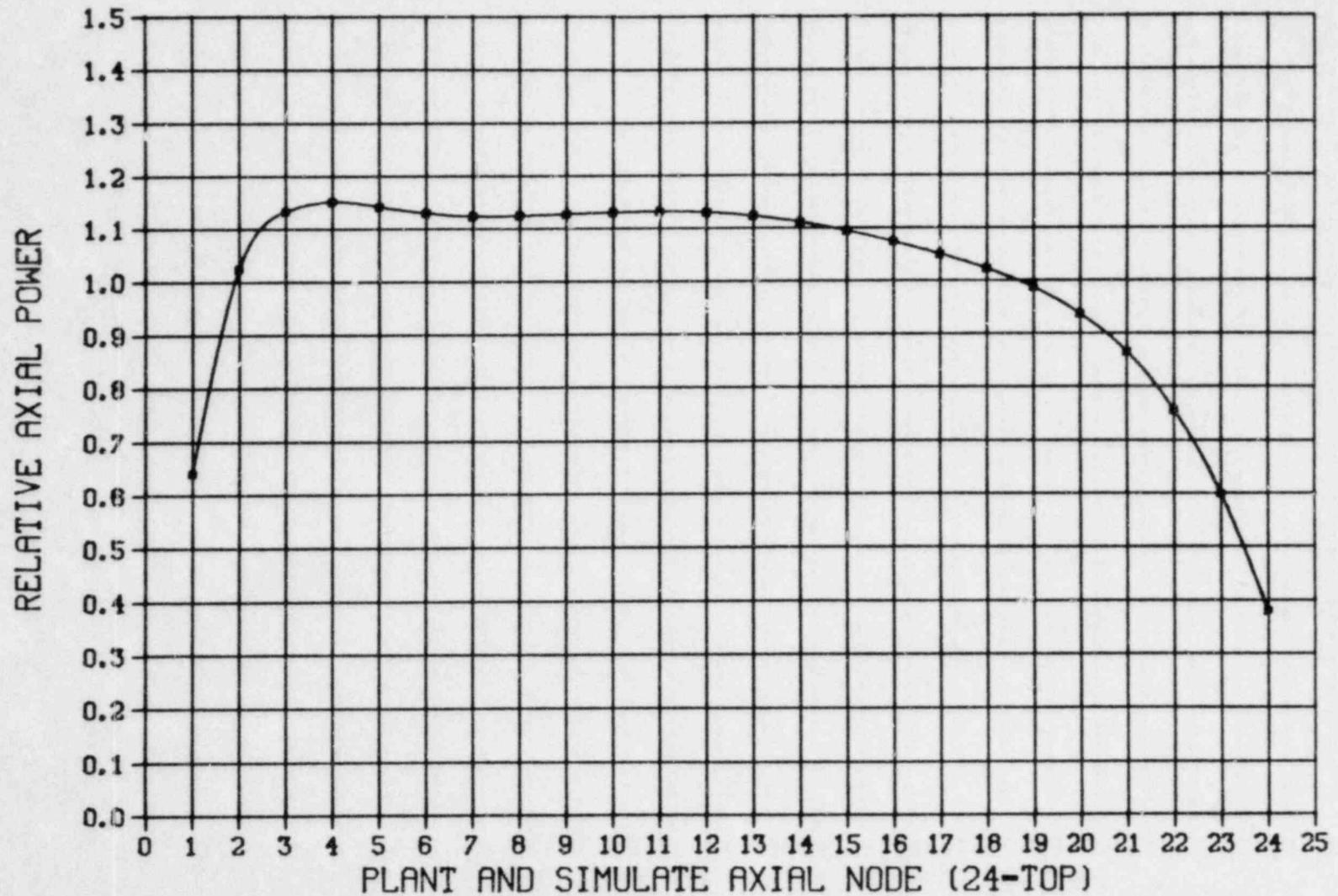


FIGURE 5.1.4

VY CYCLE 11 CORE AVERAGE AXIAL POWER DISTRIBUTION, RODDED DEPLETION-ARO AT EOFPL

VERMONT YANKEE  
CYCLE 11 HALING DEPLETION  
EOFPL BUNDLE AVERAGE EXPOSURES

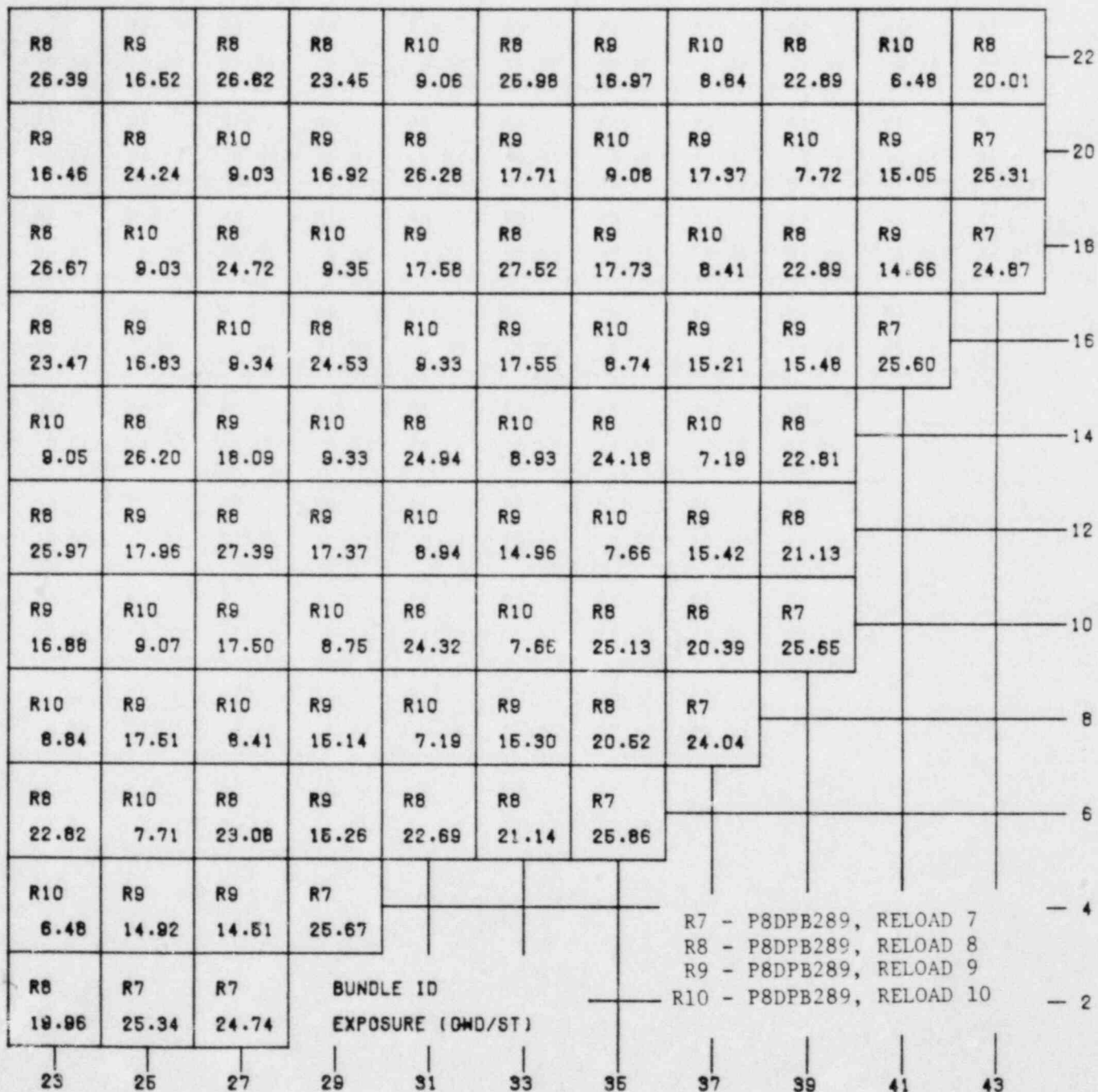


FIGURE 5.2.1

VY CYCLE 11 HALING DEPLETION, EOFPL BUNDLE AVERAGE EXPOSURES

VERMONT YANKEE  
CYCLE 11 RODDED DEPLETION  
EOFPL BUNDLE AVERAGE EXPOSURES

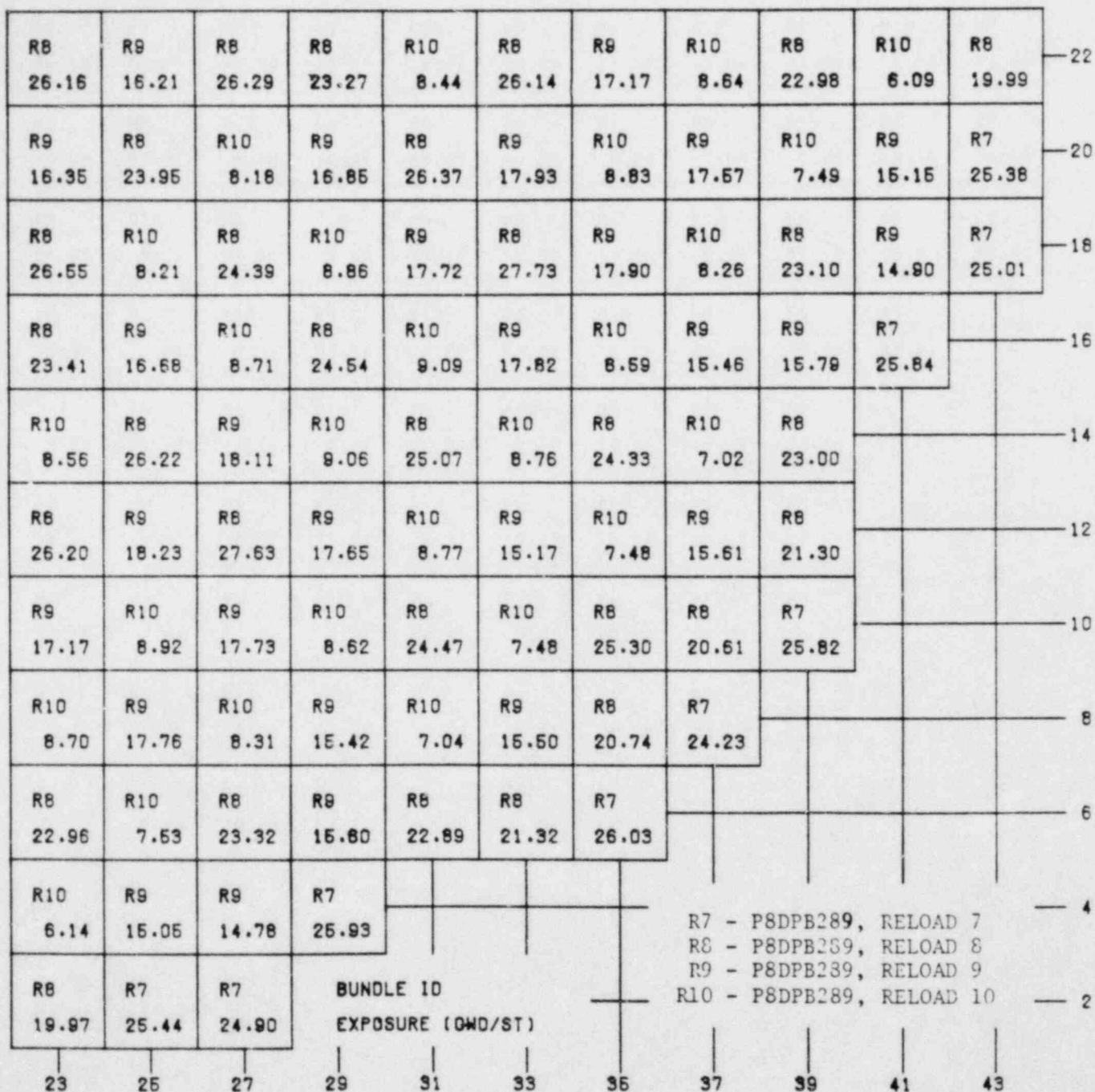
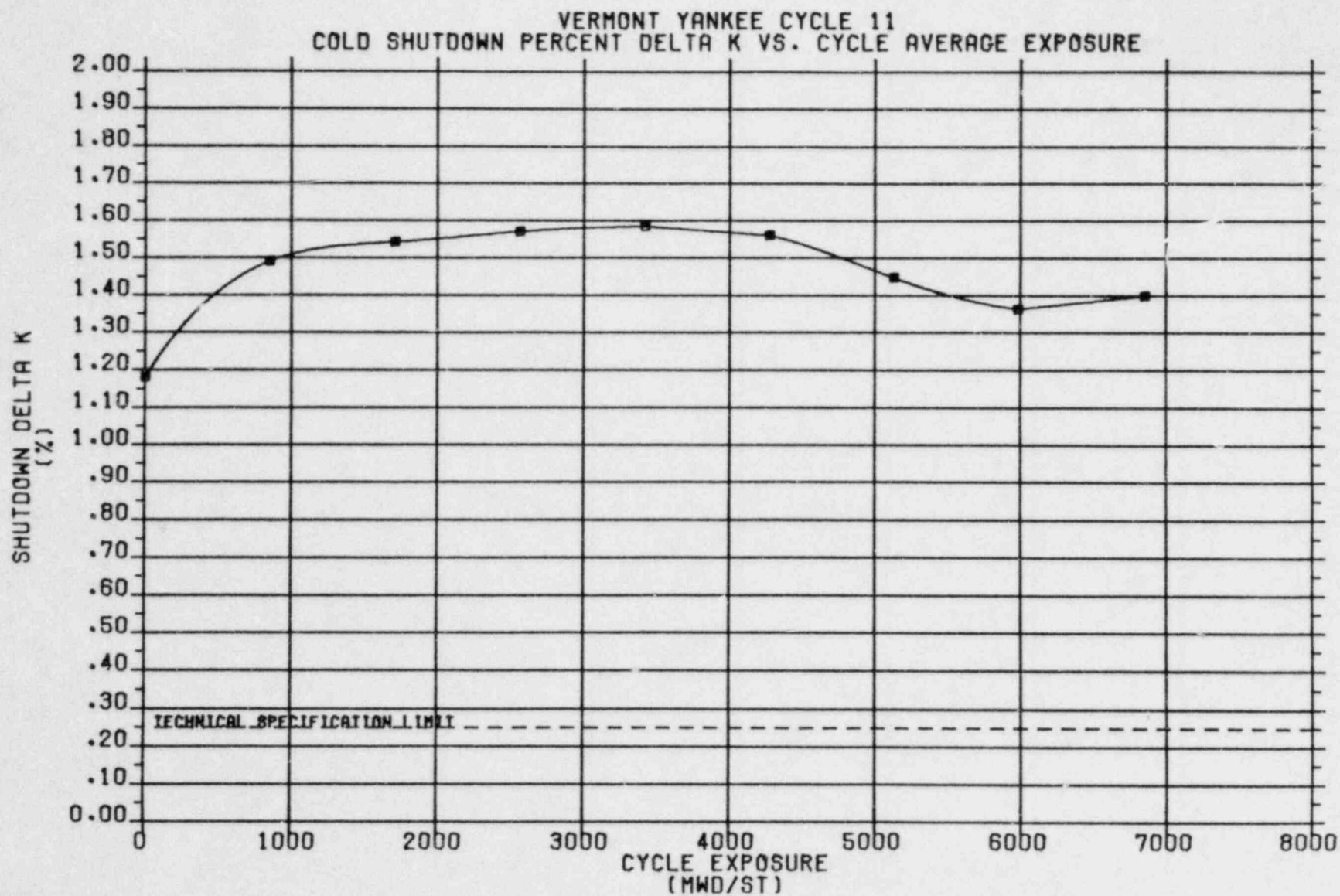


FIGURE 5.2.2

VY CYCLE 11 RODDED DEPLETION, EOFPL BUNDLE AVERAGE EXPOSURES







## 6.0 THERMAL-HYDRAULIC DESIGN

The thermal-hydraulic evaluation of the Reload Cycle was performed using the methods described in the following section.

### 6.1 Steady-State Thermal Hydraulics

Core steady-state thermal-hydraulic analyses were performed using the FIBWR [11,12] computer code. The FIBWR code incorporates a detailed geometrical representation of the complex flow paths in a BWR core, and explicitly models the leakage flow to the bypass region. FIBWR calculates the core pressure drop and total bypass flow for a given total core flow. The power distribution, inlet enthalpy, and geometry are presumed known and are supplied to FIBWR. The power distribution is derived by the 3-D neutronic simulator SIMULATE [4]. Core pressure drop and total leakage flow predicted by the FIBWR code were used in setting the initial conditions for the system's transient analysis model.

### 6.2 Reactor Limits Determination

The objective for normal operation and anticipated transient events is to maintain nucleate boiling. Avoiding a transition to film boiling protects the fuel cladding integrity. Based on Reference 13, the fuel cladding integrity safety limit for Vermont Yankee is a Lowest Allowable Minimum Critical Power Ratio (LAMCPR) of 1.07. Operating limits are specified to maintain adequate margin to onset of the boiling transition. The figure of merit utilized for plant operation is the Critical Power Ratio (CPR). This is defined as the ratio of the critical power (bundle power at which some point within the assembly experiences onset of boiling transition) to the operating bundle power. Thermal margin is stated in terms of the minimum value of the critical power ratio, MCPR, which corresponds to the most limiting fuel assembly in the core. Both the transient (safety) and normal operating thermal limits in terms of MCPR are derived based on the GEXL correlation as described in Reference 13.

Vermont Yankee Technical Specifications [9] limit the operation of the Reload Cycle fuel to a Maximum Linear Heat Generation Rate (MLHGR) of 13.4 KW/ft. The basis for a MLHGR of 13.4 KW/ft can be found in Reference 3.

## 7.0 ACCIDENT ANALYSIS

### 7.1 Core Wide Transient Analysis

Core wide transient simulations are performed to assess the impact of certain transients on the heat transfer characteristics of the fuel. The figure of merit used is the Critical Power Ratio (CPR). It is the purpose of the analysis to determine the minimum critical power ratio such that the safety limit is not violated for the transients considered.

#### 7.1.1 Methodology

The analysis requires two types of simulations. A system level simulation is performed to determine the overall plant response. Transient core inlet and exit conditions and normalized power from the system level calculation are used to perform detailed thermal-hydraulic simulations of the fuel, referred to as "hot channel calculations". The hot channel simulations provide the bundle transient  $\Delta\text{CPR}$  (the initial bundle CPR minus the minimum CPR experienced during the transient).

The system level simulations are performed with the model documented in Reference 14.

The hot channel calculations are performed with the RETRAN [15] and TCPYA01 [16] computer codes. The GEXL correlation [13] is used in TCPYA01 to evaluate critical power ratio. The calculational procedure is outlined below.

The hot channel transient  $\Delta\text{CPR}$  calculations employ a series of "inner" and "outer" iterations, as illustrated by the flow chart in Figure 7.1.1. The outer loop iterates on the hot channel initial power level. This is necessary because the  $\Delta\text{CPR}$  for a given transient varies with Initial Critical Power Ratio (ICPR). However, only the  $\Delta\text{CPR}$  corresponding to a transient MCPR equal to the safety limit (i.e.,  $1.07 + \Delta\text{CPR} = \text{ICPR}$ ) is appropriate. The approximate constancy of the  $\Delta\text{CPR}/\text{ICPR}$  ratio is useful in these iterations. Each outer iteration requires a RETRAN hot channel run to calculate the transient enthalpies, flows, pressure and saturation properties at each time step. These are required for input to the TCPYA01 code. TCYPA01 is then used

to calculate a CPR at each time step during the transient, from which a transient  $\Delta$ CPR is derived. The hot channel model assumes a chopped cosine axial power shape with a peak/average ratio of 1.4.

The inner loop iterates on the hot channel inlet flow. These iterations are necessary, because the RETRAN hot channel model calculates the entrance loss coefficient when given the initial power level, flow, and pressure drop as input. The pressure drop is assumed equal to the core average pressure drop, and the flow is varied for a given power level until the calculated entrance loss coefficient is correct. FIBWR [11, 12] is utilized to estimate the correct inlet flow for a particular power level and pressure drop.

#### 7.1.2 Initial Conditions and Assumptions

The initial conditions for the system simulations are based on maximum turbine capacity of 105% of rated steam flow. The corresponding reactor conditions are 104.5% core thermal power and 100% core flow. The core axial power distribution for each of the exposure points is based on the 3-D SIMULATE predictions associated with the generation of the reactivity data (Section 7.1.3). The core inlet enthalpy is set so that the amount of carryunder from the steam separators and the quality in the liquid region outside the separators is as close to zero as possible. For fast pressurization transients, this maximizes the initial pressurization rate and predicts a more severe neutron power spike. A summary of the initial operating state used for the system simulations is provided in Table 7.1.1.

Assumptions specific to a particular transient are discussed in the section describing the transient. In general, the following assumptions are made for all transients:

1. Scram setpoints are at Technical Specification [9] limits.
2. Protective system logic delays are at equipment specification limits.



3. Safety/relief valve and safety valve capacities are based on Technical Specification rated values.
4. Safety/relief valve and safety valve setpoints are modeled as being at the Technical Specification upper limit. Valve responses are based on slowest specified response values.
5. Control rod drive scram speed is based on the Technical Specification limits. The analysis addresses a dual set of scram speeds as given in the Technical Specifications. These are referred to as the "Measured" and the (slower) "67B" scram times.

#### 7.1.3 Reactivity Functions

The methods used to generate the fuel temperature, moderator density, and scram reactivity functions are described in detail in Reference 17. The method is outlined below.

A complete set of reactivity functions, the axial power distribution, and the kinetics parameters are generated from base states established for EOFPL, EOFPL-1000 MWD/ST, EOFPL-2000 MWD/ST, and BOC exposure statepoints. These statepoints are characterized by exposure and void history distributions, control rod patterns, and core thermal-hydraulic conditions. The latter are consistent with the assumed system transient conditions provided in Table 7.1.1.

The BOC base state is established by shuffling from the previously defined Current Cycle endpoint into the Reload Cycle loading pattern. A criticality search provides an estimate of the BOC critical rod pattern. The EOFPL and intermediate core exposure and void history distributions are calculated with a Haling depletion as described in Section 5.2. The EOFPL state is unrodded. As such, it is defined sufficiently. However, EOFPL-1000 MWD/ST and EOFPL-2000 MWD/ST exposure statepoints require base control rod patterns. These are developed to be as "black and white" as possible. That is, beginning with the rodded depletion configuration, all control rods which are more than half inserted are fully inserted, and all control rods which are less than half inserted are fully withdrawn. If the SIMULATE calculated



parameters are within operating limits, then this configuration becomes the base case. If the limits are exceeded, a minimum number of control rods are adjusted a minimum number of notches until the parameters fall within limits. Using this method, the control rod patterns and resultant power distributions are established which minimize the scram reactivity function and maximize the core average moderator density reactivity coefficient. For the transients analyzed, this tends to maximize the power response.

At each exposure statepoint, reactivity function table sets are produced for the 12 core-volumes of the Vermont Yankee RETRAN model. The fuel temperature (Doppler) data set is generated by fixing the power distribution while varying the fuel temperature associated with that power. A moderator density table set is generated specifically for each transient type. The moderator density reactivity functions for the subcooling transient are generated by quasi-statically varying the inlet subcooling only. The moderator enthalpy source distribution is in equilibrium with the calculated nuclear power. The moderator density reactivity functions for the pressurization transients are generated by quasi-statically varying the core pressure. A series of calculations are performed for various inlet moderator temperatures. The moderator enthalpy source distribution is that of the base state case.

In order to qualitatively compare the core reactivity characteristics between different base configurations, core average reactivity coefficients at selected conditions are provided in Table 7.1.2. Calculated point kinetics parameters for RETRAN are also provided.

The reactivities versus scram insertion are calculated at constant, pre-transient moderator conditions. These are fitted to yield highly detailed scram reactivity curves. The curves are combined with the appropriate rod position versus time data to generate the final RETRAN scram reactivity functions. Figures 7.1.2 through 7.1.4 display the inserted rod worths and rod positions as functions of scram time for the "Measured" scram time analysis. Figures 7.1.5 through 7.1.7 display similar curves for the "67B" scram time analysis.

#### 7.1.4 Transients Analyzed

Past licensing experience has shown that the core wide transients which result in the minimum core thermal margins are:

1. Generator load rejection with complete failure of the turbine bypass system.
2. Turbine trip with complete failure of the turbine bypass system.
3. Loss of feedwater heating.

The "feedwater controller failure" (maximum demand) transient is not a severe transient for Vermont Yankee, because of the plant's 110% steam flow bypass system. Past analyses have shown this transient to be considerably less severe than any of the above for all exposure points. Brief descriptions and the results of the core wide transients analyzed are provided in the following section.

#### 7.2 Core Wide Transient Analysis Results

The transients selected for consideration were analyzed at exposure points of EOFPL, EOFPL-1000 MWD/ST, and EOFPL-2000 MWD/ST; the loss of feedwater heating transient was also evaluated at BOC conditions. A summary of the results of the analyses is provided in Table 7.2.1.

##### 7.2.1 Turbine Trip Without Bypass Transient (TTWOBP)

The transient is initiated by a rapid closure (0.1 second closing time) of the turbine stop valves. It is assumed that the steam bypass valves, which normally open to relieve pressure, remain closed. A reactor protection system signal is generated by the turbine stop valve closure switches. Control rod drive motion is conservatively assumed to occur 0.27 seconds after the start of turbine stop valve motion. The ATWS recirculation pump trip is assumed to occur at a setpoint of 1150 psig dome pressure. A pump trip time delay of 1.0 second is assumed to account for logic delay and M-G set generator field collapse. In simulating the transient, the bypass piping volume up to the

valve chest is lumped into the control volume upstream of the turbine stop valves. Predictions of the salient system parameters at the three exposure points are shown in Figures 7.2.1 through 7.2.3 for the "Measured" scram time analysis.

#### 7.2.2 Generator Load Rejection Without Bypass Transient (GLRWOBP)

The transient is initiated by a rapid closure (0.3 seconds closing time) of the turbine control valves. As in the case of the turbine trip transient, the bypass valves are assumed to fail. A reactor protection system signal is generated by the hydraulic fluid pressure switches in the acceleration relay of the turbine control system. Control rod drive motion is conservatively assumed to occur 0.28 seconds after the start of turbine control valve motion. The same modeling regarding the ATWS pump trip and bypass piping is used as in the turbine trip simulation. The influence of the accelerating main turbine generator on the recirculation system is simulated by specifying the main turbine generator electrical frequency as a function of time for the M-G set drive motors. The main turbine generator frequency curve is based on a 100% power plant startup test and is considered representative for the simulation. The system model predictions for the three exposure points are shown in Figures 7.2.4 through 7.2.6 for the "Measured" scram time analysis.

#### 7.2.3 Loss of Feedwater Heating Transient (LOFWH)

A feedwater heater can be lost in such a way that the steam extraction line to the heater is shut off or the feedwater flow bypasses one of the heaters. In either case, the reactor will receive cooler feedwater, which will produce an increase in the core inlet subcooling, resulting in a reactor power increase.

The response of the system due to the loss of 100<sup>0</sup>F of the feedwater heating capability was analyzed. This represents the current licensing assumption for the maximum expected single heater or group of heaters that can be tripped or bypassed by a single event.

Vermont Yankee has a scram setpoint of 120% of rated power as part of the Reactor Protection System (RPS) on high neutron flux. In this analysis, no credit was taken for scram on high neutron flux, thereby allowing the reactor power to reach its peak without scram. This approach was selected to provide a bounding and conservative analysis.

The transient response of the system was evaluated at several exposures during the cycle. The transient evaluation at EOFPL-2000 MWD/ST was found to be the limiting case between BOC to EOFPL. The results of the system response to a loss of 100<sup>0</sup> F feedwater heating capability evaluated at EOFPL-2000 MWD/ST as predicted by the RETRAN code are presented in Figure 7.2.7.

### 7.3 Overpressurization Analysis Results

Compliance with ASME vessel code limits is demonstrated by an analysis of the Main Steam Isolation Valves (MSIV) closing with failure of the MSIV position switch scram. EOFPL conditions were analyzed. The system model used is the same as that used for the core wide transient analysis (Section 7.1.1). The initial conditions and modeling assumptions discussed in Section 7.1.2 are applicable to this simulation.

The transient is initiated by a simultaneous closure of all four MSIV's. A 3.0 second closing time, which is the Technical Specification minimum, is assumed. A reactor scram signal is generated on APRM high flux. Control rod drive motion is conservatively assumed to occur 0.28 seconds after reaching the high flux setpoint. The system response is shown in Figure 7.3.1 for the "Measured" scram time analysis.

The maximum pressures at the bottom of the reactor vessel calculated for the "Measured" scram time analysis and for the "67B" scram time analysis are given in Table 7.3.1. These results are within the allowable code limit of 10% above vessel design pressure for upset conditions, or 1375 psig.

### 7.4 Local Rod Withdrawal Error Transient Results

The rod withdrawal error is a local core transient caused by an operator erroneously withdrawing a control rod in the continuous withdrawal



mode. If the core is operating at its operating limits for MCPR and LHGR at the time of the error, then withdrawal of a control rod could increase both local and core power levels with the potential for overheating the fuel.

There is a broad spectrum of core conditions and control rod patterns which could be present at the time of such an error. For most normal situations it would be possible to fully withdraw a control rod without exceeding 1% clad plastic strain or violating the CPR based fuel cladding integrity safety limit.

To bound the most severe of postulated rod withdrawal error events, a portion of the core MCPR operating limit envelope is specifically defined such that the cladding limits are not violated. The consequences of the error depend on the local power increase, the initial MCPR of the neighboring locations and the ability of the Rod Block Monitor System to stop the withdrawing rod before MCPR reaches 1.07.

The most severe transient postulated begins with the core operating according to normal procedures and within normal operating limits. The operator makes a procedural error and attempts to fully withdraw the maximum worth control rod at maximum withdrawal speed. The core limiting locations are close to the error rod. They experience the spatial power shape transient as well as the overall core power increase.

The core conditions and control rod pattern for the bounding case are specified using the following set of concurrent worst case assumptions:

1. The rod should have high reactivity worth. This is provided for by analysis of the core at peak reactivity exposure for each test pattern with xenon free conditions superimposed. The xenon free conditions and the additional control rod inventory needed to maintain criticality exaggerates the worth of control rods substantially when compared to normal operation with normal xenon levels. A fully inserted high worth rod is selected as the error rod.
2. The core is initially at 104.5% power and 100% flow.



3. The core power distribution is adjusted with the available control rods to place the locations within the four by four array of bundles around the error rod as nearly on the operating limits as practical.

The Rod Block Monitor System's ability to terminate the bounding case is evaluated on the following bases:

1. Technical Specifications [9] allow each of the separate RBM channels to remain operable if at least half of the LPRM inputs at every level are operable. For the interior RBM channels tested in this analysis, there are a maximum of four LPRM inputs per level. One RBM channel averages the inputs from the A and C levels; the other channel averages the inputs from the B and D levels. Considering the inputs for a single channel, there are eleven failure combinations of none, one and two failed LPRM strings. The RBM channel responses are evaluated separately at these eleven input failure conditions. Then, for each channel taken separately, the lowest response as a function of error rod position is chosen for comparison to the RBM setpoint.
2. The event is analyzed separately in each of the four quadrants of the core due to the differing LPRM string physical locations relative to the error rod.

Technical Specifications require that both RBM channels be operable during normal operation. Thus, the first channel calculated to intercept the RBM setpoint is assumed to stop the rod. To allow for control system delay times, the rod is assumed to move two inches after the intercept and stop at the following notch.

The analysis is performed using the three dimensional steady state SIMULATE core model [4]. Necessary properties of that model for use in this analysis are:

1. Accurate bundle power calculation as shown by the PDQ and gamma scan comparisons.

2. Accurate LPRM signal calculation as shown by the detailed TIP trace comparisons.
3. Accurate control rod worths and core power coefficient as shown by the consistent core eigenvalues.

Two separate cases are presented from numerous explicit SIMULATE analyses. The reactor conditions and case descriptions are shown in Figures 7.4.1 and 7.4.2. Case 1 analyzes the bounding event with the abnormal xenon condition at the most reactive point in the cycle for the given rod pattern configuration. The initial conditions for Case 2 approximate the 104.5% power conditions with an expected control rod pattern and equilibrium xenon. The  $\Delta$ CPR and MLHGR values for both cases are shown in Table 7.4.1. The  $\Delta$ CPR values are evaluated such that the implied operating limit MCPR equals  $1.07 + \Delta$ CPR. This is done by conserving the figure of merit ( $\Delta$ CPR/Initial CPR) shown by the SIMULATE calculations. The use of this method provides valid  $\Delta$ CPR values in the analysis of normal operating states where locations near the assumed error rod are not initially near the MCPR operating limit. Case 2 is the worst of all the rod withdrawal transients analyzed from 104.5% power, full flow and normal rod pattern conditions. Case 2 is bounded by Case 1 with substantial MCPR margin.

For Case 1; Figures 7.4.3 and 7.4.4 show the end of transient control rod position. This is determined from the point where the weakest RBM channel response first intercepts the RBM setpoint. For this same bounding case, the operating limit  $\Delta$ CPR envelope component versus Rod Block Monitor setpoint is taken from the Table 7.4.1. The same table demonstrates margin to the 1% plastic strain limit. The MLHGR values include the 2.2% power spiking penalty.

## 7.5 Misloaded Bundle Error Analysis Results

### 7.5.1 Rotated Bundle Error

The primary result of an assembly rotation is a large increase in local pin peaking and R-factor as higher enrichment pins are placed adjacent to the surrounding wide water gaps. In addition, there may be a small increase in reactivity, depending on the exposure and void fraction states. The R-factor

increase results in a CPR reduction, while the local pin peaking factor increase results in a higher pin linear heat generation rate. The objective of the analysis is to insure that in the worst possible rotation, the safety limit linear heat generation rate and CPR are not violated with the most limiting monitored bundles on their operating limits.

To analyze the CPR response, rotated bundle R-factors as a function of exposure are developed by adding the largest possible  $\Delta R$ -factor resulting from a rotation to the exposure dependent R-factors of the properly oriented bundles [13]. Using these rotated bundle R-factors, the MCPR values resulting from a bundle rotation are determined using SIMULATE. This is done for each control rod sequence throughout the cycle. These MCPR values are, in addition, modified slightly to account for the change in reactivity resulting from the rotation. For each sequence, the MCPR for the properly oriented assemblies is adjusted by a ratio necessary to place the corresponding rotated CPR on its 1.07 safety limit. The maximum of these adjusted MCPR's is the rotated bundle operating limit.

To determine the Maximum Linear Heat Generation Rate (MLHGR) resulting from a rotation, the ratios of the maximum rotated bundle local peaking factor to the maximum properly oriented bundle local peaking are determined for the expected range of exposure and void conditions. The maximum of this ratio is applied to the operating limit LHGR of 13.4 kw/ft. This maximum rotated bundle LHGR is in addition modified to account for the possible reactivity increase resulting from the rotation. It is also increased by the 2.2% power spiking penalty.

The results of the rotated bundle analysis are given in Table 7.5.1.

#### 7.5.2 Mislocated Bundle Error

Misloading a high reactivity assembly into a region of high neutron importance results in a location of high relative assembly average power. Since the assembly is assumed to be properly oriented (not rotated), R-factors used for the misloaded bundle are the standard values for the fuel type.

The analysis consists of an iterative procedure which successively eliminates potential misloading locations from any MCPR safety limit violations. The first step is to use SIMULATE to determine the largest possible  $\Delta$ CPR which could result, at any location, as the result of misloading a high reactivity assembly into the location. This maximum  $\Delta$ CPR is then subtracted from all the other bundle CPR's in the core. This is done at the various cycle exposures. Even with this maximum  $\Delta$ CPR applied, some locations will never exceed the MCPR safety limit of 1.07. These locations are eliminated from further investigation.

The next iteration consists of applying the same procedure to the locations which appeared to violate the safety limit when the maximum  $\Delta$ CPR from the first iteration was applied. Since these locations are of higher reactivity than those eliminated in the first iteration, they will result in a smaller  $\Delta$ CPR when misloaded. Using this smaller  $\Delta$ CPR, some of the remaining locations will be eliminated from potential CPR safety limit violations. This procedure is continued until all locations are shown to be above the MCPR safety limit due to a misloading, or until a limiting location is identified.

Using the above procedure, it has been demonstrated that for the Reload Cycle all possible mislocations result in calculated MCPR's above the 1.07 safety limit, assuming an initial operating CPR limit of 1.22. This makes the mislocated bundle analysis less limiting than the rotated bundle analysis.

#### 7.6 Control Rod Drop Accident Results

The control rod sequences are a series of rod withdrawal and banked withdrawal instructions specifically designed to minimize the worths of individual control rods. The sequences are examined so that, in the event of the uncoupling and subsequent free fall of the rod, the incremental rod worth is acceptable. Incremental worth refers to the fact that rods beyond Group 2 are banked out of the core and can only fall the increment from all in to the rod drive withdrawal position. Acceptable worth is one which produces a maximum fuel enthalpy less than 280 calories/gram.

Some out-of-sequence control rods could accrue potentially high worths. However, the Rod Worth Minimizer (RWM) will prevent withdrawing an



out-of-sequence rod if accidentally selected. The RWM is functionally tested before each startup.

The sequence entered into the RWM will take the plant from All Rods In (ARI) to well above 20% core thermal power. Above 20% power even multiple operator errors will not create a potential rod drop situation above 280 calories per gram [18, 19]. Below 20% power, however, the sequences must be examined for incremental rod worth. This is done using the full core, xenon free SIMULATE model at the projected most reactive point in the cycle. This assures that the maximum amount of reactivity is held in the rods.

Both the A and B sequences were examined. It was found that the highest worth occurred in the first rod pull of the second group. Any of the first four rod arrays shown in Figures 7.6.1 and 7.6.2 may be designated as the first group pulled. But, then a specific second group must follow as Table 7.6.1 illustrates. For added conservatism, the highest worth rod in the second group was deliberately assigned to be the first rod pulled. This assures that in any sequence followed at the plant, the worths will always be less than those calculated here. The results of the calculations are presented in Table 7.6.2.

Beyond Group 2, procedures [20] apply which severely reduce the rod incremental worths. This makes the xenon free, hot standby worths much less than the cold, xenon free worths as demonstrated in Reference 10.

## 7.7 Stability Analysis Results

The analysis of reactor stability has been performed by General Electric as described in Section S.2.4 of Reference 3. The 105% power rod line was analyzed and the resultant decay ratio as a function of reactor power level is provided in Figure 7.7.1.

The reactor core stability decay ratio is calculated at natural circulation conditions and a power level corresponding to the 105% power rod line. The calculated core stability decay ratio and the channel hydrodynamic performance decay ratio is given in Table 7.7.1.



TABLE 7.1.1

VY CYCLE 11 SUMMARY OF SYSTEM TRANSIENT MODEL  
INITIAL CONDITIONS FOR CORE WIDE TRANSIENT ANALYSES

Core Thermal Power (MWth)	1664.0
Turbine Steam Flow (% NBR)	105
Total Core Flow ( $10^6$ lbm/hr)	48.0
Core Bypass Flow ( $10^6$ lbm/hr)	5.3
Core Inlet Enthalpy (BTU/lbm)	520.9
Steam Dome Pressure (psia)	1034.7
Turbine Inlet Pressure (psia)	986.0
Total Recirculation Flow ( $10^6$ lbm/hr)	23.4
Core Plate Differential Pressure (psi)	18.5
Narrow Range Water Level (in.)	35
Average Fuel Gap Conductance	(See Section 4.2)

TABLE 7.1.2

## VY CYCLE 11 TRANSIENT ANALYSIS REACTIVITY COEFFICIENTS AT SELECTED CONDITIONS

Calculated Parameter	Cycle Exposure Point (MWD/ST)			
	EOFPL	EOFPL-1000	EOFPL-2000	BOC
Axial Shape Index <sup>(1)</sup>	-0.0805	-0.1854	-0.1938	-0.0760
Moderator Density Coefficient (Subcooling), $\beta/\Delta u$ <sup>(2)</sup> Pressure = 1050 psia Subcooling = 30 BTU/lbm	20.75	20.64	26.04	20.13
Moderator Density Coefficient (Pressurization), $\beta/\Delta u$ Pressure = 1050 psia Inlet Enthalpy = 520 BTU/lbm	23.12	22.10	28.69	(3)
Fuel Temperature Coefficient at 1130°F, $\beta/^\circ\text{F}$	-0.278	-0.277	-0.276	-0.259
Effective Delayed Neutron Fraction	0.005400	0.005494	0.005547	0.005958
Prompt Neutron Generation Time in Microseconds	42.64	42.52	41.90	39.65

Notes: (1) Axial Shape Index (ASI) =  $\frac{P_T - P_B}{P_T + P_B}$

(2)  $\Delta u$  = change in density, in percent

(3) Pressurization transients are not calculated at BOC

TABLE 7.2.1

VY CYCLE 11 CORE WIDE TRANSIENT ANALYSIS RESULTS

<u>Transient</u>	<u>Exposure</u>	Peak Prompt Power (Fraction of Initial Value)	Peak Avg. Heat Flux (Fraction of Initial Value)	<u><math>\Delta</math>CPR P8X8R</u>
Turbine Trip Without Bypass, "Measured" Scram Time	EOFPL	2.936	1.186	.19
	EOFPL-1000	2.097	1.108	.13
	EOFPL-2000	1.007	1.000	.00
Turbine Trip Without Bypass, "67B" Scram Time	EOFPL	3.466	1.236	.25
	EOFPL-1000	2.574	1.189	.20
	EOFPL-2000	1.433	1.007	.01
Generator Load Rejection Without Bypass, "Measured" Scram Time	EOFPL	2.802	1.168	.19
	EOFPL-1000	2.008	1.094	.11
	EOFPL-2000	1.000	1.000	.00
Generator Load Rejection Without Bypass, "67B" Scram Time	EOFPL	3.405	1.227	.26
	EOFPL-1000	2.590	1.193	.20
	EOFPL-2000	1.310	1.000	.00
Loss of 100°F Feedwater Heating	EOFPL	1.203	1.196	.16
	EOFPL-1000	1.216	1.208	.17
	EOFPL-2000	1.221	1.213	.18
	BOC	1.199	1.191	.15

TABLE 7.3.1

VY CYCLE 11 OVERPRESSURIZATION ANALYSIS RESULTS

<u>Conditions</u>	<u>Maximum Pressure at Reactor Vessel Bottom (psig)</u>
"Measured" Scram Time	1281
"67B" Scram Time	1306

TABLE 7.4.1

VY CYCLE 11 ROD WITHDRAWAL ERROR TRANSIENT SUMMARY  
WITH LIMITING INSTRUMENT FAILURE

Case 1  
Conditions in Figure 7.4.1

<u>RBM Setpoint</u>	<u>Rod Position</u>	<u>ΔCPR P8X8R</u>	<u>MLHGR (kw/ft) P8X8R</u>
104	10	.12	15.4
105	10	.12	15.4
106	12	.16	16.4
107	12	.16	16.4
108	18	.22	17.8

Case 2  
Conditions in Figure 7.4.2

<u>RBM Setpoint</u>	<u>Rod Position</u>	<u>ΔCPR P8X8R</u>	<u>MLHGR (kw/ft)* P8X8R</u>
104	30	.08	13.1
105	38	.11	14.1
106	40	.11	14.4
107	42	.12	14.6
108	44	.12	14.7

\* Not initially on limits

TABLE 7.5.1

VY CYCLE 11 ROTATED BUNDLE ANALYSIS RESULTS

<u>Initial MCPR</u>	<u>Resulting MCPR</u>	<u>Resulting LHGR (kw/ft)</u>
1.24	1.07	17.46

TABLE 7.6.1

CONTROL ROD DROP ANALYSIS - ROD ARRAY PULL ORDER

The order in which rod arrays are pulled is specific once the choice of first group is made.

<u>First Group Pulled is:</u>	<u>Second Group Pulled Must Be:</u>	<u>Successive Group Is Banked Out</u>
Array 1	Array 2	Array 3 or 4
Array 2	Array 1	Array 3 or 4
Array 3	Array 4	Array 1 or 2
Array 4	Array 3	Array 1 or 2

TABLE 7.6.2

VY CYCLE 11 CONTROL ROD DROP ANALYSIS RESULTS

Maximum Incremental Rod Worth Calculated Cold, Xenon Free	.83% $\Delta K$
Bounding Analysis Worth for Enthalpy Less than 280 Calories per Gram (References 18, 19 and 20)	1.30% $\Delta K$

TABLE 7.7.1VY CYCLE 11 STABILITY ANALYSIS RESULTS

	<u>Decay Ratio</u>
Reactor Total Core Stability	.83
Channel Hydrodynamic Performance	.30



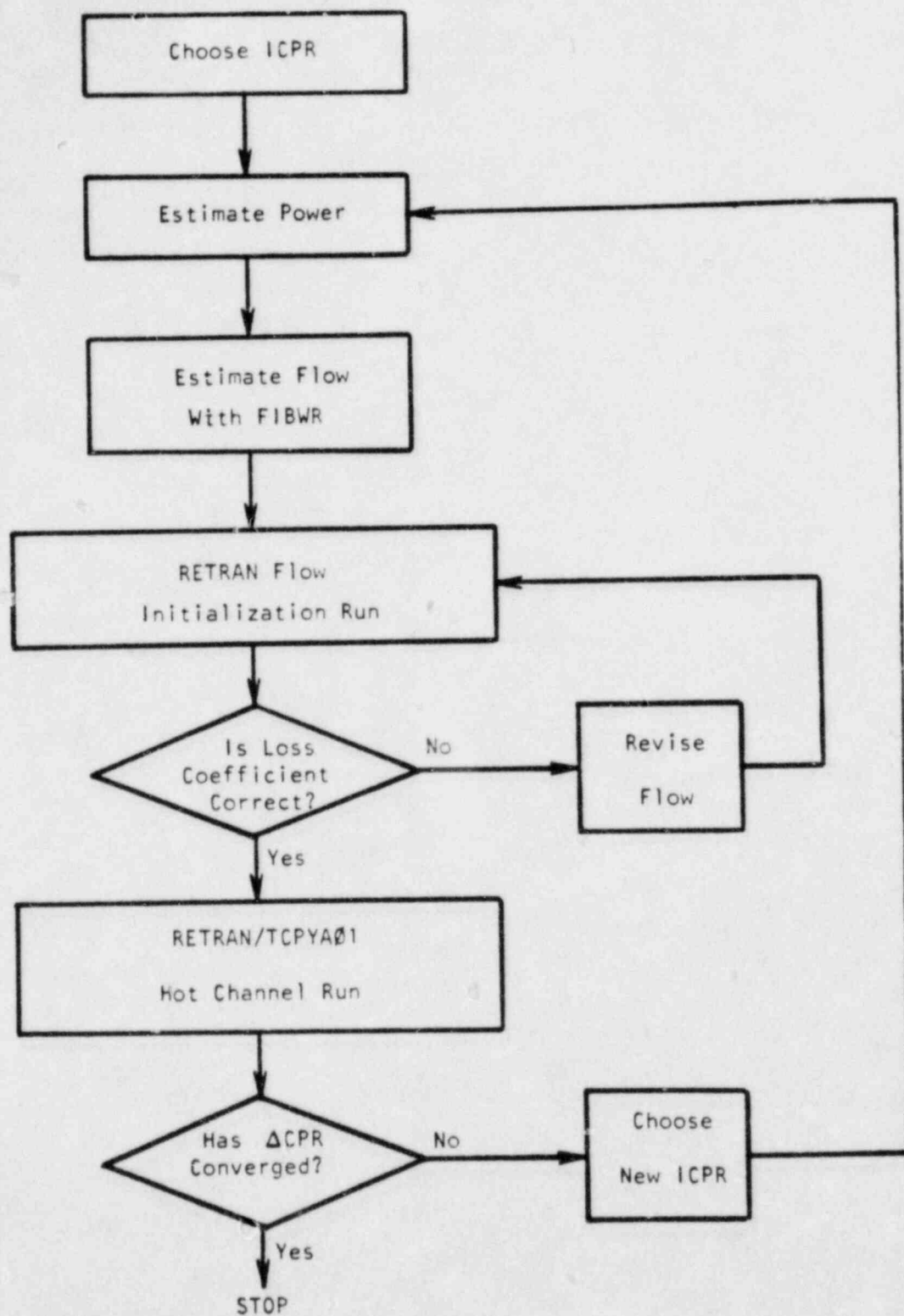


FIGURE 7.1.1

FLOW CHART FOR THE CALCULATION OF  $\Delta\text{CPR}$  USING THE RETRAN/TCPYA01 CODES

VY CYCLE 11 - MST, EOFPL

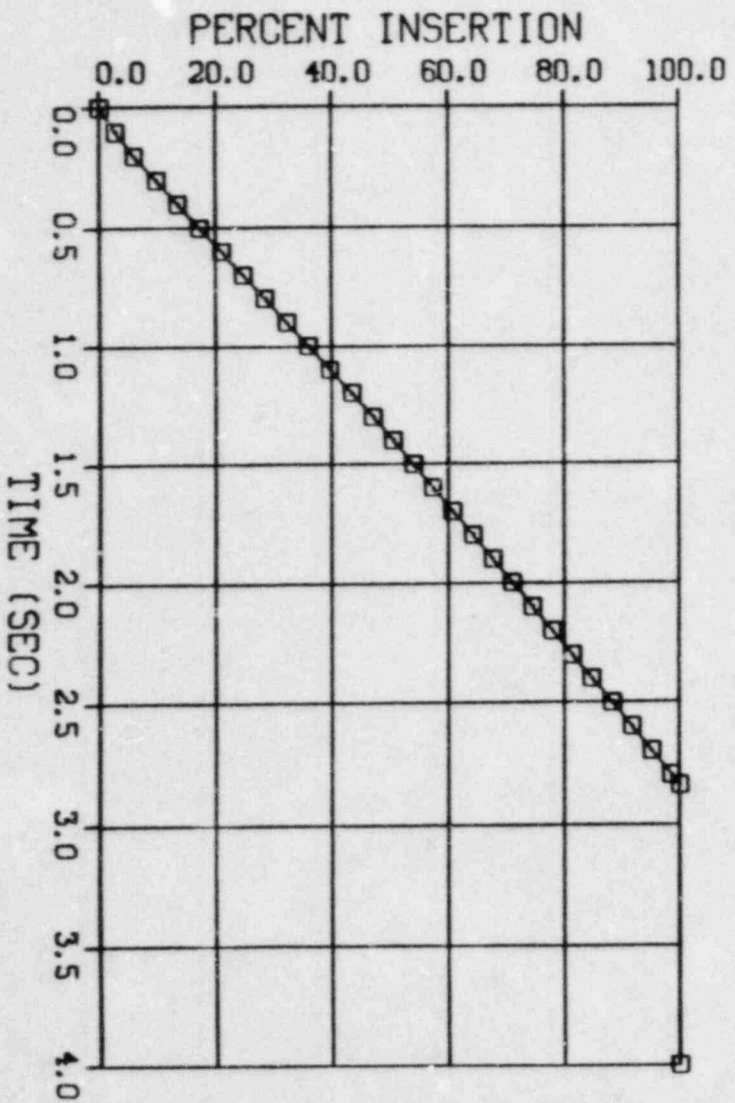
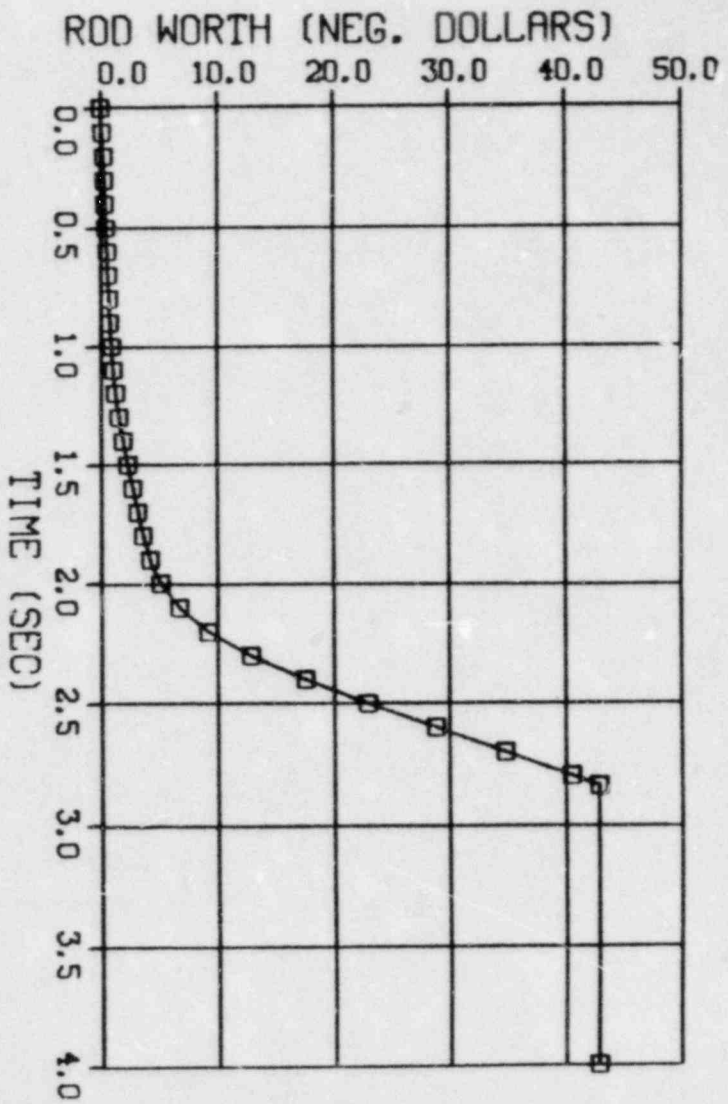


FIGURE 7.1.2

INSERTED ROD NORTH AND ROD POSITION VERSUS TIME FROM  
INITIAL ROD MOVEMENT AT EOFPL11, "MEASURED" SCRAM TIME

VY CYCLE 11 - MST, EOFPL-1000

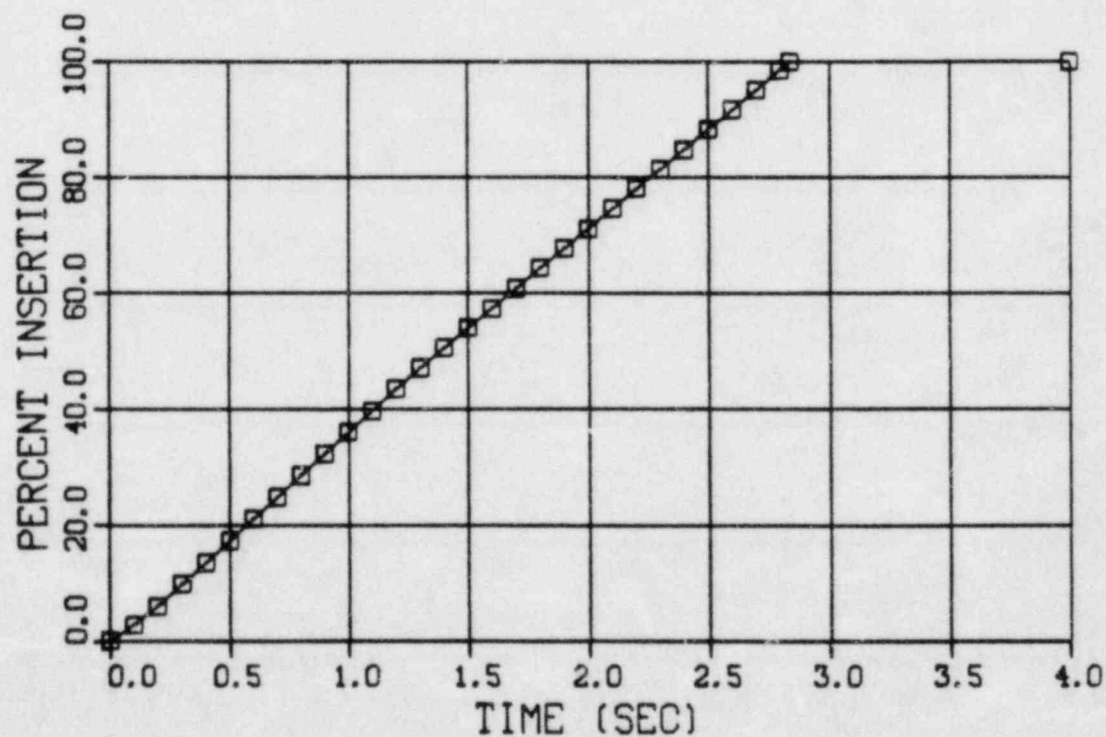
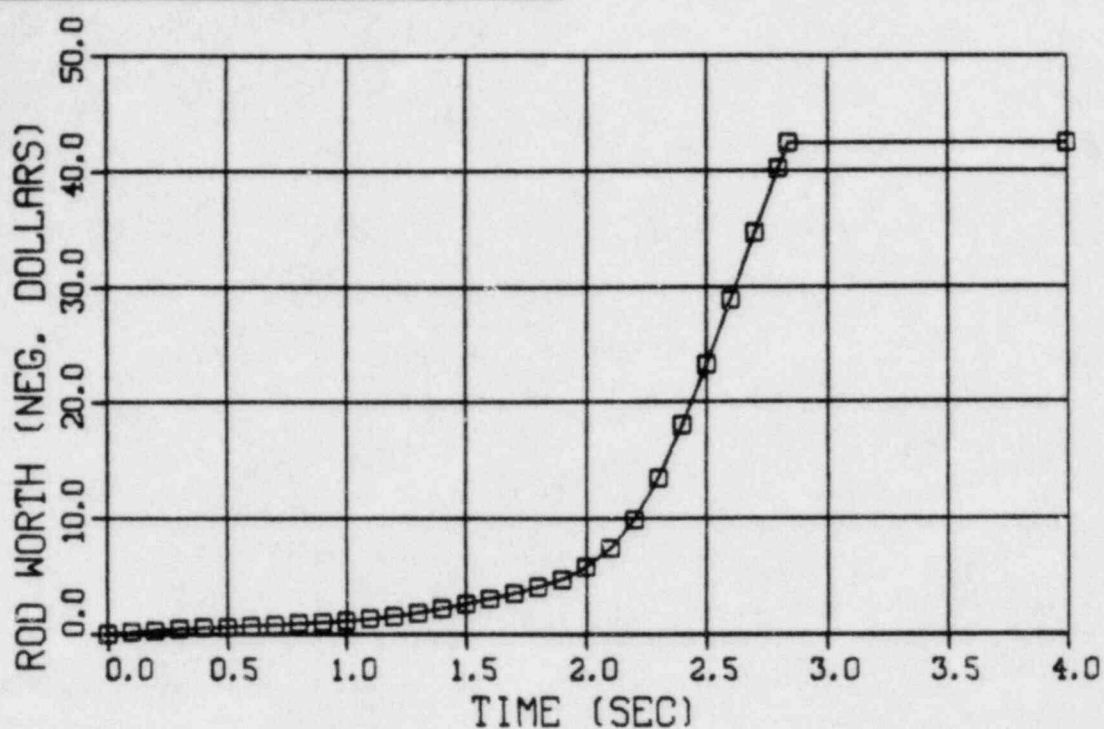


FIGURE 7.1.3

INSERTED ROD WORTH AND ROD POSITION VERSUS TIME FROM INITIAL ROD  
MOVEMENT AT EOFPL11-1000 MWD/ST, "MEASURED" SCRAM TIME

VY CYCLE 11 - MST, EOFPL-2000

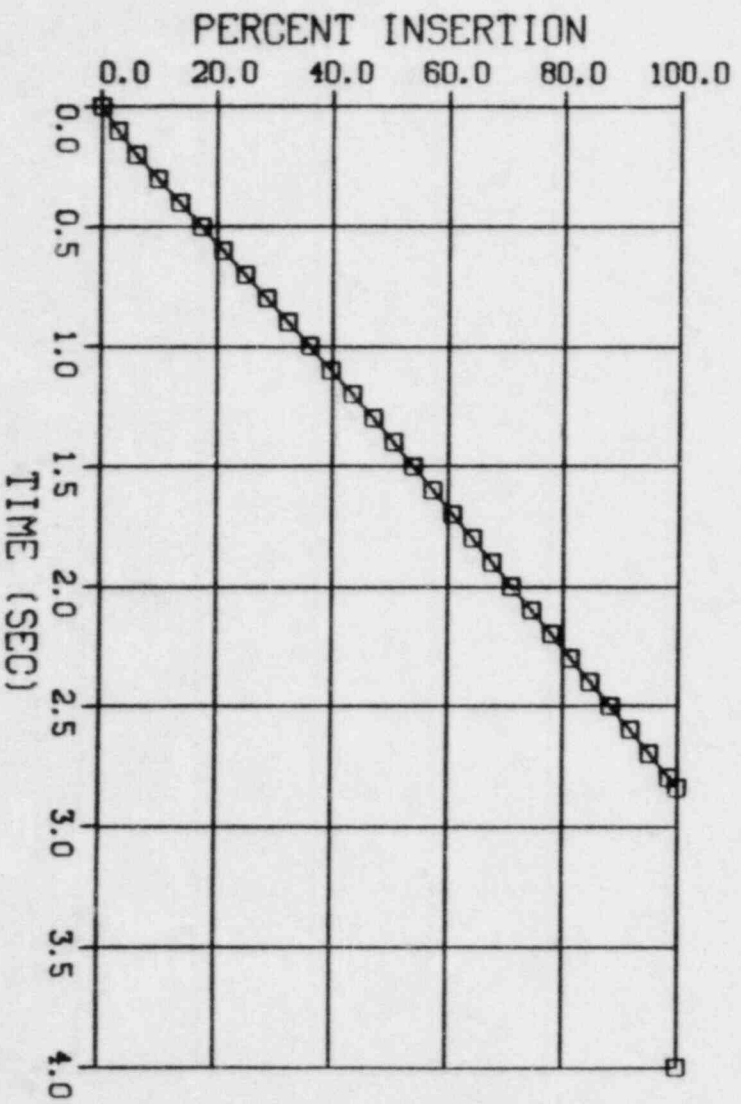
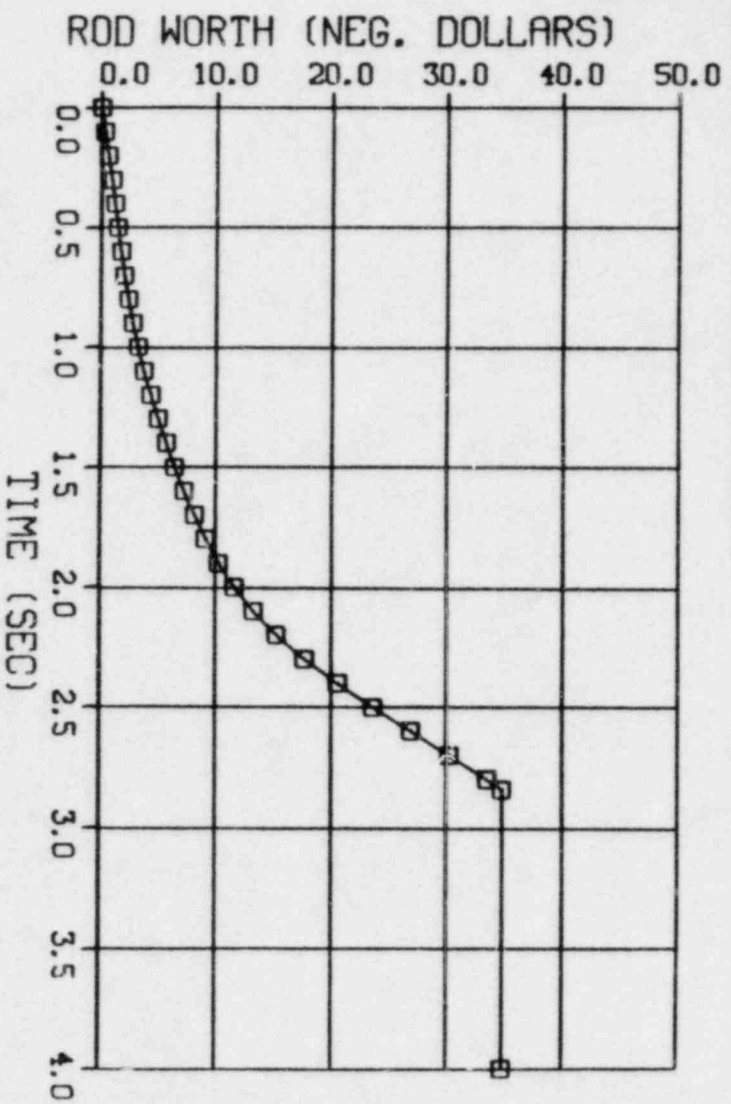


FIGURE 7.1.4

INSERTED ROD WORTH AND ROD POSITION VERSUS TIME FROM INITIAL ROD  
MOVEMENT AT EOFPL1-2000 MWD/ST, "MEASURED" SCRAM TIME

VY CYCLE 11 - 67B SCRAM, EOFPL

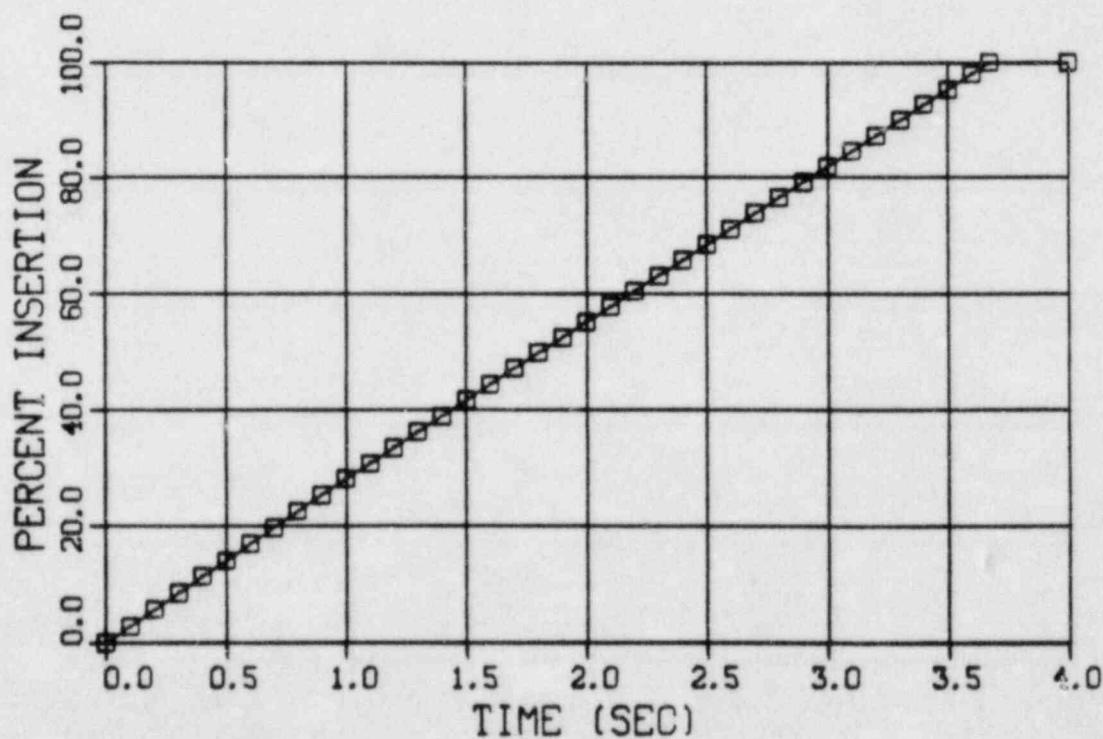
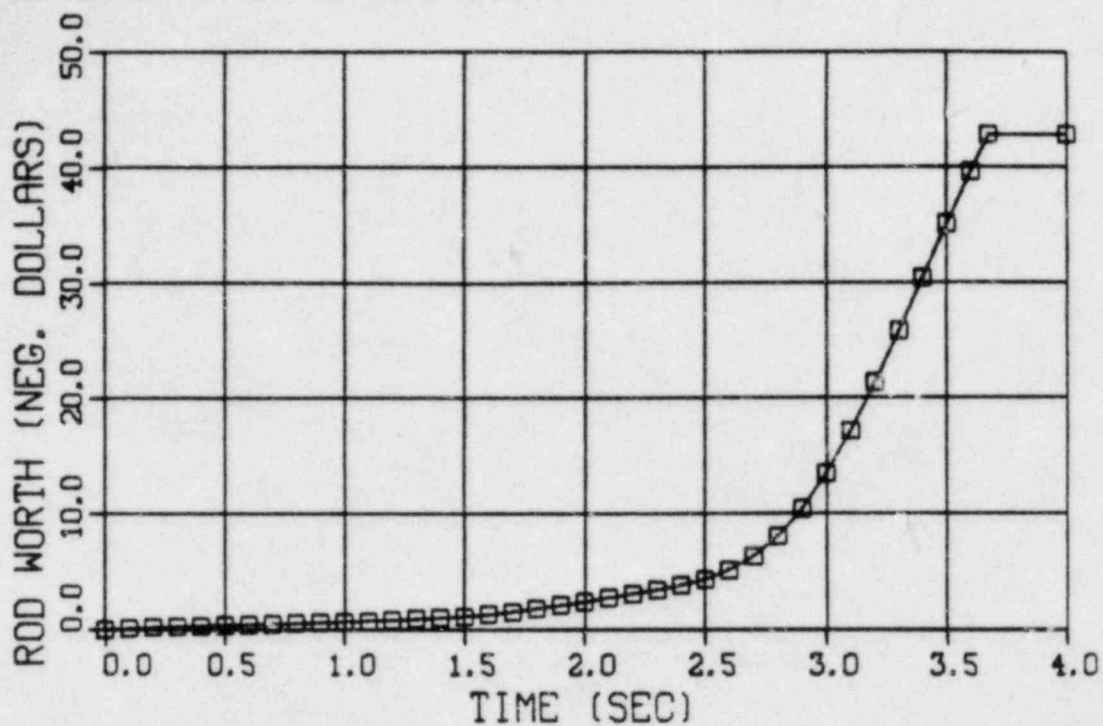


FIGURE 7.1.5

INSERTED ROD WORTH AND ROD POSITION VERSUS TIME FROM  
INITIAL ROD MOVEMENT AT EOFPL11, "67B" SCRAM TIME



VY CYCLE 11 - 67B SCRAM, EOFPL-1000

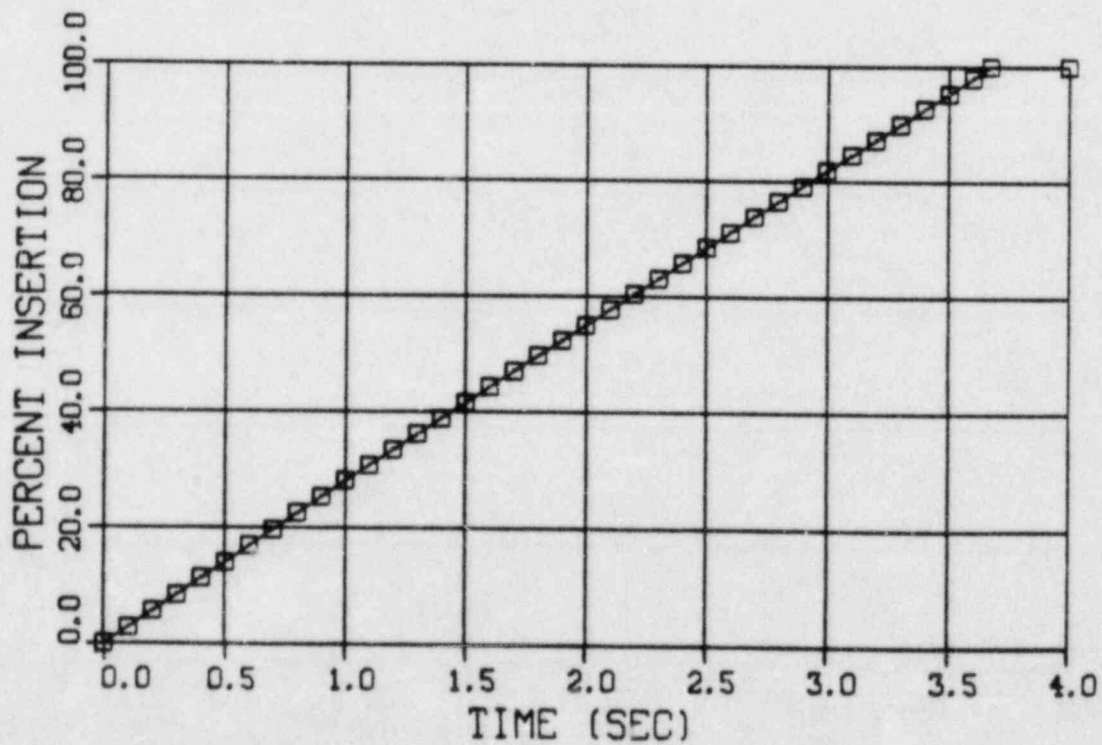
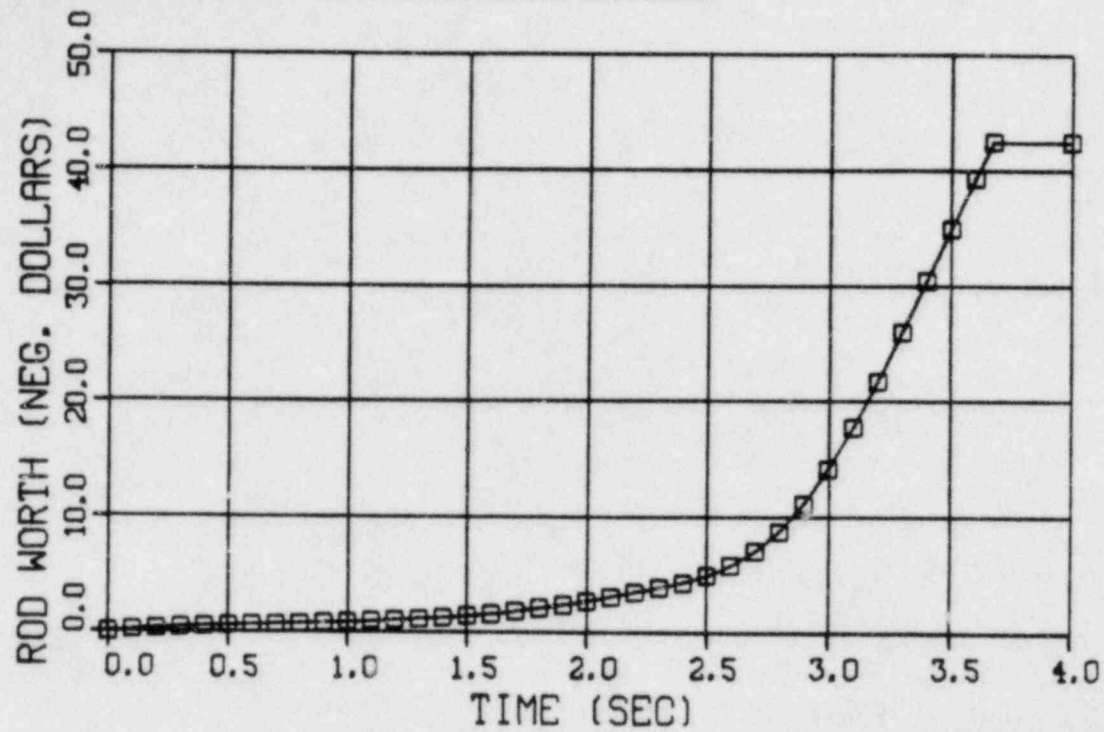


FIGURE 7.1.6

INSERTED ROD WORTH AND ROD POSITION VERSUS TIME FROM INITIAL ROD  
MOVEMENT AT EOFPL11-1000 MWD/ST, "67B" SCRAM TIME

VY CYCLE 11 - 67B SCRAM, EOFPL-2000

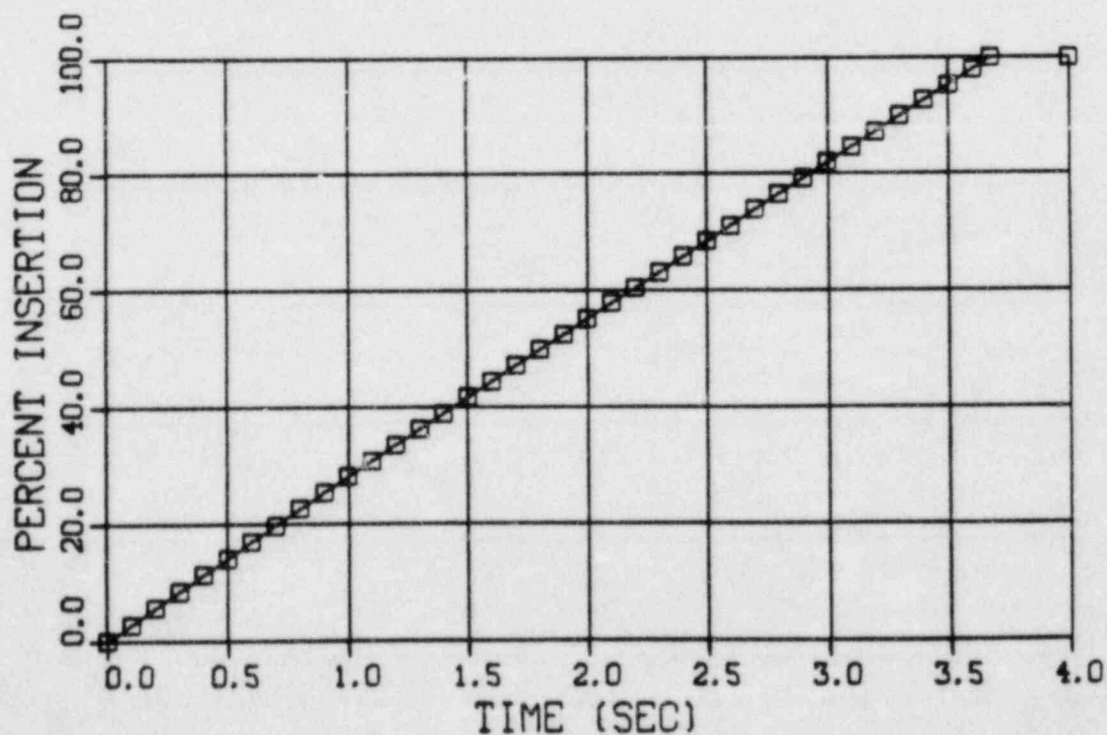
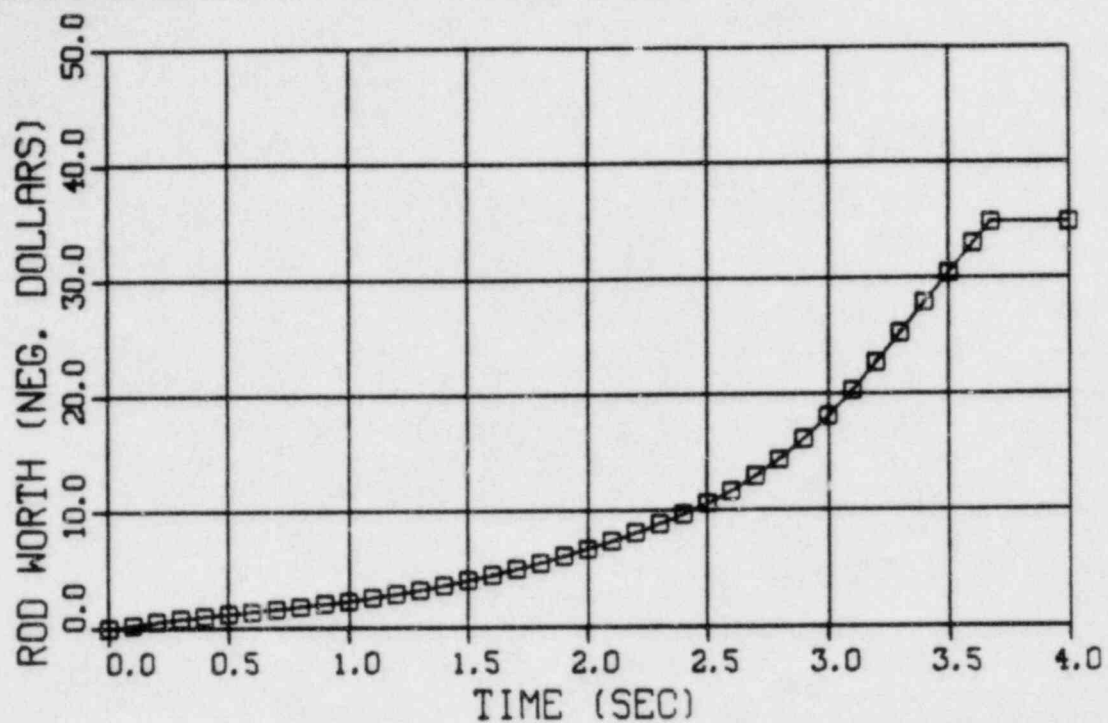


FIGURE 7.1.7

INSERTED ROD WORTH AND ROD POSITION VERSUS TIME FROM INITIAL ROD  
MOVEMENT AT EOFPL11-2000 MWD/ST, "67B" SCRAM TIME

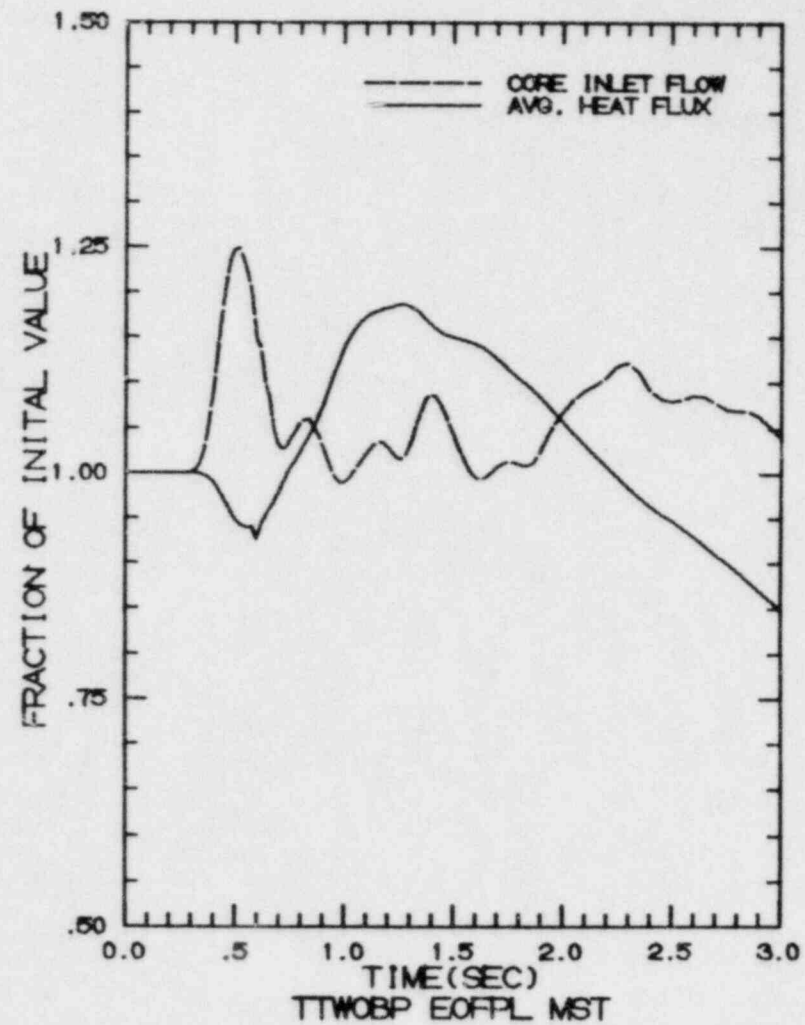
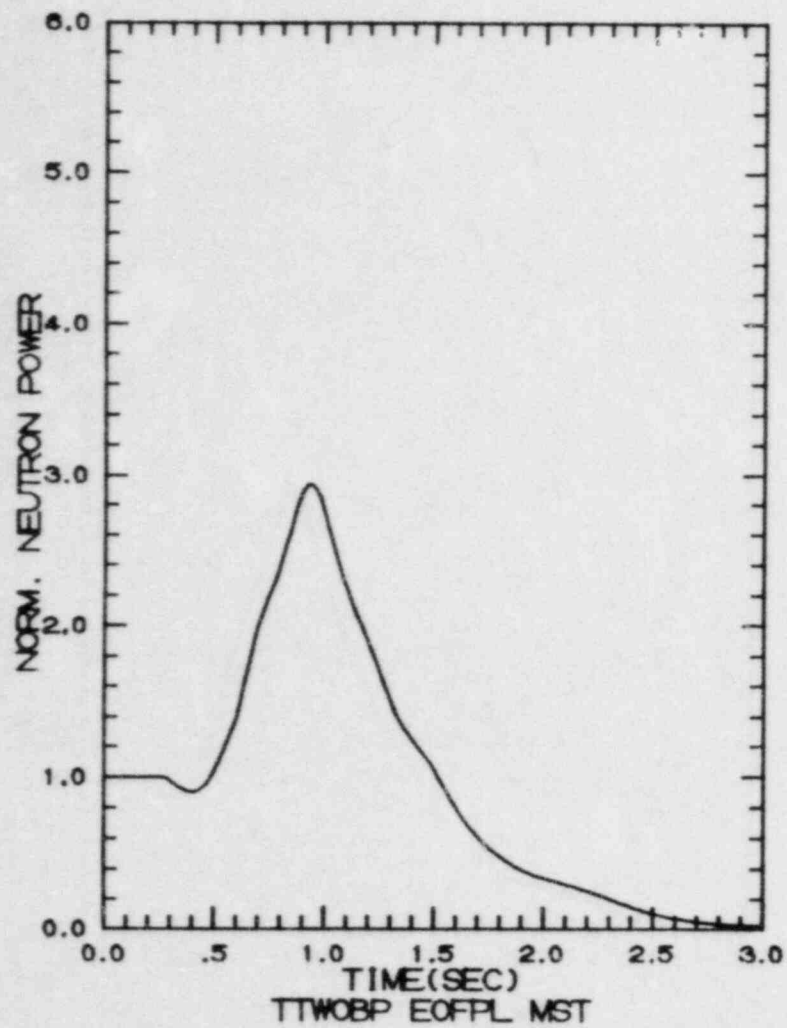


FIGURE 7.2.1-1

TURBINE TRIP WITHOUT BYPASS, EOFPL11  
TRANSIENT RESPONSE VERSUS TIME. "MEASURED" SCRAM TIME

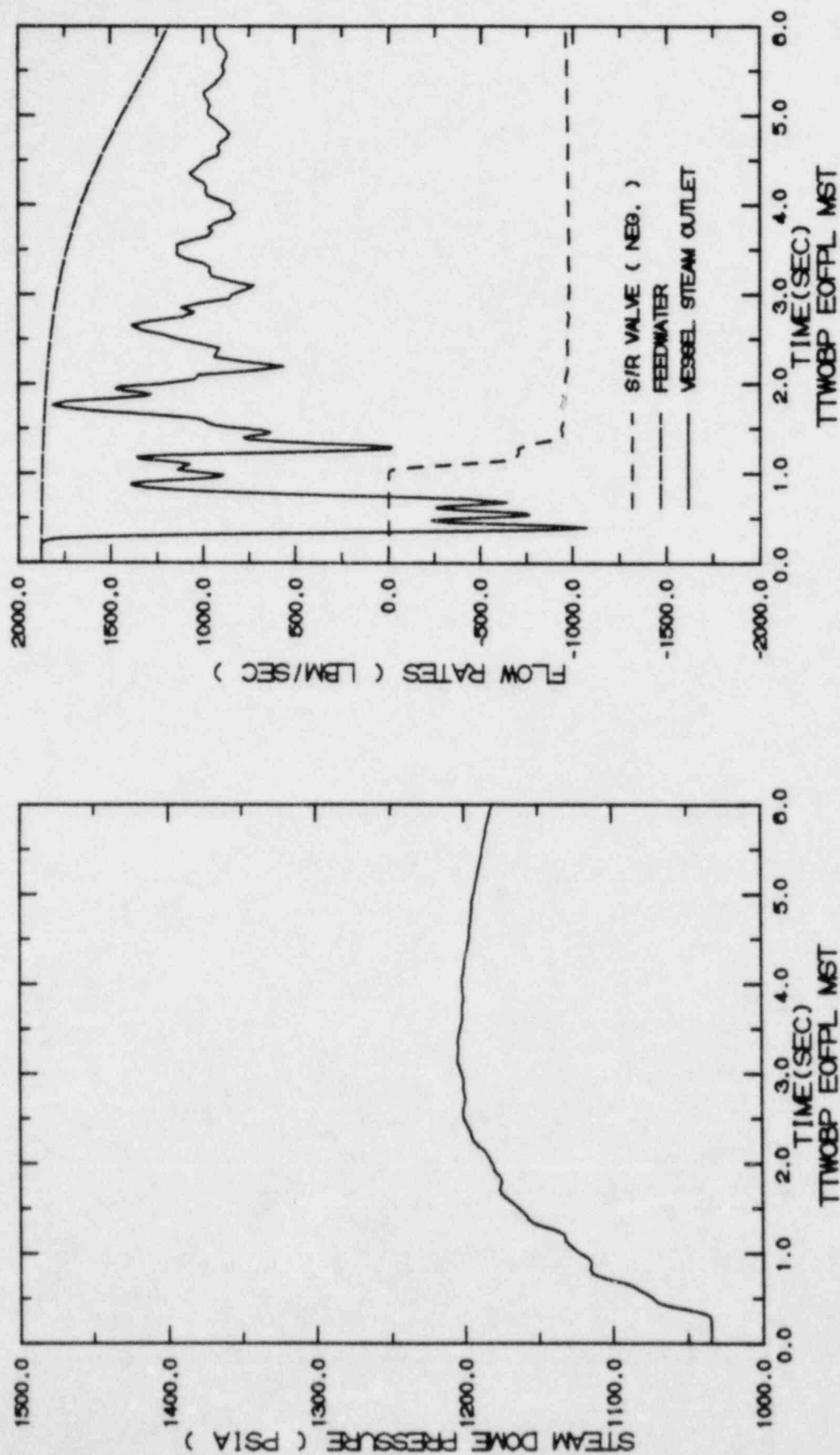


FIGURE 7.2.1-2  
 TURBINE TRIP WITHOUT BYPASS, EOFPL11  
 TRANSIENT RESPONSE VERSUS TIME, "MEASURED" SCRAM TIME

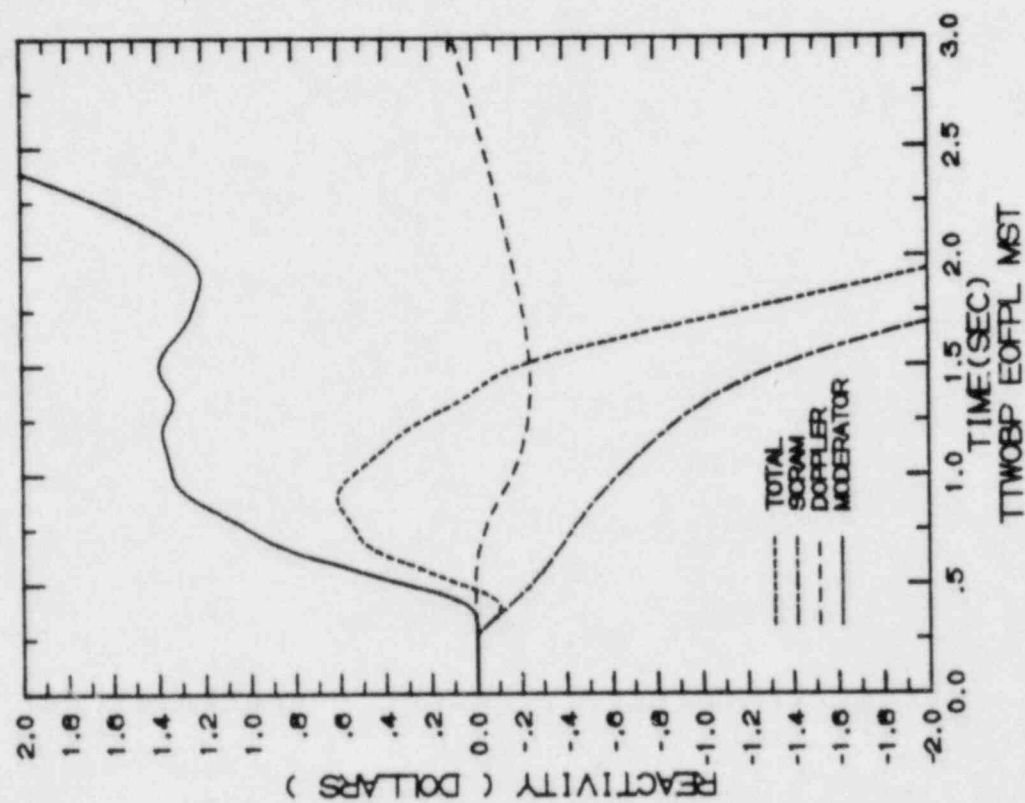


FIGURE 7.2.1-3

TURBINE TRIP WITHOUT BYPASS, EOFPL11  
TRANSIENT RESPONSE VERSUS TIME, "MEASURED" SCRAM TIME



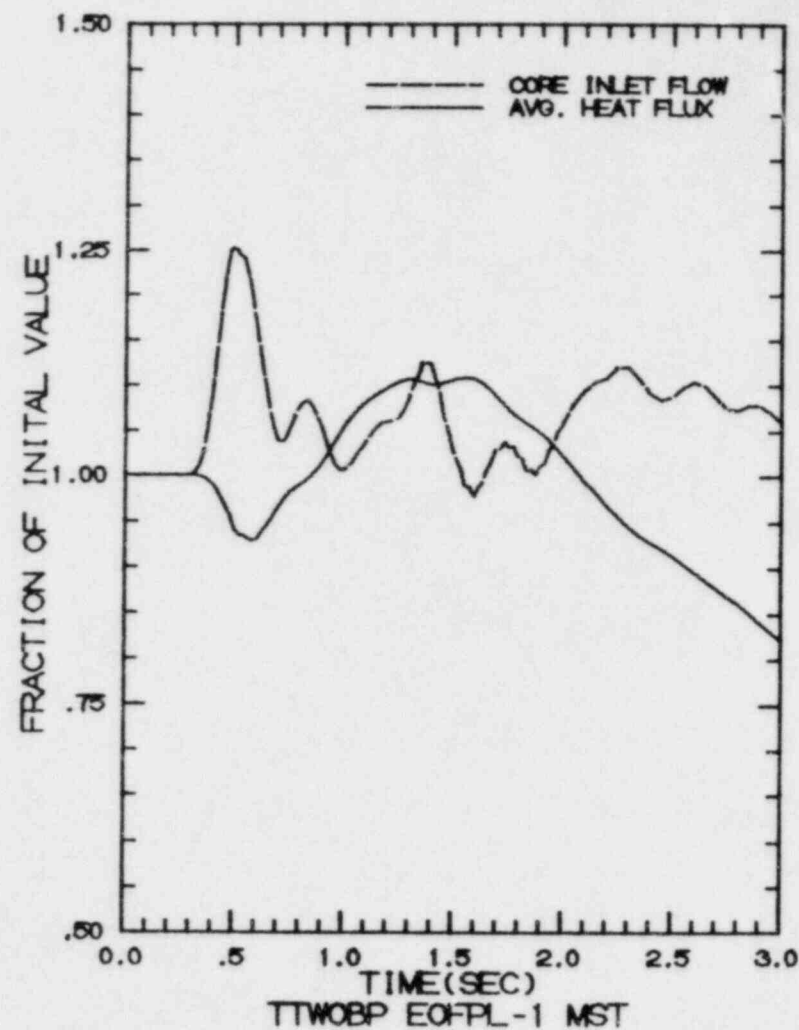
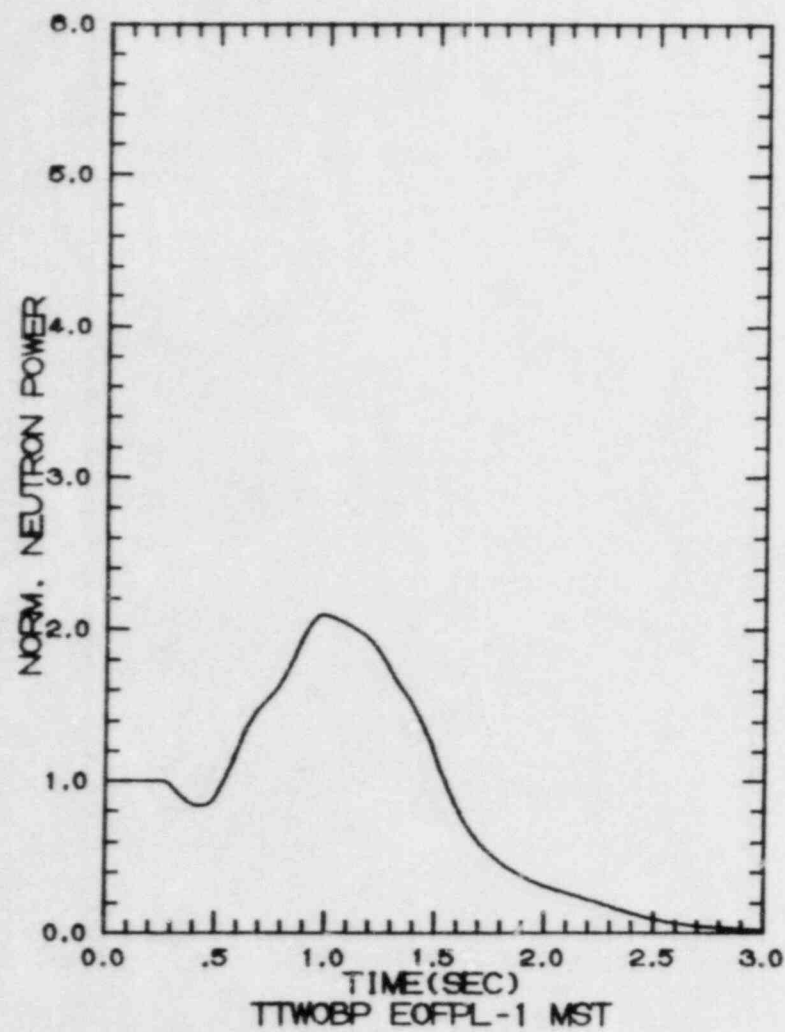


FIGURE 7.2.2-1

TURBINE TRIP WITHOUT BYPASS, EOFPL11-1000 MWD/ST  
TRANSIENT RESPONSE VERSUS TIME, "MEASURED" SCRAM TIME

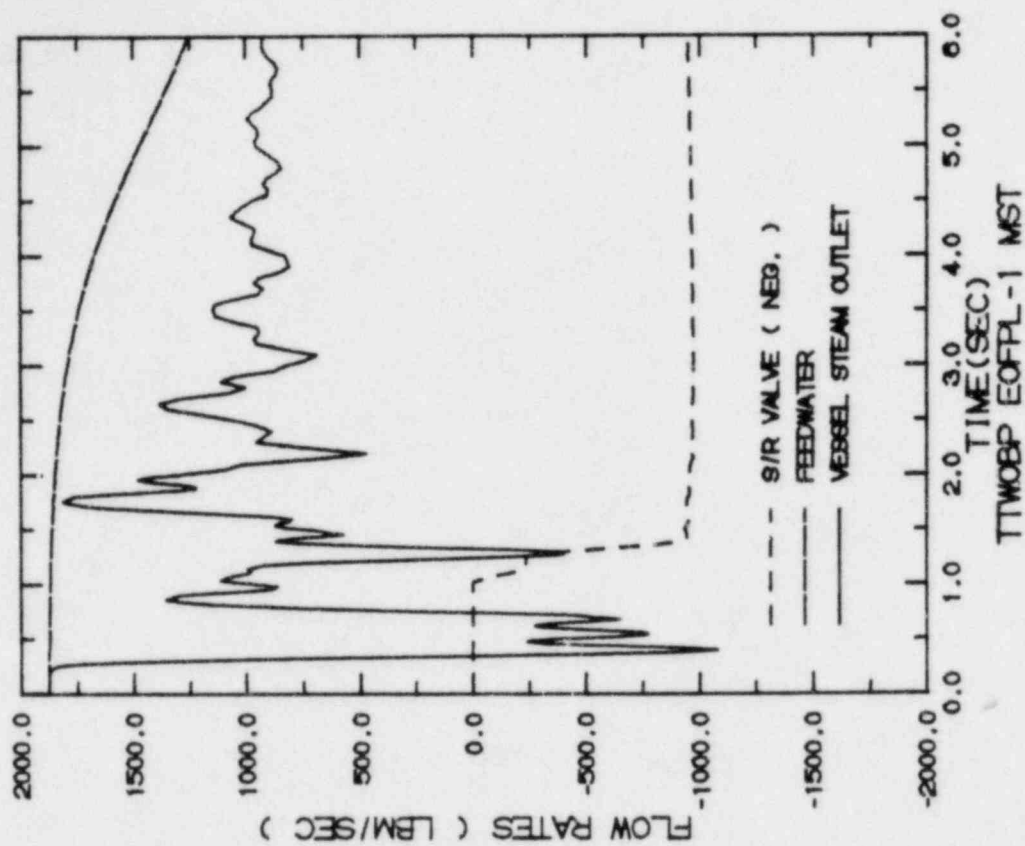
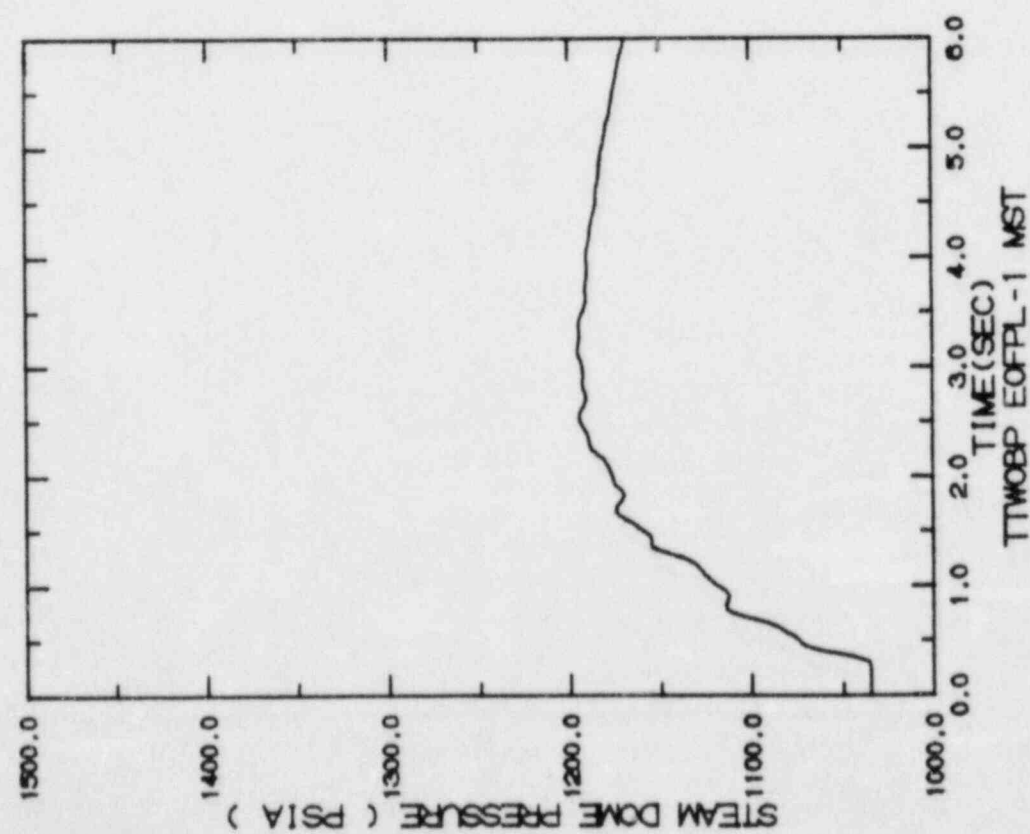


FIGURE 7.2.2-2

TURBINE TRIP WITHOUT BYPASS, EOFPL1-1000 MWD/ST

TRANSIENT RESPONSE VERSUS TIME, "MEASURED" SCRAM TIME

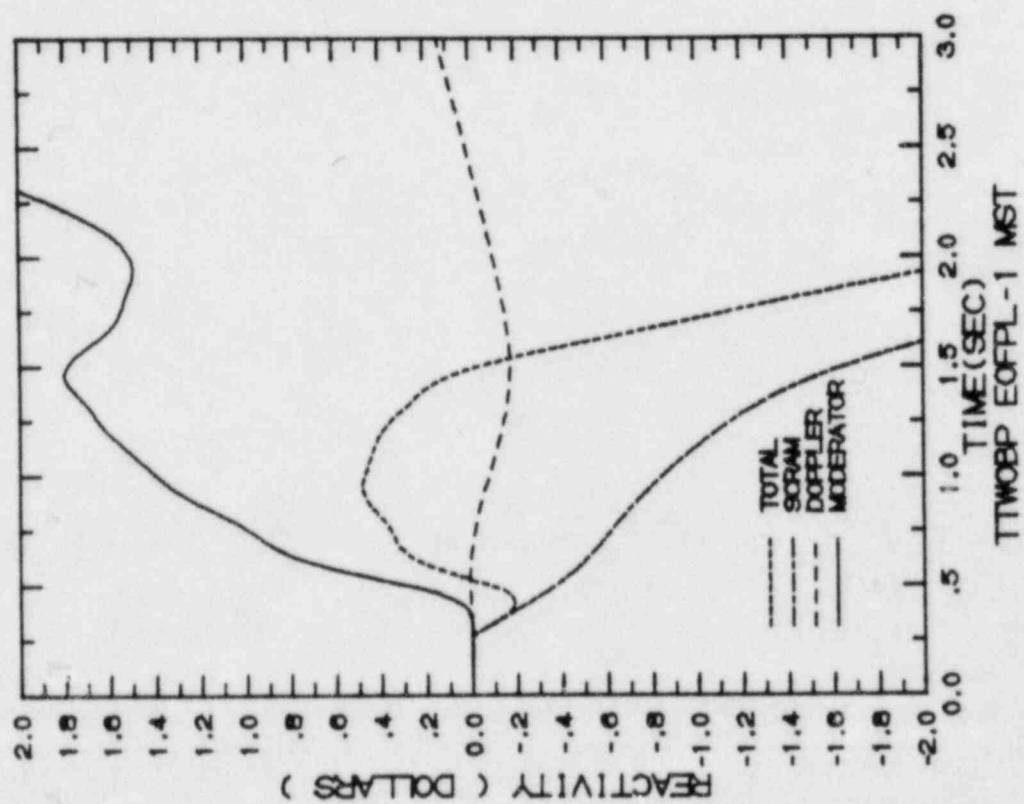


FIGURE 7.2.2-3

TURBINE TRIP WITHOUT BYPASS, EOPPL1-1000 MWD/ST  
TRANSIENT RESPONSE VERSUS TIME, "MEASURED" SCRAM TIME

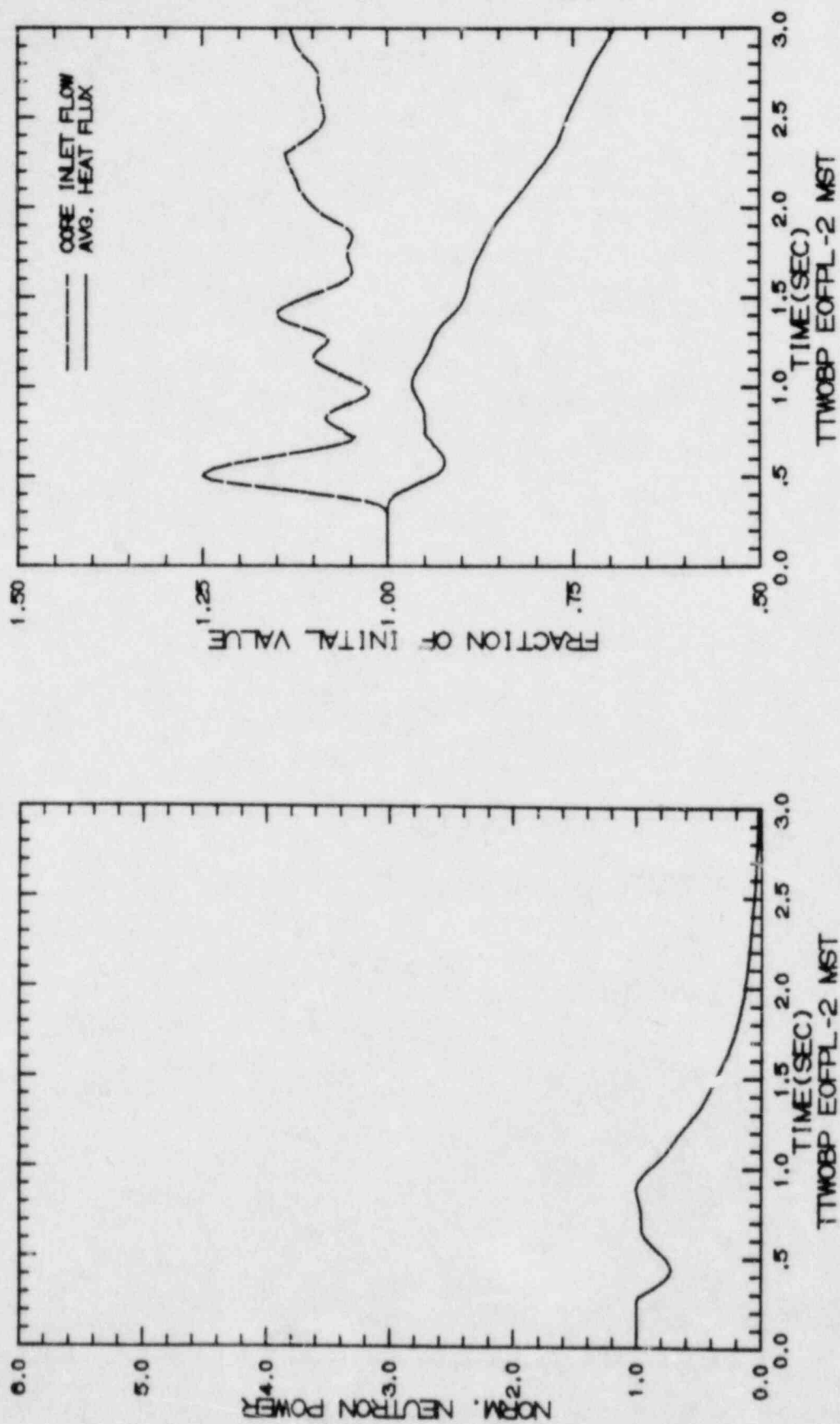


FIGURE 7.2.3-1

TURBINE TRIP WITHOUT BYPASS, EOFPL11-2000 MWD/ST  
TRANSIENT RESPONSE VERSUS TIME, "MEASURED" SCRAM TIME



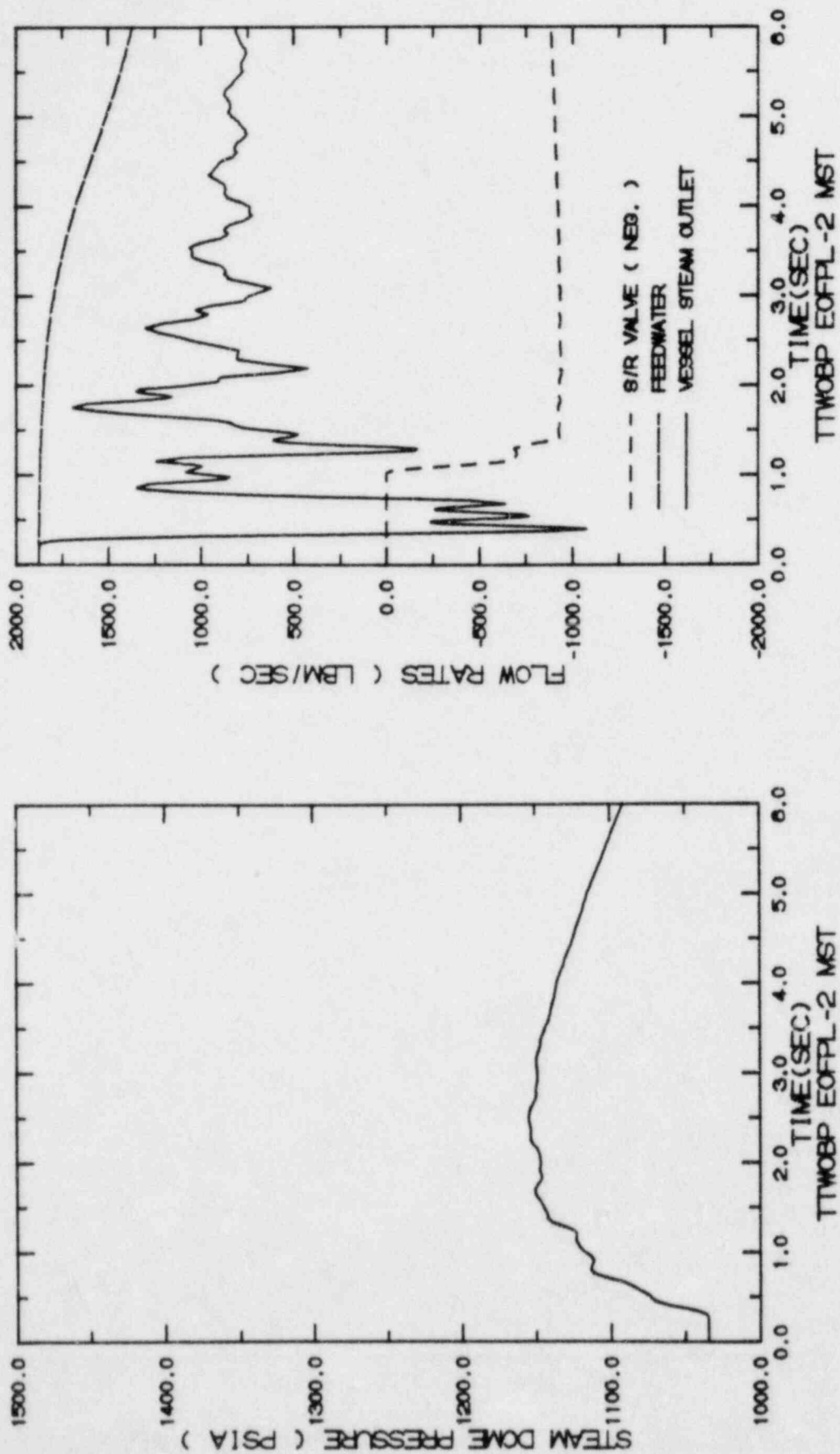


FIGURE 7.2.3-2  
 TURBINE TRIP WITHOUT BYPASS, EOFPL11-2000 MWD/ST  
 TRANSIENT RESPONSE VERSUS TIME, "MEASURED" SCRAM TIME

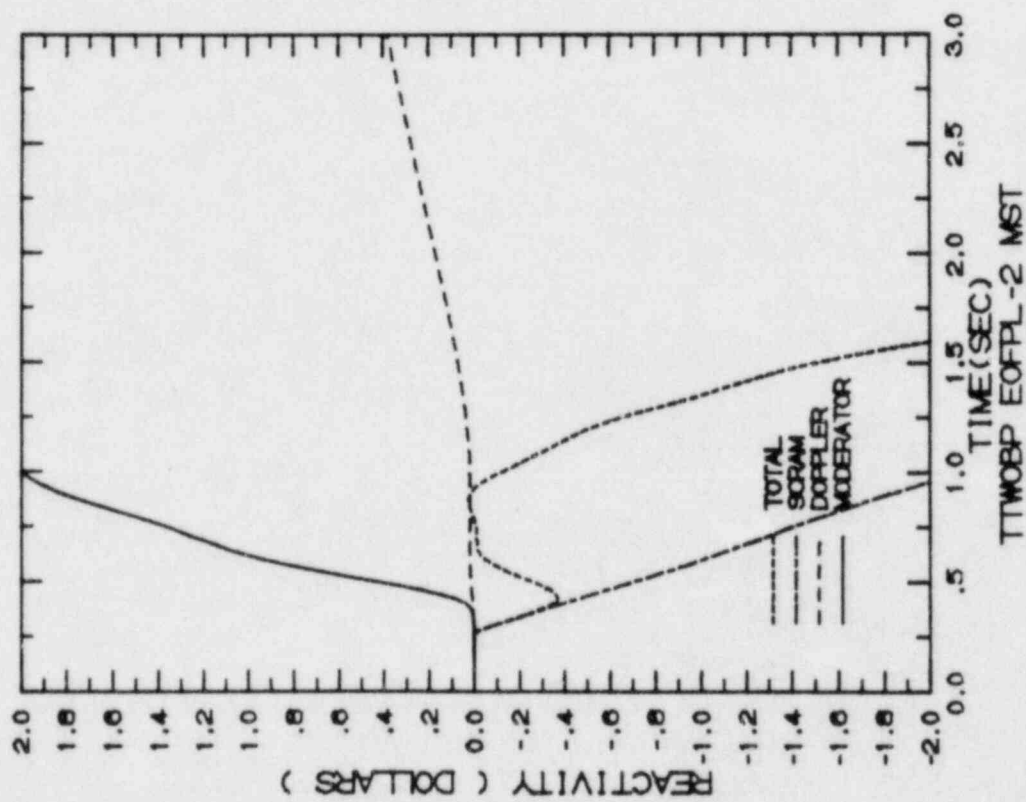


FIGURE 7.2.3-3

TURBINE TRIP WITHOUT BYPASS, EOFPL11-2000 MWD/ST  
TRANSIENT RESPONSE VERSUS TIME, "MEASURED" SCRAM TIME

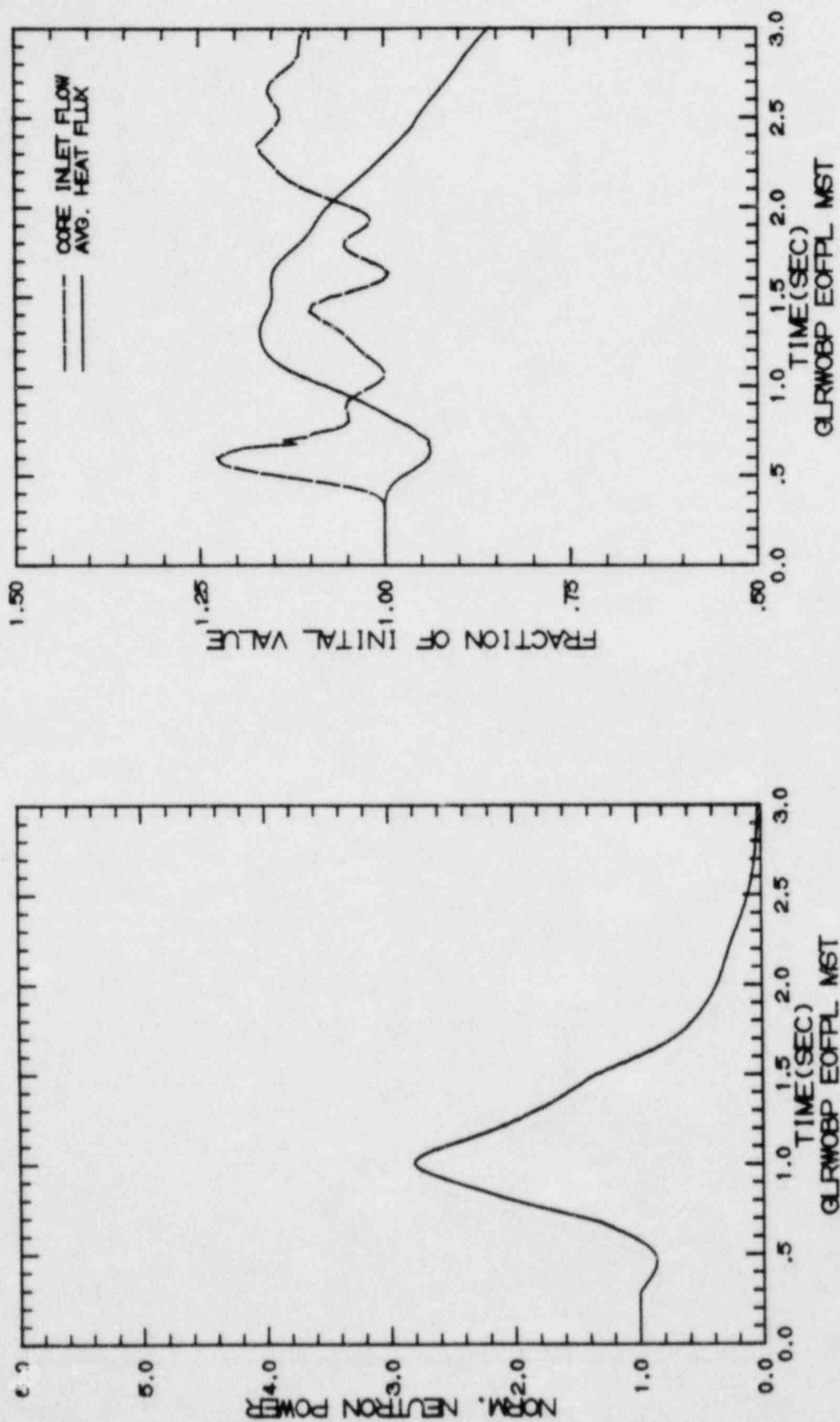


FIGURE 7.2.4-1

GENERATOR LOAD REJECTION WITHOUT BYPASS, EOFPL11  
TRANSIENT RESPONSE VERSUS TIME, "MEASURED" SCRAM TIME

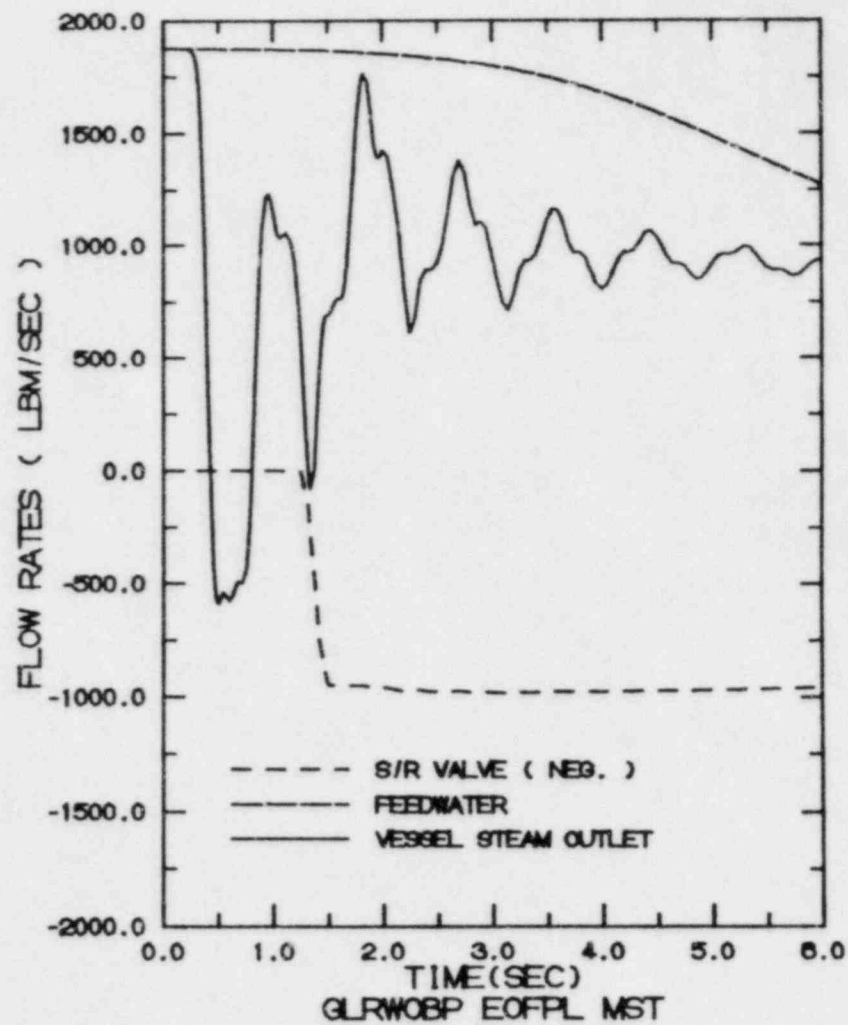
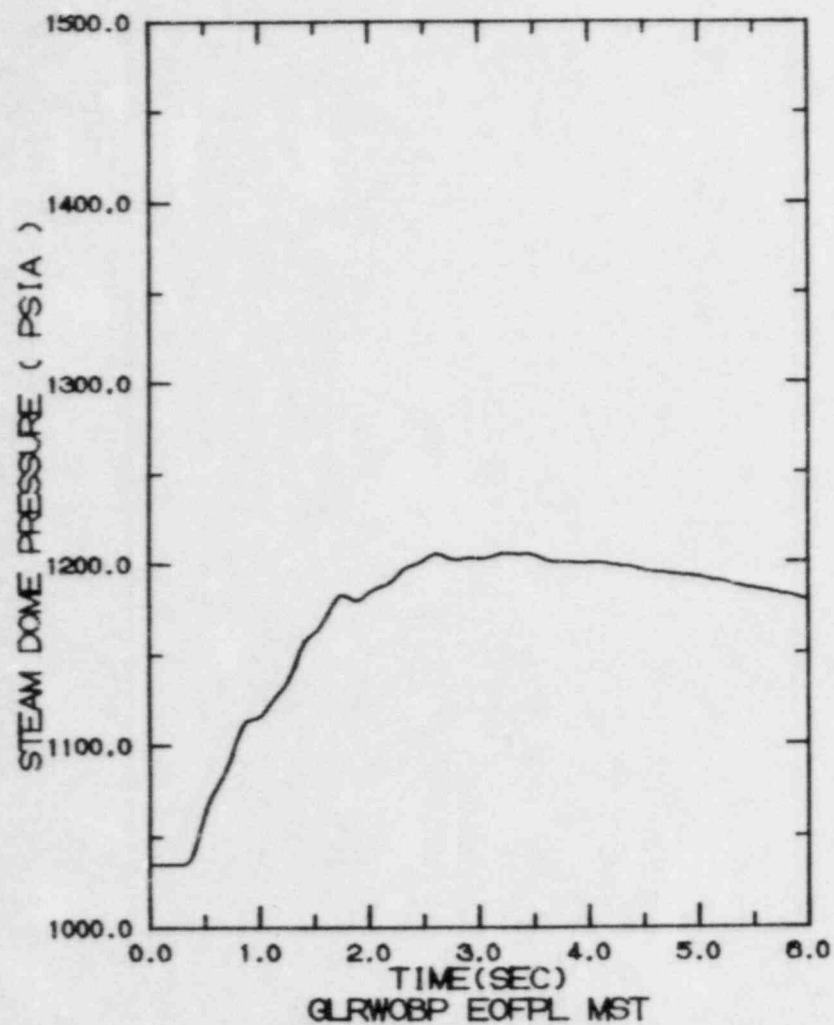


FIGURE 7.2.4-2

GENERATOR LOAD REJECTION WITHOUT BYPASS, EOFPL11  
TRANSIENT RESPONSE VERSUS TIME, "MEASURED" SCRAM TIME

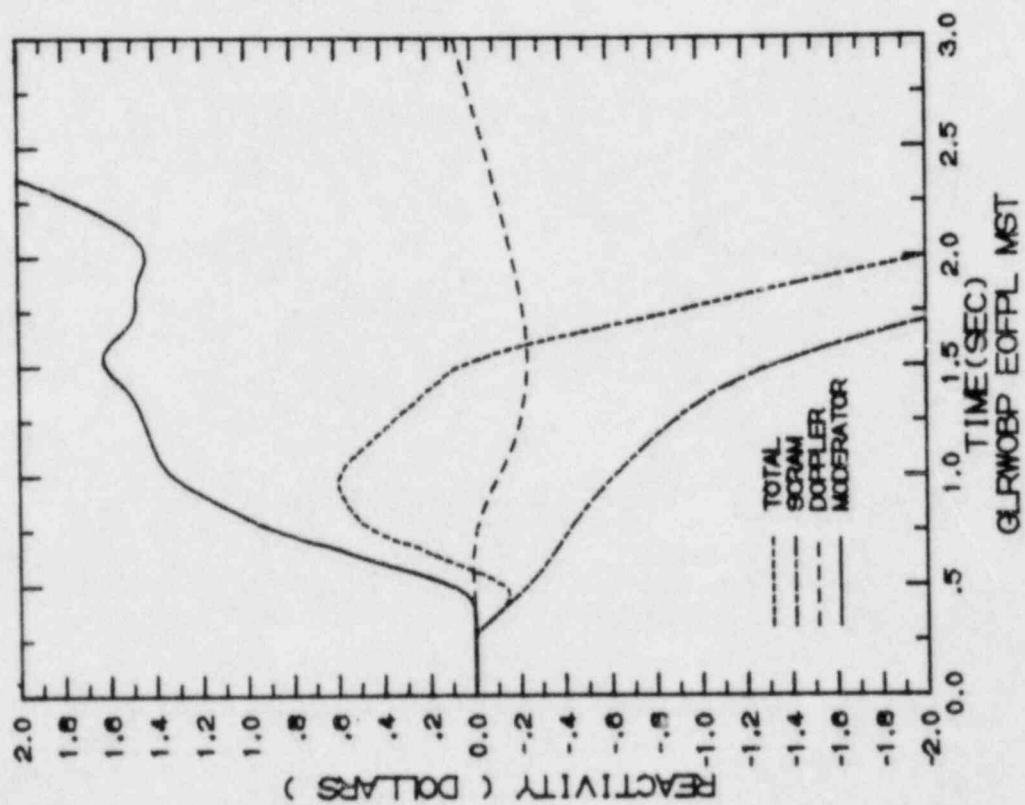


FIGURE 7.2.4-3

GENERATOR LOAD REJECTION WITHOUT BYPASS, EOFFPL11  
TRANSIENT RESPONSE VERSUS TIME, "MEASURED" SCRAM TIME



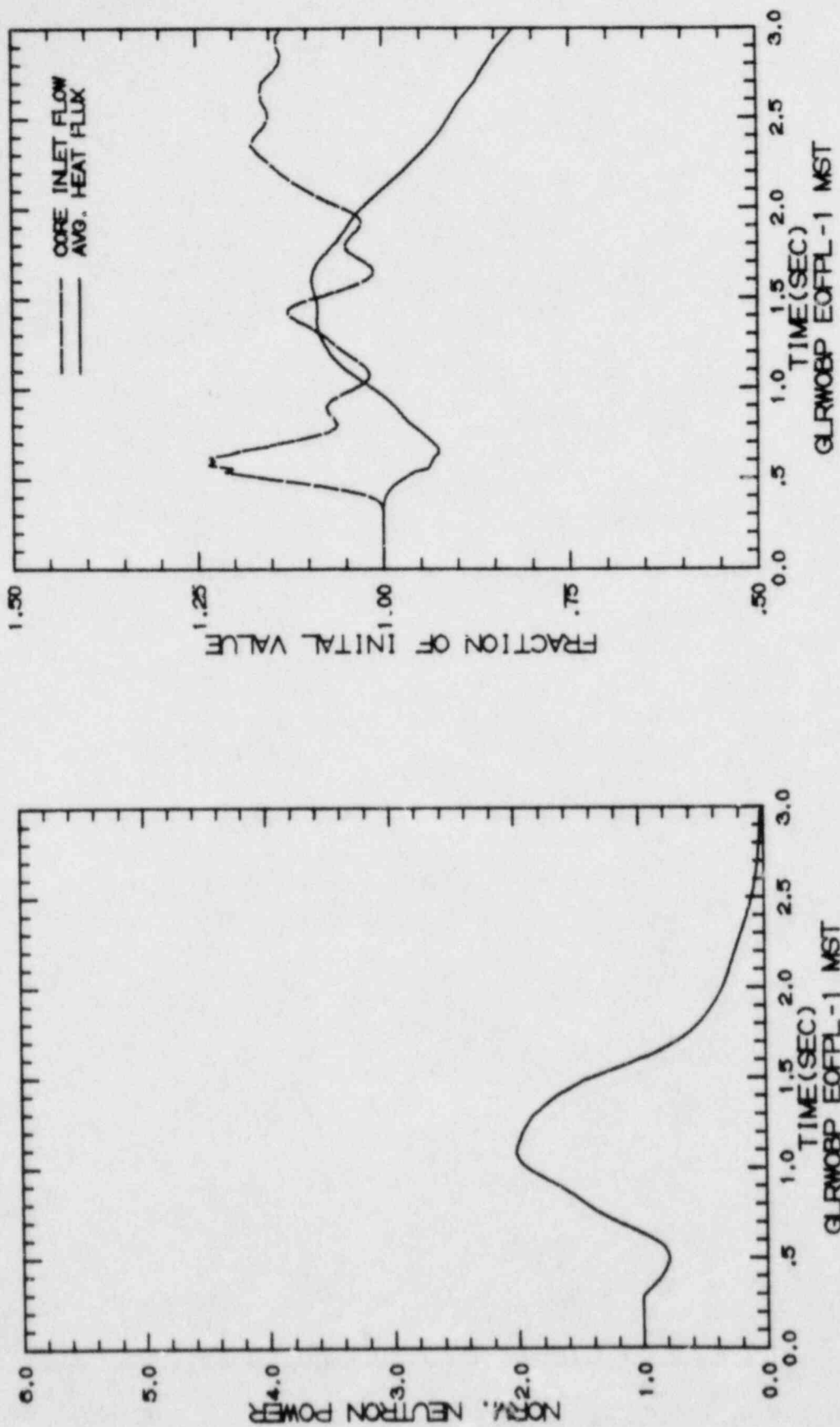


FIGURE 7.2.5-1  
 GENERATOR LOAD REJECTION WITHOUT BYPASS, EOFFPL11-1000 MWD/ST  
 TRANSIENT RESPONSE VERSUS TIME, "MEASURED" SCRAM TIME

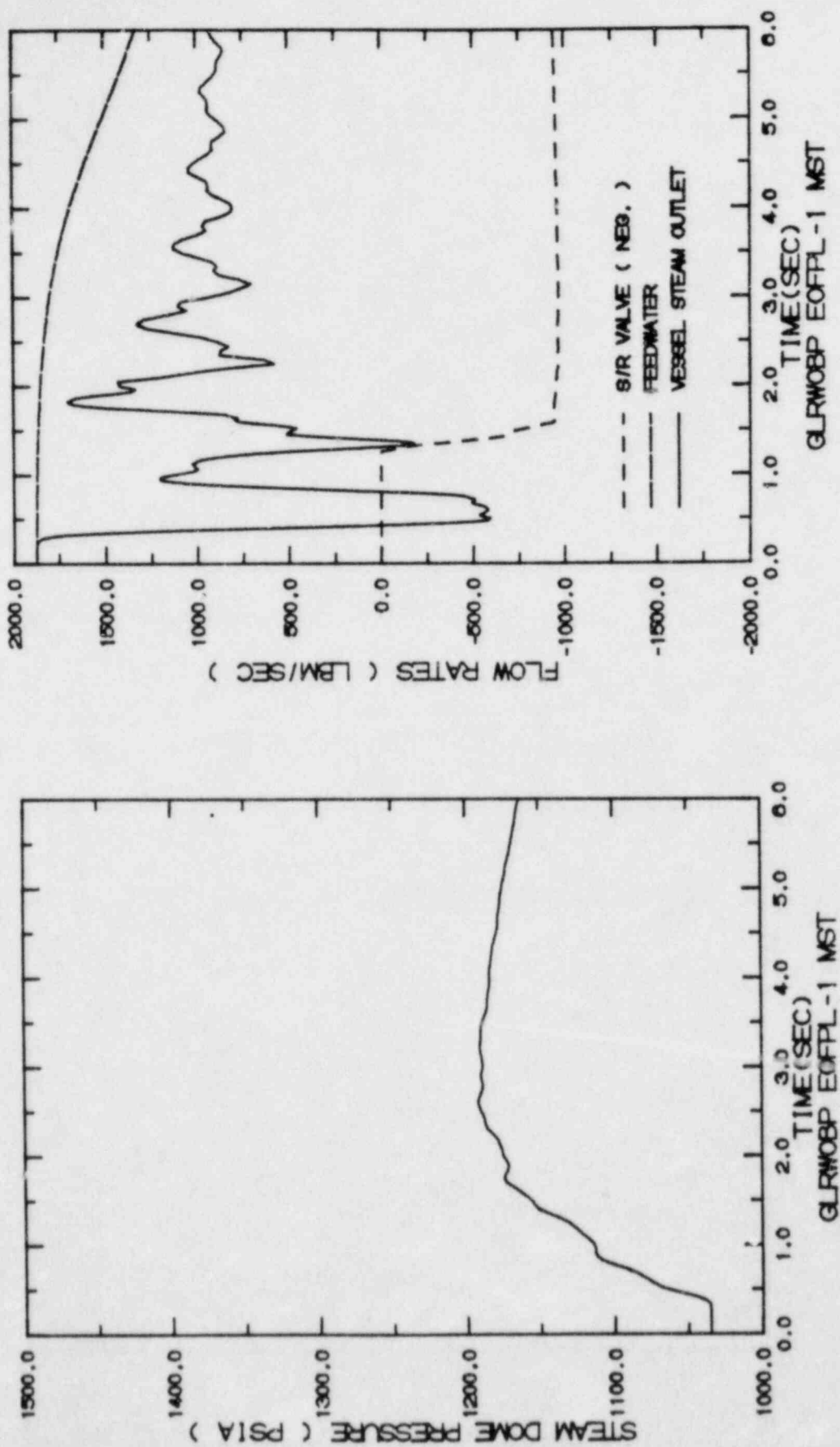


FIGURE 7.2.5-2

GENERATOR LOAD REJECTION WITHOUT BYPASS, EOPPL11-1000 MWD/ST  
TRANSIENT RESPONSE VERSUS TIME, "MEASURED" SCRAM TIME

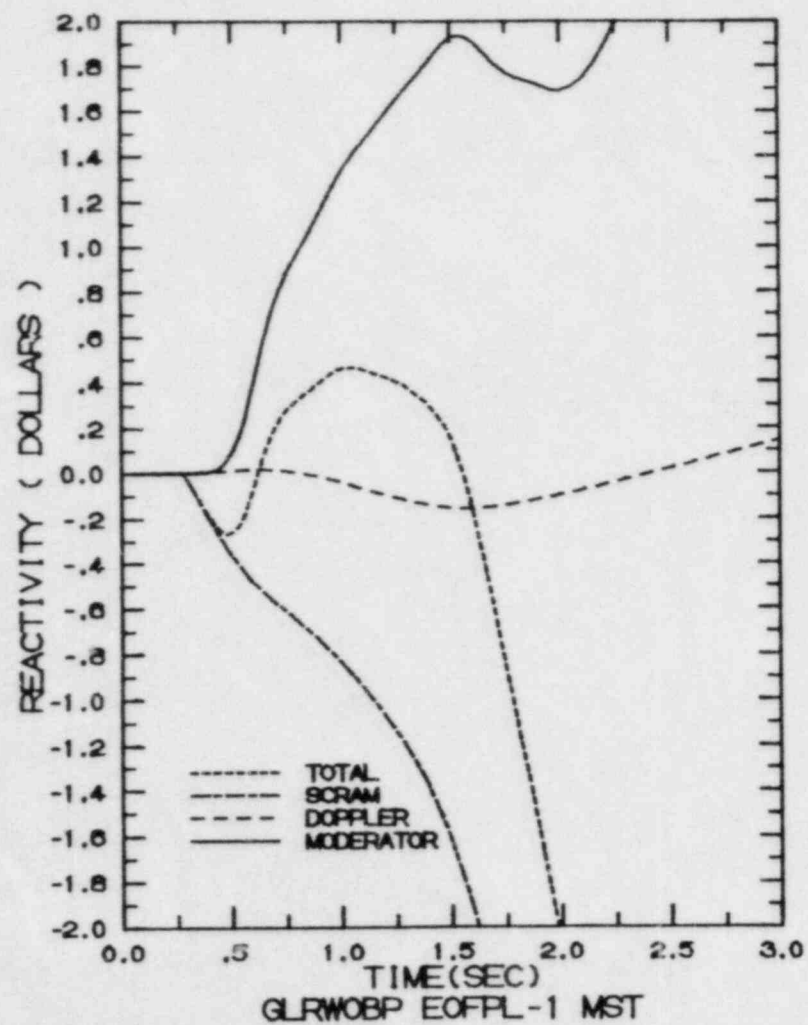


FIGURE 7.2.5-3

GENERATOR LOAD REJECTION WITHOUT BYPASS, EOPPL11-1000 MWD/ST  
TRANSIENT RESPONSE VERSUS TIME, "MEASURED" SCRAM TIME

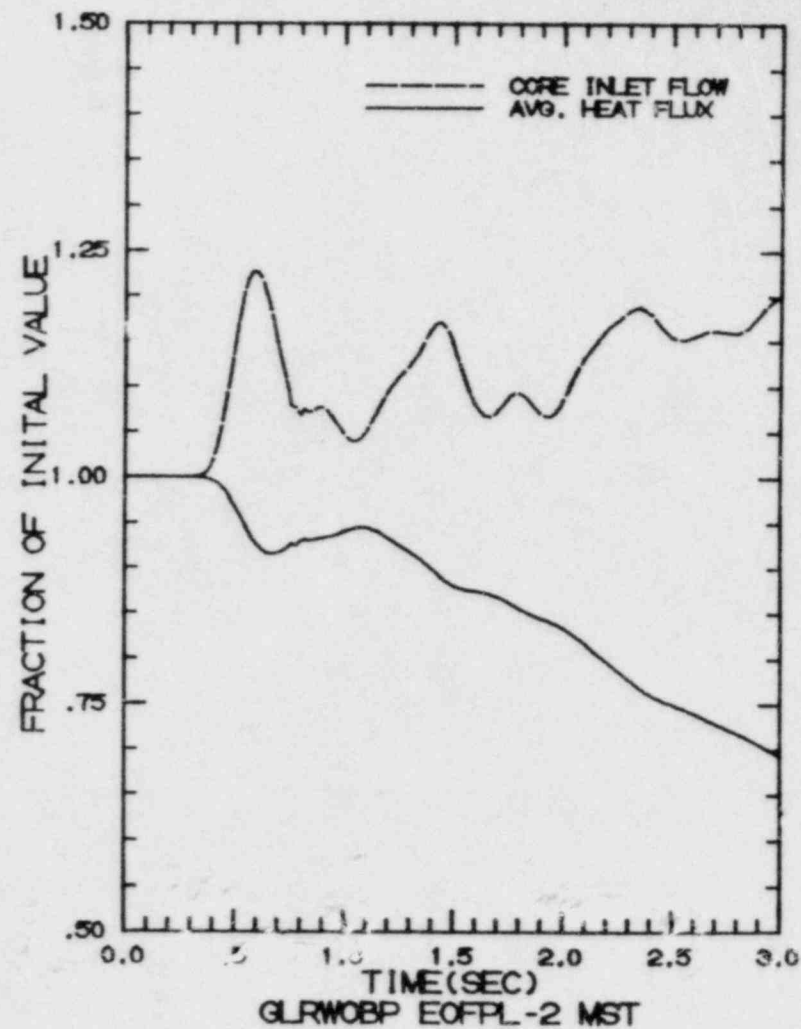
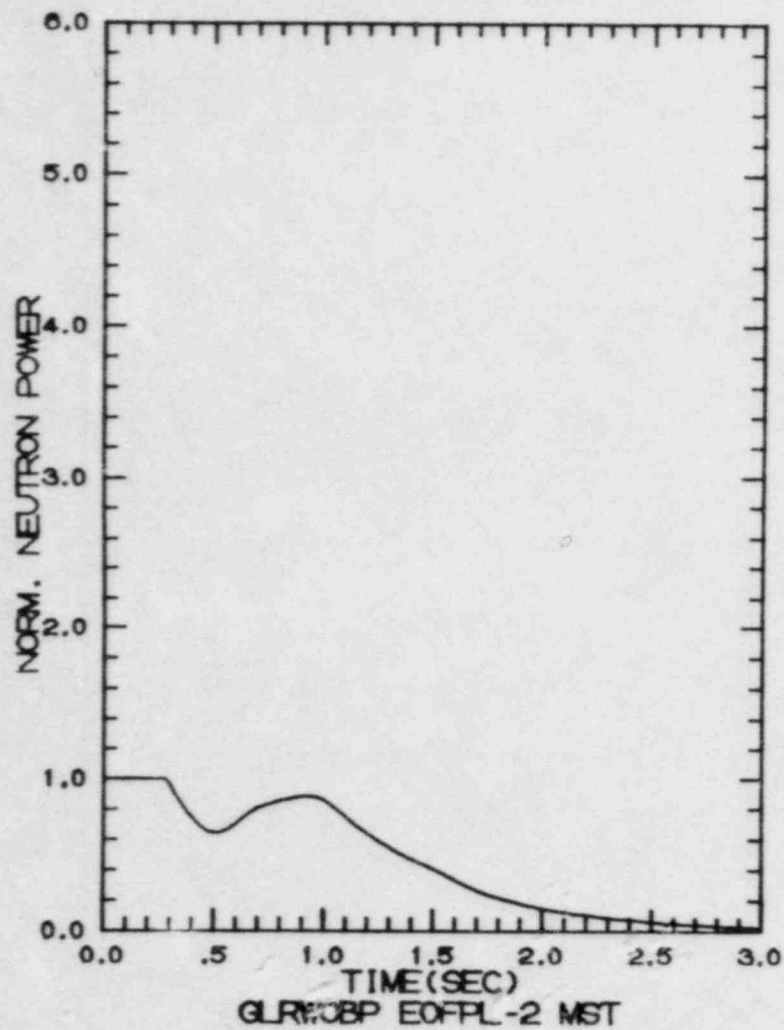


FIGURE 7.2.6-1

GENERATOR LOAD REJECTION WITHOUT BYPASS, EOFPL11-2000 MW/ST  
TRANSIENT RESPONSE VERSUS TIME, "MEASURED" SCRAM TIME

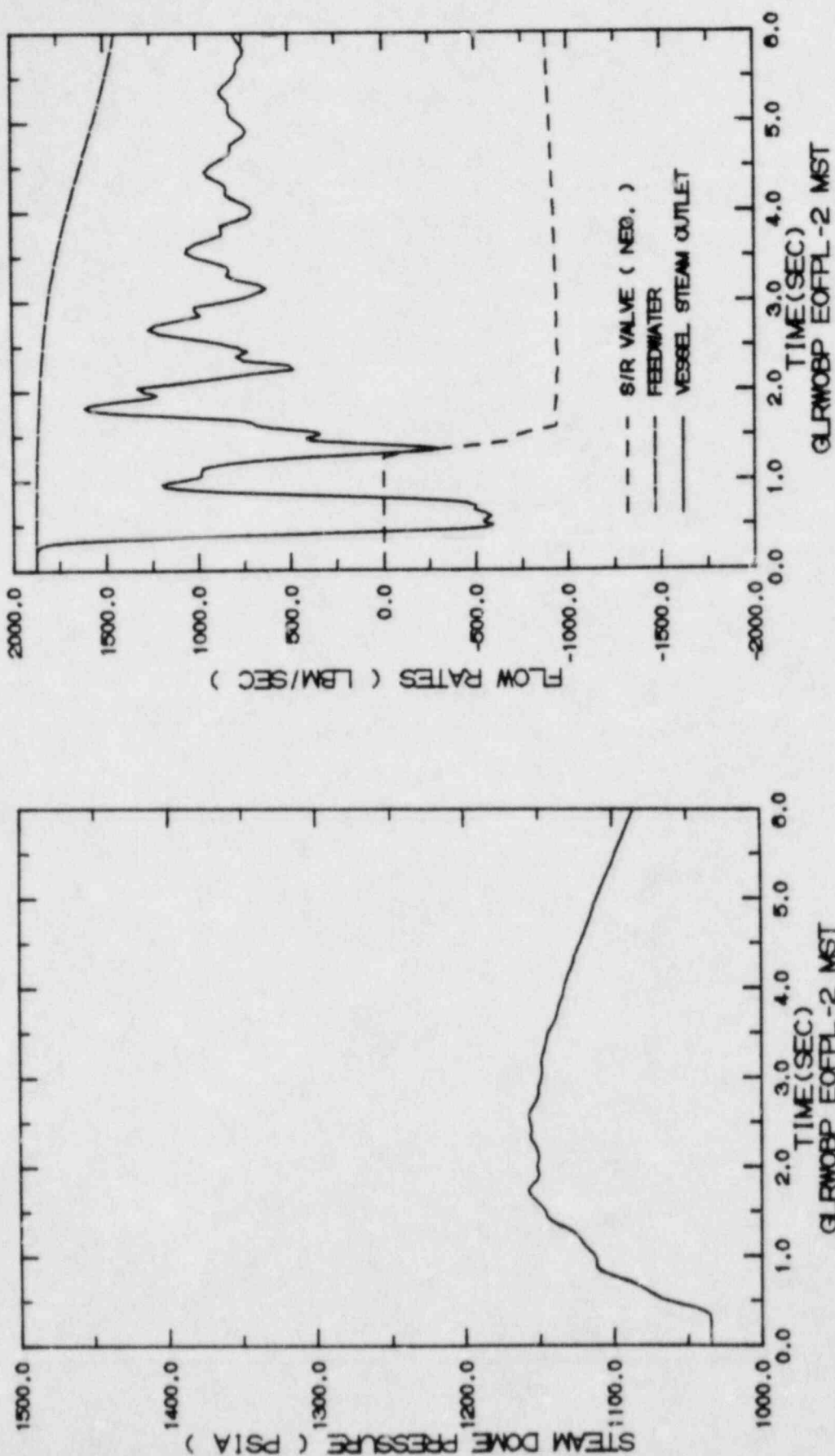


FIGURE 7.2.6-2

GENERATOR LOAD REJECTION WITHOUT BYPASS, EOPPL1-2000 MWL/ST  
TRANSIENT RESPONSE VERSUS TIME, "MEASURED" SCRAM TIME



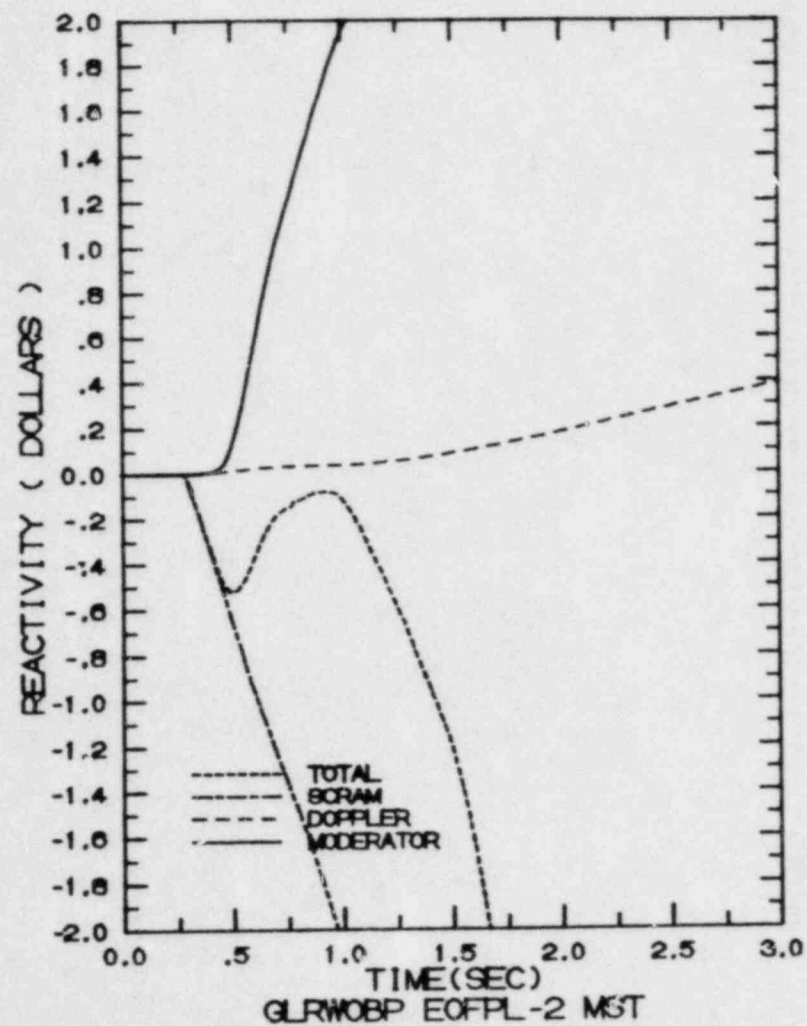


FIGURE 7.2.6-3

GENERATOR LOAD REJECTION WITHOUT BYPASS, EOFPL11-2000 MWD/ST  
TRANSIENT RESPONSE VERSUS TIME, "MEASURED" SCRAM TIME

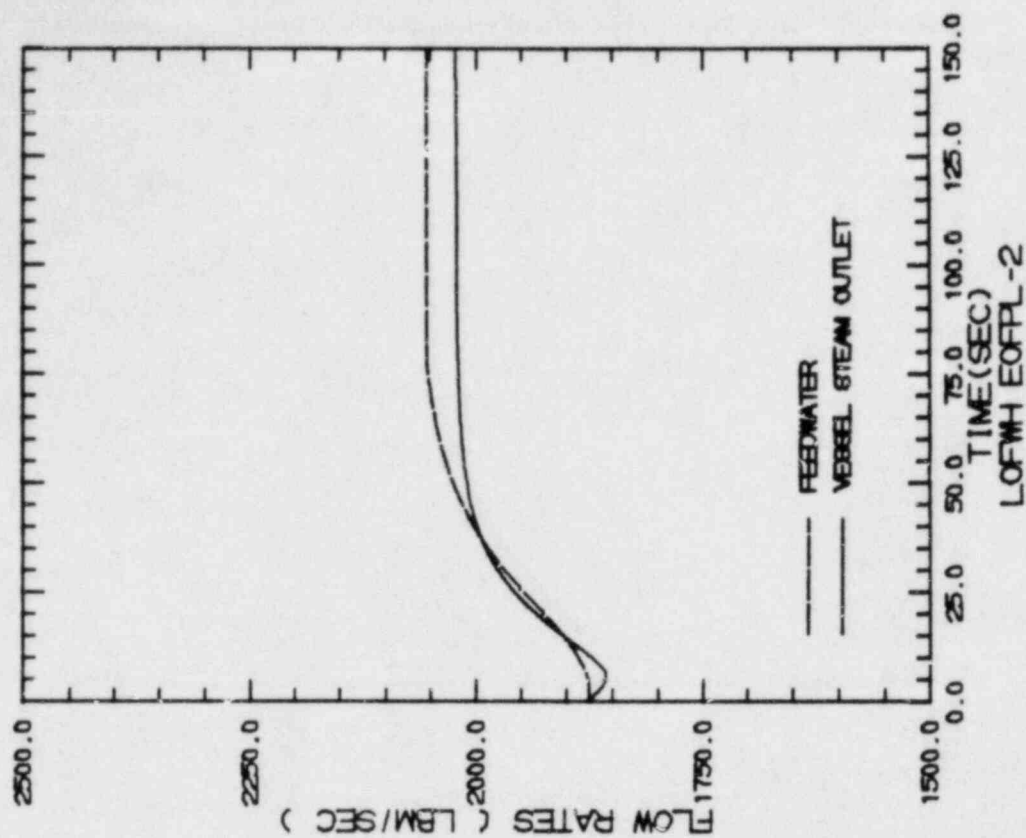
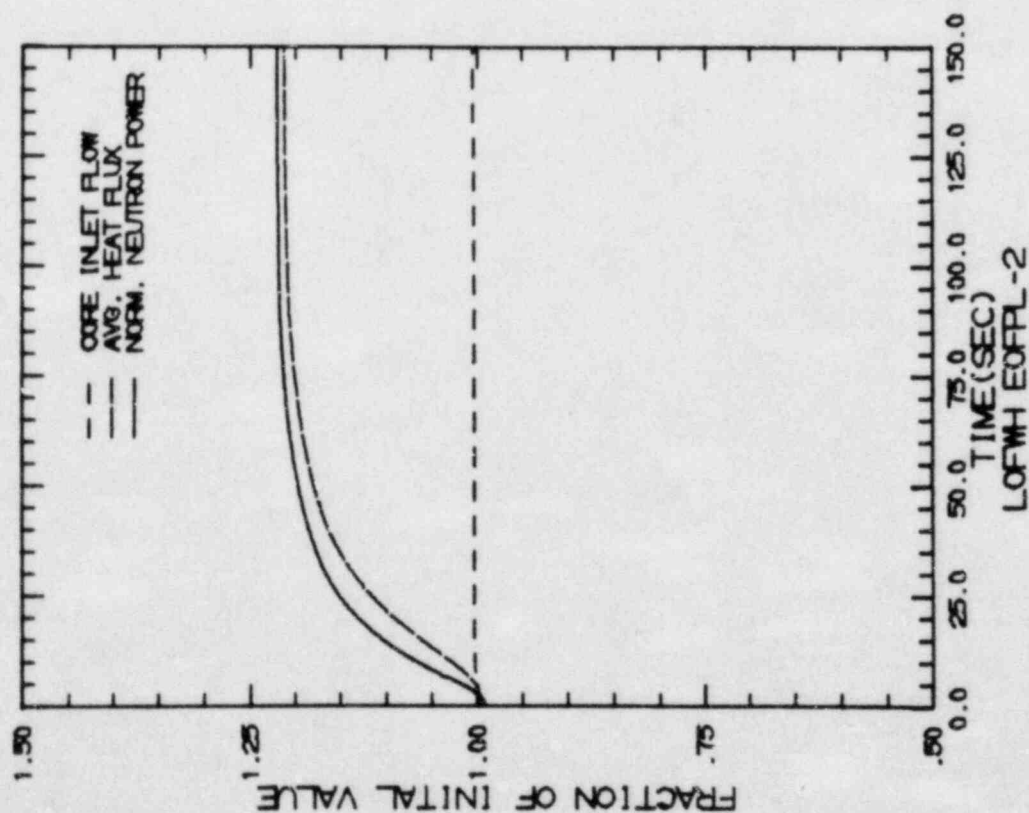


FIGURE 7.2.7-1

LOSS OF 100°F FEEDWATER HEATING, EOFPL11-2000 MWD/ST (LIMITING CASE)  
TRANSIENT RESPONSE VERSUS TIME

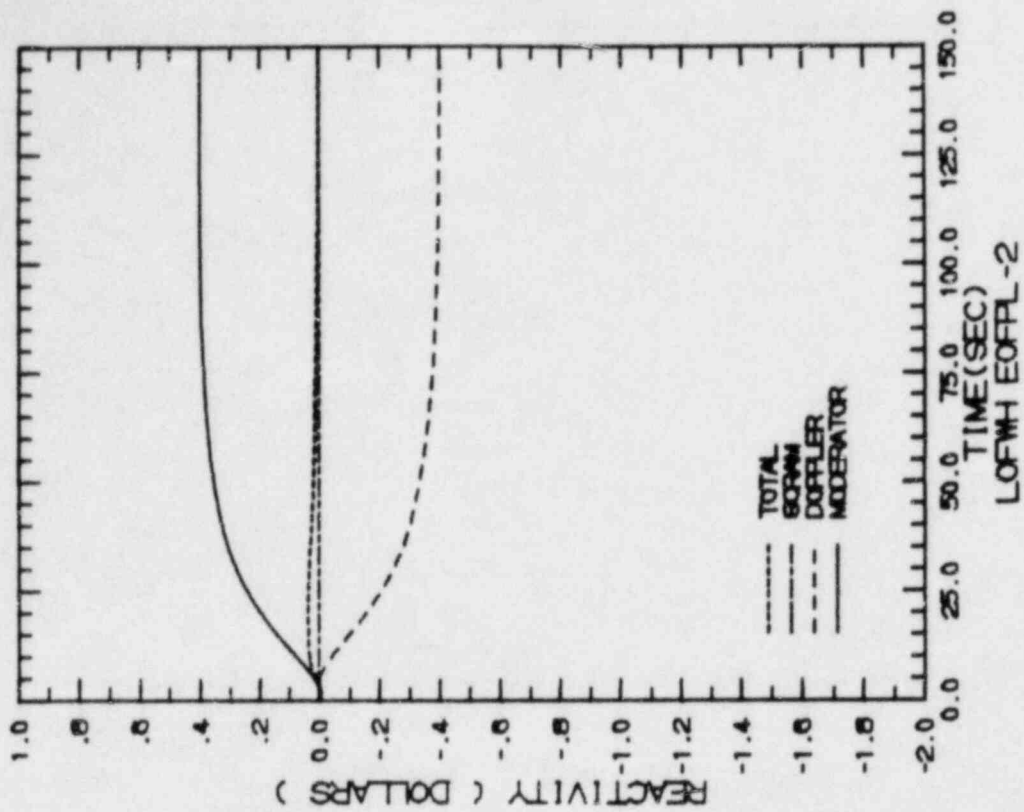
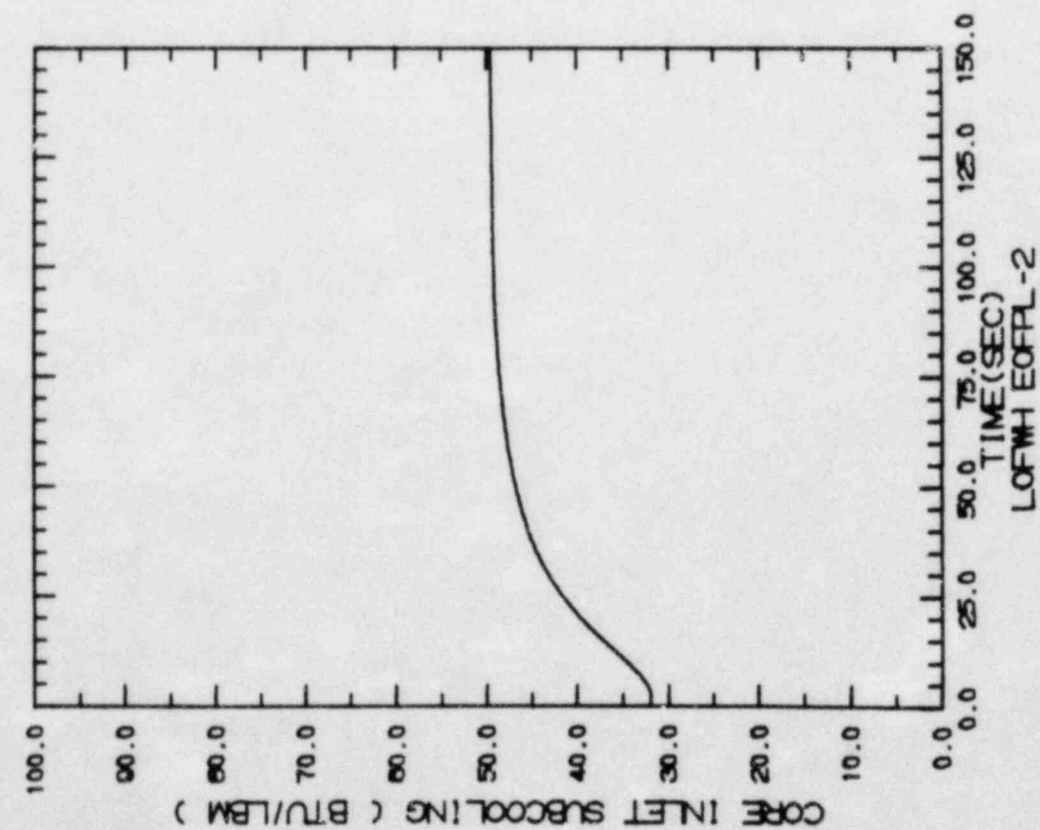


FIGURE 7.2.7-2

LOSS OF 100°F FEEDWATER HEATING, EOFFL11-2000 MWD/ST (LIMITING CASE)  
TRANSIENT RESPONSE VERSUS TIME

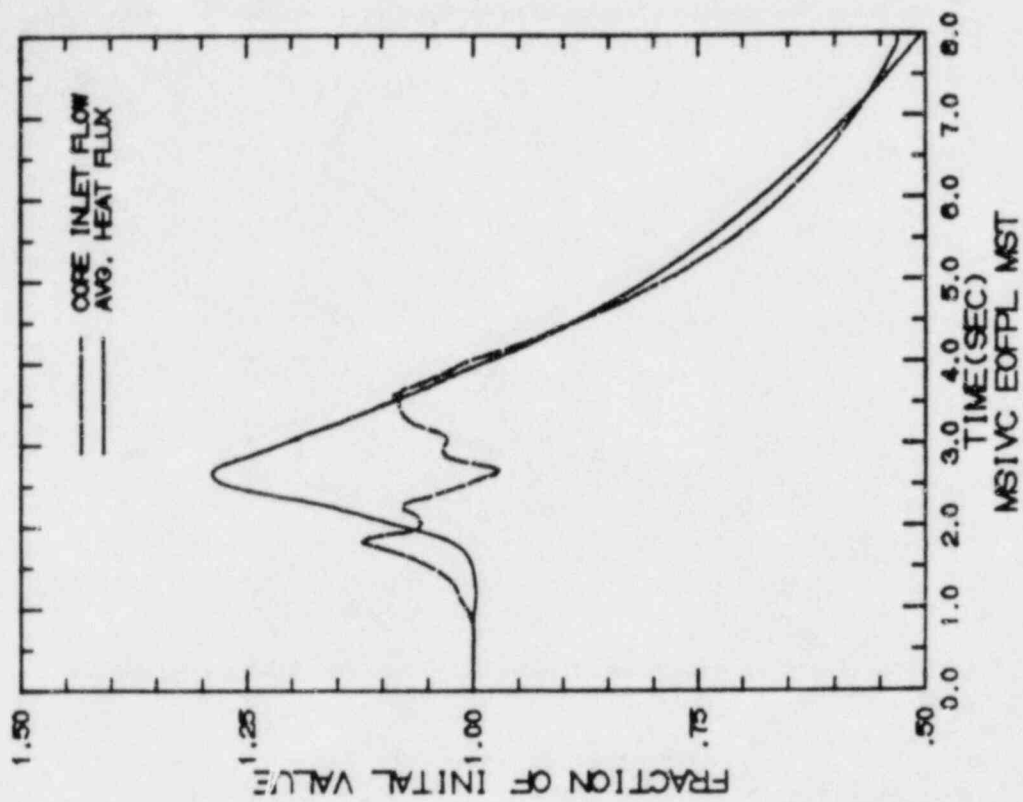
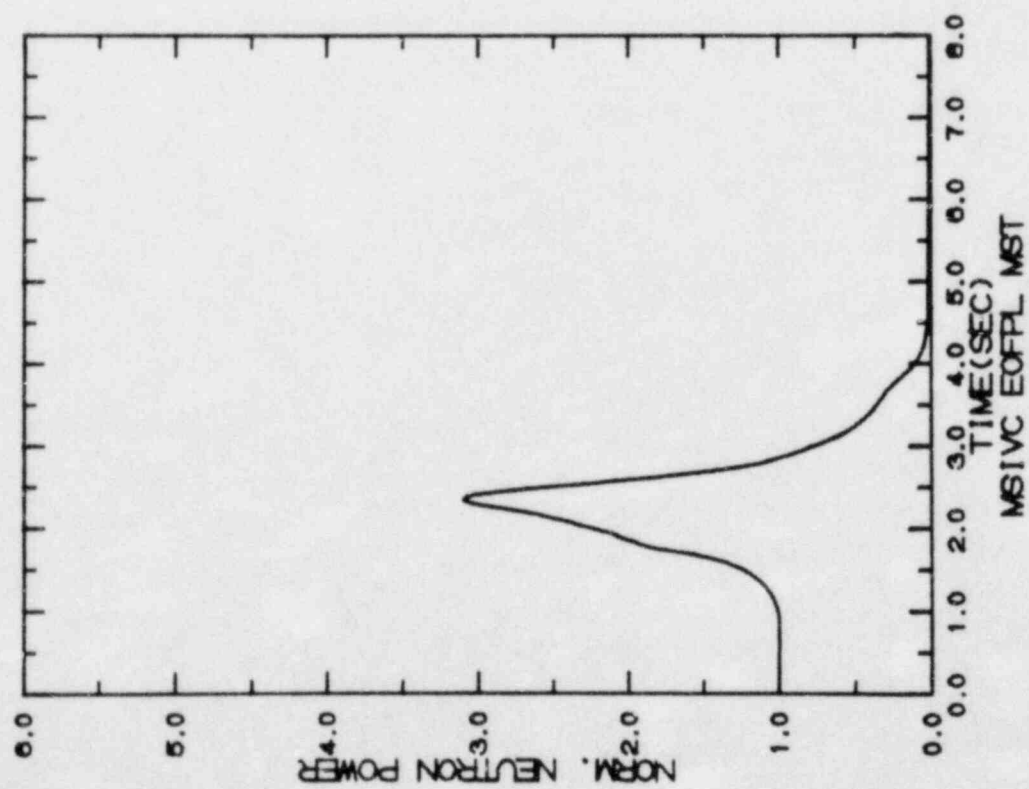


FIGURE 7.3.1-1

MSIV CLOSURE, FLUX SCRAM, EOFPL11  
TRANSIENT RESPONSE VERSUS TIME, "MEASURED" SCRAM TIME

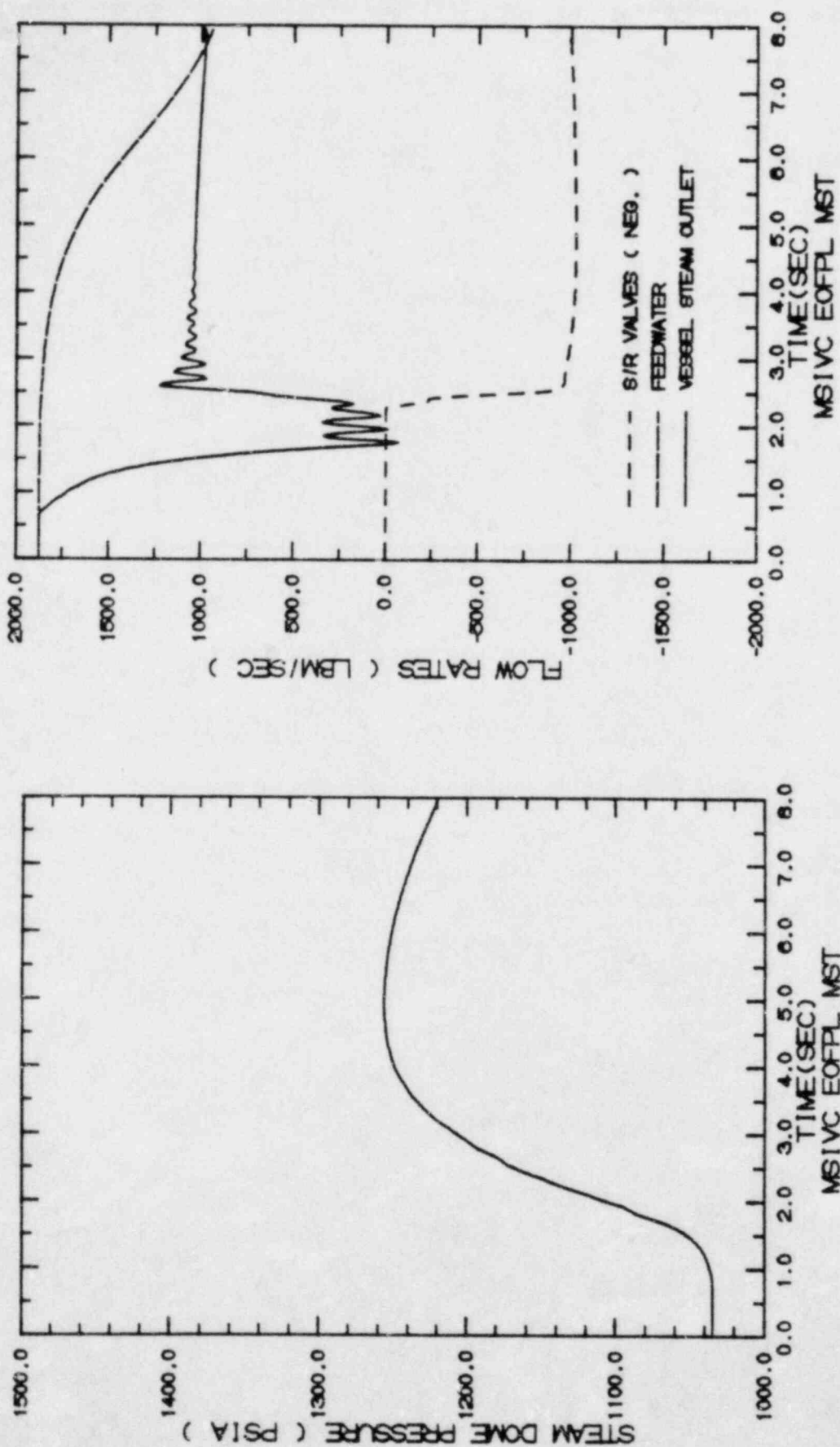


FIGURE 7.3.1-2  
 MSIV CLOSURE, FLUX SCRAM, EOFPL11  
 TRANSIENT RESPONSE VERSUS TIME, "MEASURED" SCRAM TIME



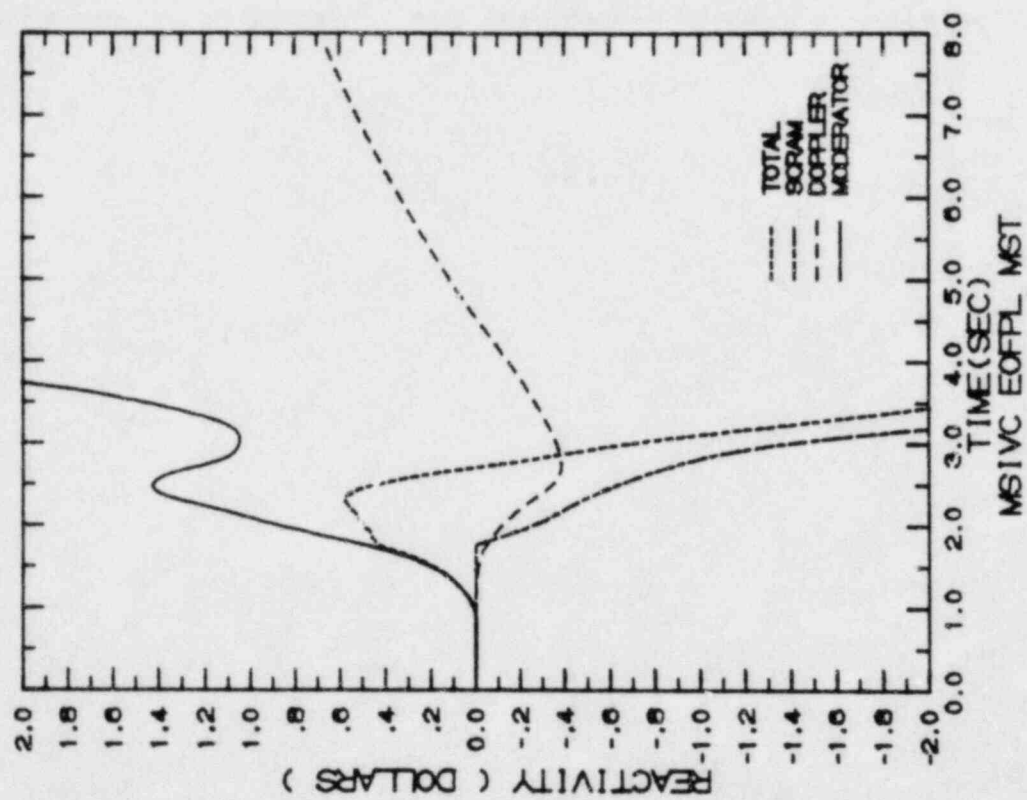
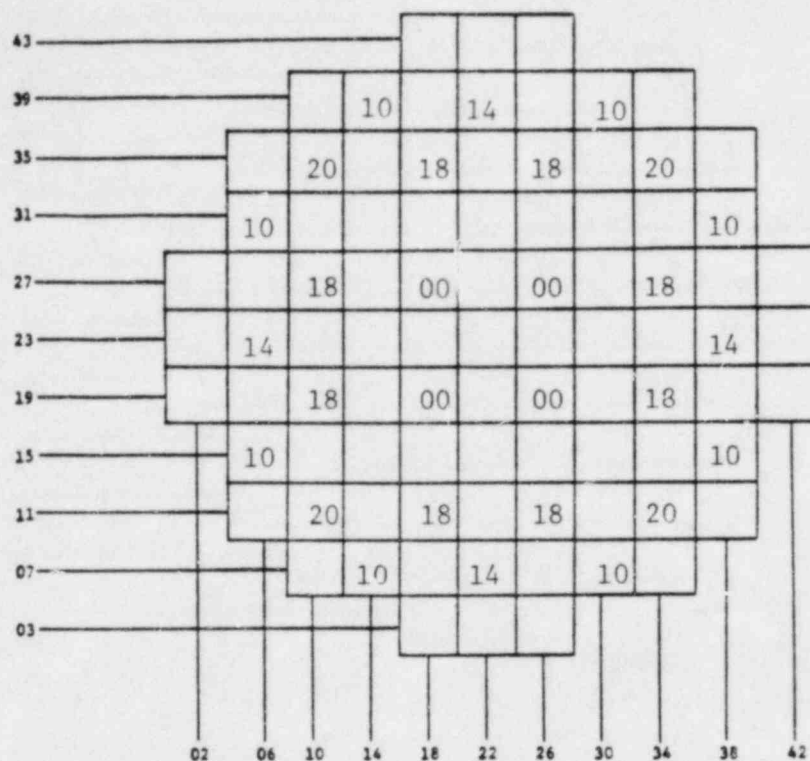


FIGURE 7.3.1-3

MSIV CLOSURE, FLUX SCRAM, EOFPL11  
TRANSIENT RESPONSE VERSUS TIME, "MEASURED" SCRAM TIME

# CONTROL ROD PATTERN



## Reactor Conditions:

Core Thermal Power = 1664 Mwt  
 Core Flow = 48 Mlb/hr  
 Cycle Exposure = 2565 MWD/ST  
 Xenon Free  
 Initial MCPR = 1.357  
 Initial LHGR = 13.4 kw/ft

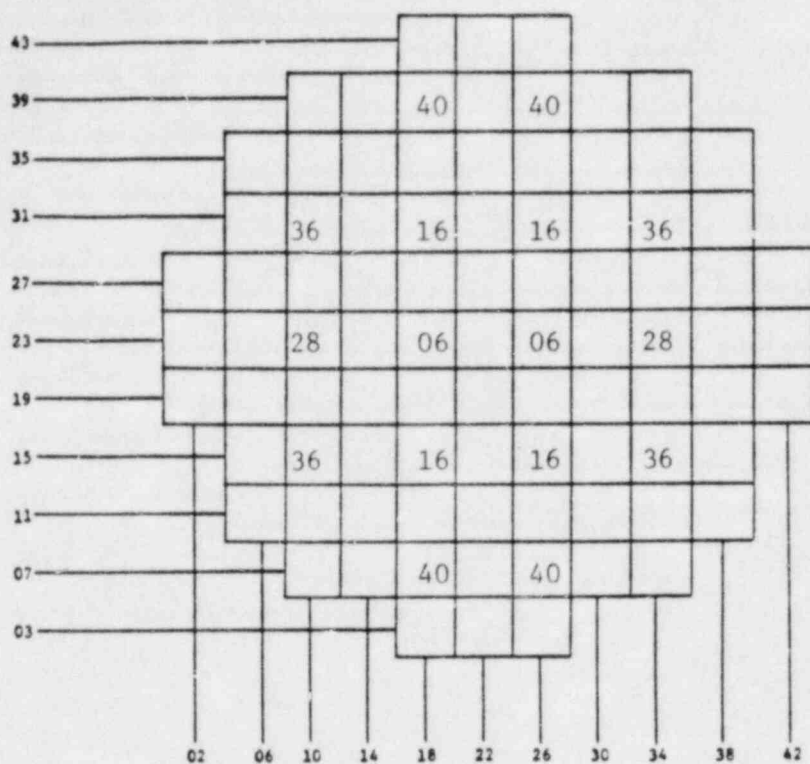
## Case Description

- o Operator attempts full withdrawal of the fully inserted rod at coordinates (26, 27).
- o Bounding Case.

**FIGURE 7.4.1**

REACTOR INITIAL CONDITIONS FOR THE VY CYCLE 11 ROD WITHDRAWAL ERROR CASE 1

# CONTROL ROD PATTERN



## Reactor Conditions:

Core Thermal Power	= 1664 Mwt
Core Flow	= 48 Mlb/hr
Cycle Exposure	= 4275 MWD/ST
Equilibrium Xenon	
Initial MCPR	= 1.386
Initial LHGR	= 12.8 kw/ft

## Case Description

- o Operator attempts full withdrawal of the partially inserted rod at coordinates (26, 31).
- o Normal Xenon condition and control rod pattern.

**FIGURE 7.4.2**

REACTOR INITIAL CONDITIONS FOR THE VY CYCLE 11 ROD WITHDRAWAL ERROR CASE 2

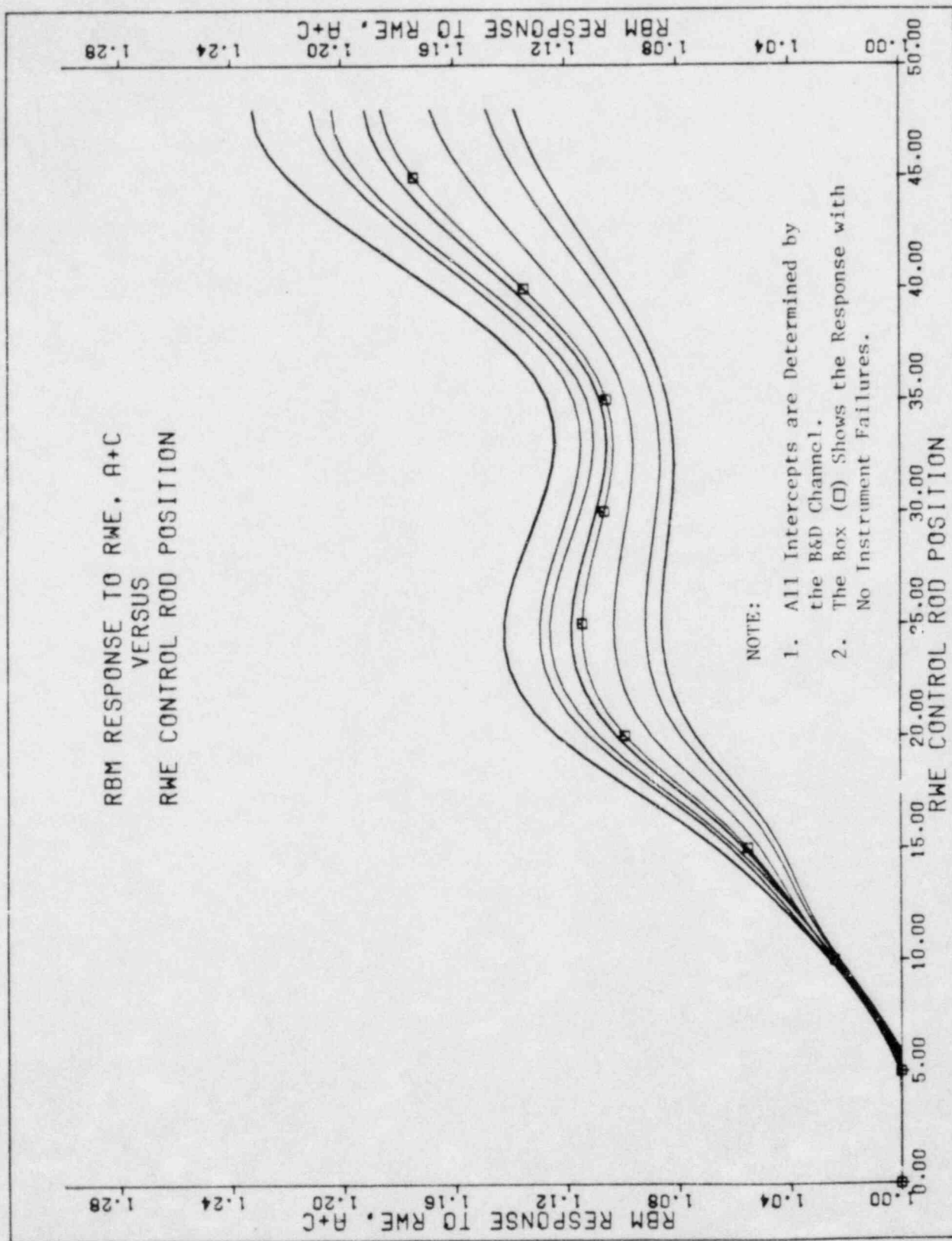


FIGURE 7.4.3

VY CYCLE 11 RWE CASE 1-SETPOINT INTERCEPTS DETERMINED BY THE A+C CHANNEL

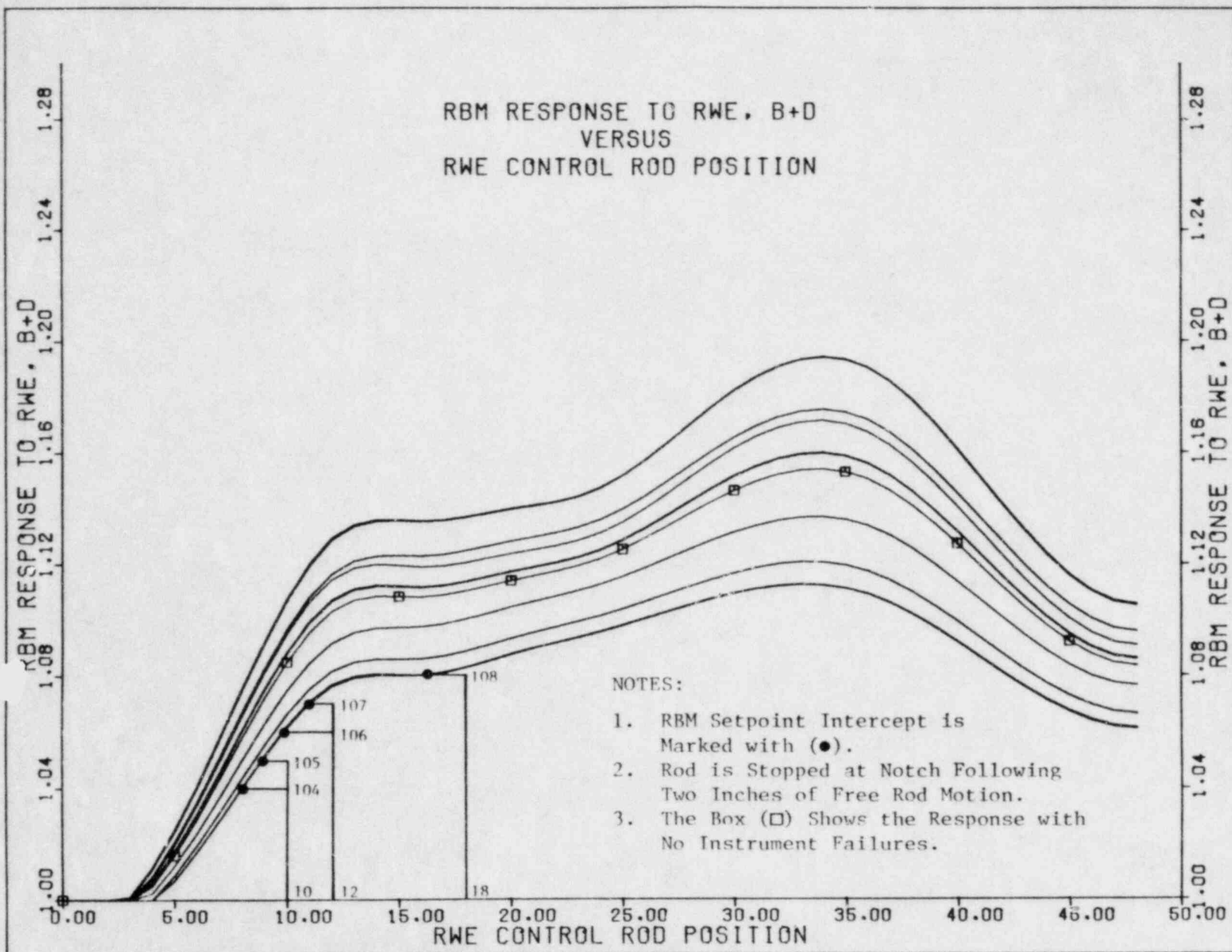


FIGURE 7.4.4

VY CYCLE 11 RWE CASE 1-SETPOINT INTERCEPTS DETERMINED BY THE B+D CHANNEL



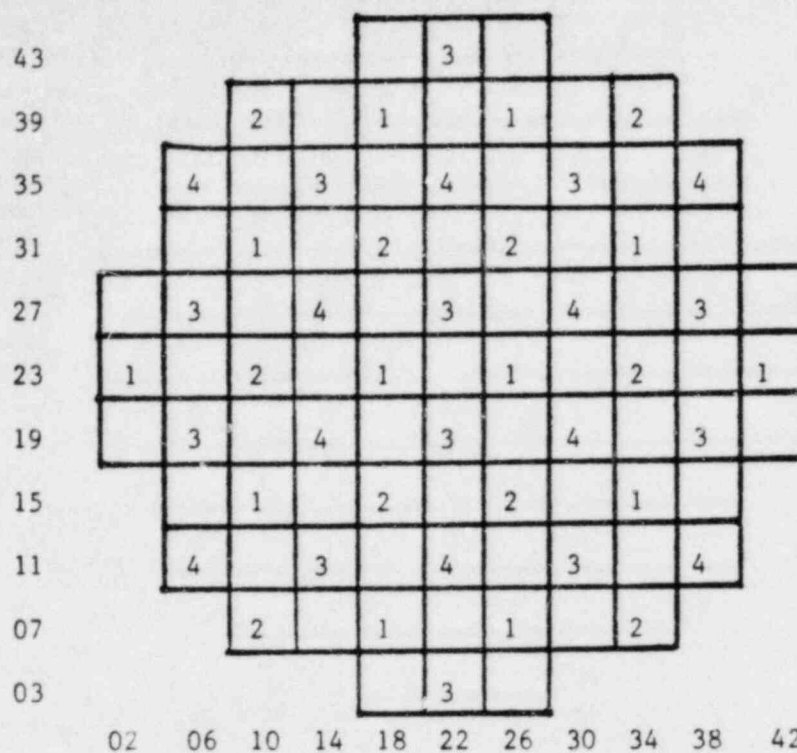


FIGURE 7.6.1 FIRST FOUR ROD ARRAYS PULLED IN THE A SEQUENCES

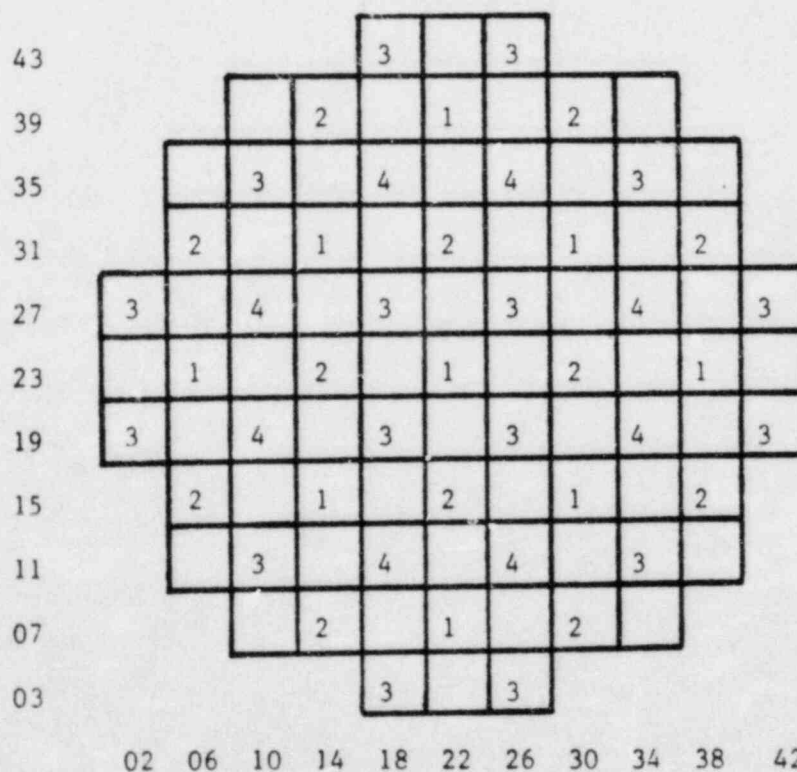


FIGURE 7.6.2 FIRST FOUR ROD ARRAYS PULLED IN THE B SEQUENCES

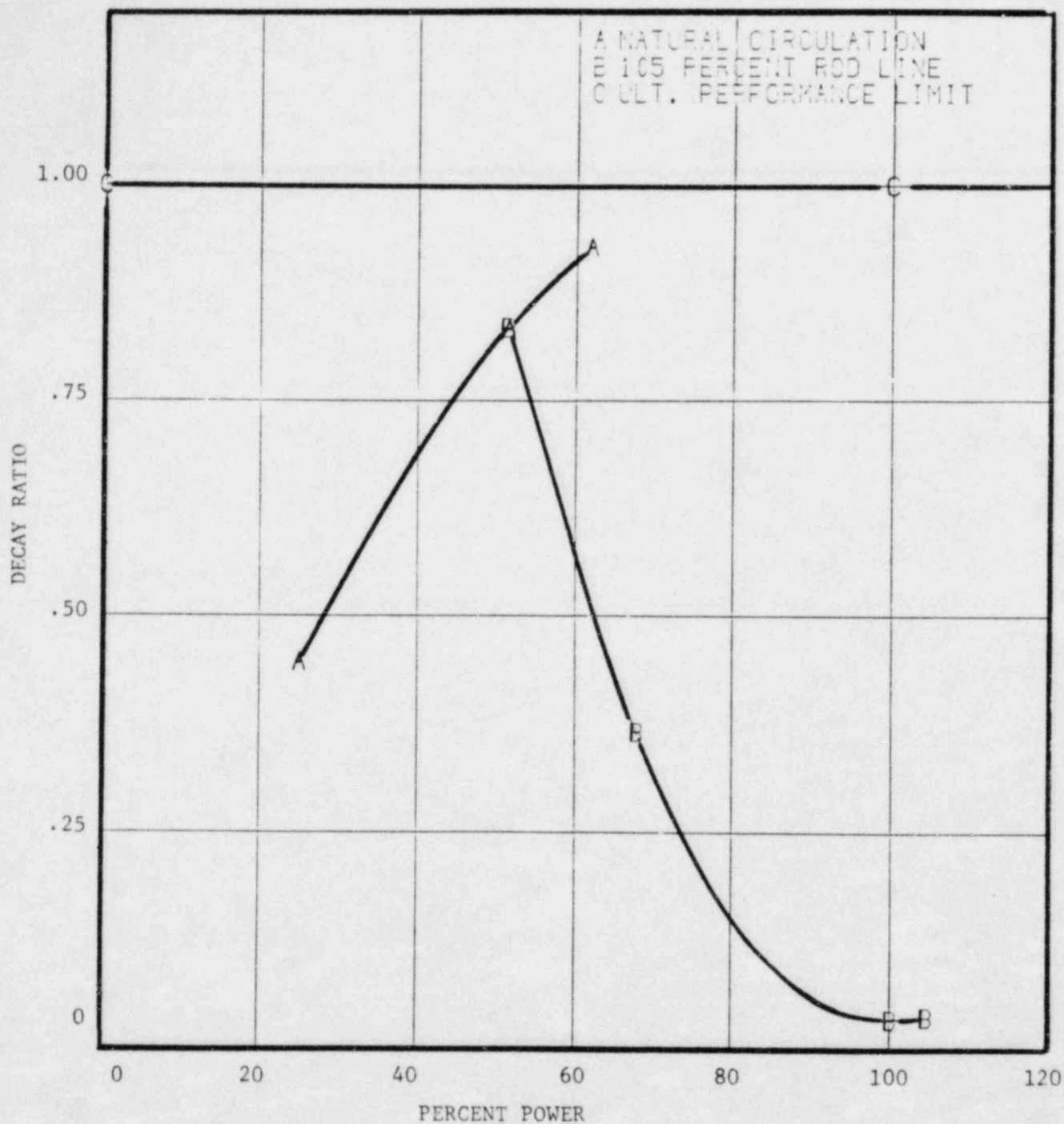


FIGURE 7.7.1

VV CYCLE 11 CORE DECAY RATIO VERSUS POWER

## 8.0 STARTUP PROGRAM

Following refueling and prior to vessel reassembly, fuel assembly position and orientation will be verified and videotaped by underwater television.

The Vermont Yankee Startup Program will include process computer data checks, shutdown margin demonstration, in-sequence critical measurement, rod scram tests, power distribution comparisons, TIP reproducibility, and TIP symmetry checks. The content of the Startup Test Report will be similar to that sent to the Office of Inspection and Enforcement in the past [22].

## 9.0 LOSS-OF-COOLANT ACCIDENT ANALYSIS

The results of the complete evaluation of the loss-of-coolant accident for Vermont Yankee as documented in Reference 23 provide required support for the operation of the Reload Cycle. No new fuel types have been introduced in this reload, therefore, the MAPLHGR limits as a function of average planar exposure remain the same as in the Current Cycle [9].

## APPENDIX A

### CALCULATED CYCLE DEPENDENT LIMITS

The MCPR limits appropriate for the Reload Cycle are calculated by adding the calculated  $\Delta$ CPR to the safety limit LAMCPR of 1.07. This is done for each of the analyses in Section 7 at each of the exposure statepoints. For an exposure interval between statepoints, the highest MCPR limit at either end is assumed to apply to the whole interval.

Table A.1 provides the highest calculated MCPR limits for the Reload Cycle for each of the exposure intervals for the various scram speeds and for the various rod block lines.

With regard to MAPLHGR, no new fuel types have been introduced. The MAPLHGR limits given in Reference 9 apply to the Reload Cycle. The MCPR limits in Reference 9 are also bounding for the Reload Cycle. These are found in Reference 9 as Table 3.11-2 and are reproduced here as Table A.2. On Table A.2, as in the Technical Specifications, End of Cycle (EOC) is understood to mean End of Full Power Life (EOFPL).



TABLE A.1

VERMONT YANKEE NUCLEAR POWER STATION  
LIMITING CYCLE 11 MCPR RESULTS

<u>Value of "N" in RBM</u> <u>Equation(1)</u>	<u>Average Control Rod</u> <u>Scram Time</u>	<u>Cycle</u> <u>Exposure Range</u>	<u>MCPR for</u> <u>P8X8R Fuel</u>
42%	"MEASURED"	BOC to EOFPL-2 GWD/T	1.29
		EOFPL-2 GWD/T to EOFPL-1 GWD/T	1.29
		EOFPL-1 GWD/T to EOFPL	1.29
	"57B"	BOC to EOFPL-2 GWD/T	1.29
		EOFPL-2 GWD/T to EOFPL-1 GWD/T	1.29
		EOFPL-1 GWD/T to EOFPL	1.33
41%	"MEASURED"	BOC to EOFPL-2 GWD/T	1.25
		EOFPL-2 GWD/T to EOFPL-1 GWD/T	1.25
		EOFPL-1 GWD/T to EOFPL	1.26
	"67B"	BOC to EOFPL-2 GWD/T	1.25
		EOFPL-2 GWD/T to EOFPL-1 GWD/T	1.27
		EOFPL-1 GWD/T to EOFPL	1.33
≤ 40%	"MEASURED"	BOC to EOFPL-2 GWD/T	1.25
		EOFPL-2 GWD/T to EOFPL-1 GWD/	1.25
		EOFPL-1 GWD/T to EOFPL	1.26
	"67B"	BOC to EOFPL-2 GWD/T	1.25
		EOFPL-2 GWD/T to EOFPL-1 GWD/T	1.27
		EOFPL-1 GWD/T to EOFPL	1.33

## NOTES:

- (1) The Rod Block Monitor (RBM) trip setpoints are determined by the equation shown in Table 3.2.5 of the Technical Specifications [Reference 9].

TABLE A.2

VERMONT YANKEE NUCLEAR POWER STATION  
TECHNICAL SPECIFICATION MCPR OPERATING LIMITS

Value of "N" in RBM Equation(1)	Average Control Rod Scram Time	Cycle Exposure Range	MCPR Operating Limit for Fuel Type (2)		
			8X8	8X8R	P8X8R
42%	Equal or better than L.C.O. 3.3 C.1.1	BOC to EOC-2 GWD/T	1.29	1.29	1.29
		EOC-2 GWD/T to EOC-1 GWD/T	1.29	1.29	1.29
		EOC-1 GWD/T to EOC	1.30	1.30	1.30
	Equal or better than L.C.O. 3.3 C.1.2	BOC to EOC-2 GWD/T	1.29	1.29	1.29
		EOC-2 GWD/T to EOC-1 GWD/T	1.33	1.31	1.31
		EOC-1 GWD/T to EOC	1.36	1.35	1.35
41%	Equal or better than L.C.O. 3.3 C.1.1	BOC to EOC-2 GWD/T	1.25	1.25	1.25
		EOC-2 GWD/T to EOC-1 GWD/T	1.26	1.25	1.25
		EOC-1 GWD/T to EOC	1.30	1.30	1.30
	Equal or better than L.C.O. 3.3 C.1.2	BOC to EOC-2 GWD/T	1.25	1.25	1.25
		EOC-2 GWD/T to EOC-1 GWD/T	1.33	1.31	1.31
		EOC-1 GWD/T to EOC	1.36	1.35	1.35
≤ 40%	Equal or better than L.C.O. 3.3 C.1.1	BOC to EOC-2 GWD/T	1.25	1.25	1.25
		EOC-2 GWD/T to EOC-1 GWD/T	1.26	1.25	1.25
		EOC-1 GWD/T to EOC	1.30	1.30	1.30
	Equal or better than L.C.O. 3.3 C.1.2	BOC to EOC-2 GWD/T	1.25	1.25	1.25
		EOC-2 GWD/T to EOC-1 GWD/T	1.33	1.31	1.31
		EOC-1 GWD/T to EOC	1.36	1.35	1.35
75%	Special Testing at Natural Circulation (Notes 3, 4)		1.30	1.31	1.31

## NOTES:

- (1) The Rod Block Monitor (RBM) trip setpoints are determined by the equation shown in Table 3.2.5 of the Technical Specifications.
- (2) The current analyses for MCPR Operating Limits do not include 7X7 fuel. On this basis, further evaluation of MCPR operating limits is required before 7X7 fuel can be used in Reactor Power Operation.
- (3) For the duration of pump trip and stability testing.
- (4)  $K_f$  factors are not applied during the pump trip and stability testing.

## REFERENCES

1. M. A. Sironen, R. A. Woehlke, and J. A. McGahan, Vermont Yankee Cycle 8 Summary Report, YAEC-1305, August 1982.
2. M. A. Sironen and P. A. McGahan, Vermont Yankee Cycle 9 Summary Report, YAEC-1367, June 1983.
3. General Electric Standard Application for Reactor Fuel (GESTARII), NEDE-24011-P-A-5, GE Company Proprietary, August 1982.
4. D. M. VerPlanck, Methods for the Analysis of Boiling Water Reactors Steady State Core Physics, YAEC-1238, March 1981.
5. E. E. Pilat, Methods for the Analysis of Boiling Water Reactors Lattice Physics, YAEC-1232, December 1980.
6. S. P. Schultz and K. E. St. John, Methods for the Analysis of Oxide Fuel Rod Steady-State Thermal Effects (FROSSTEY) Code/Model Description Manual, YAEC-1249P, April 1981.
7. S. P. Schultz and K. E. St. John, Methods for the Analysis of Oxide Fuel Rod Steady-State Thermal Effects (FROSSTEY) Code Qualification and Application, YAEC-1265P, June 1981.
8. D. C. Albright, H2ODA: An Improved Water Properties Package, YAEC-1237, March 1981.
9. Appendix A to Operating License DPR-28 Technical Specifications and Bases for Vermont Yankee Nuclear Power Station, Docket No. 50-271.
10. A. A. F. Ansari, et al., Vermont Yankee Cycle 9 Core Performance Analysis, YAEC-1275, August 1981.
11. A. A. F. Ansari, Methods for the Analysis of Boiling Water Reactors: Steady-State Core Flow Distribution Code (FIBWR), YAEC-1234, December 1980.
12. A. A. F. Ansari, R. R. Gay, and B. J. Gitnick, FIBWR: A Steady-State Core Flow Distribution Code for Boiling Water Reactors - Code Verification and Qualification Report, EPRI NP-1923, Project 1754-1 Final Report, July 1981.
13. General Electric Company, GEXL Correlation Application to BWR 2-6 Reactors, NEDE-25422, GE Company Proprietary, June 1981.
14. A. A. F. Ansari and J. T. Cronin, Methods for the Analysis of Boiling Water Reactors: A Systems Transient Analysis Model (RETRAN), YAEC-1233, April 1981.
15. EPRI, RETRAN - A Program for One-Dimensional Transient Thermal-Hydraulic Analysis of Complex Fluid Flow Systems, CCM-5, December 1978.

16. A. A. F. Ansari, K. J. Burns, and D. K. Beller, Methods for the Analysis of Boiling Water Reactors: Transient Critical Power Ratio Analysis (RETRAN-TCPYA01), YAE-1299P, March 1982.
17. J. M. Holzer, Methods for the Analysis of Boiling Water Reactors Transient Core Physics, YAE-1239P, August 1981.
18. C. J. Paone, et al., Rod Drop Accident Analysis for Large Boiling Water Reactors, NEDO-10527, March 1972.
19. R. C. Stirn, et al., Rod Drop Accident Analysis for Large Boiling Water Reactors Addendum No. 1, Multiple Enrichment Cores With Axial Gadolinium, NEDO-10527, Supplement 1, July 1972.
20. D. Radcliffe and R. E. Bates, "Reduced Notch Worth Procedure", SIL-316, November 1979.
21. R. C. Stirn, et al., Rod Drop Accident Analysis for Large Boiling Water Reactor Addendum No. 2 Exposed Cores, NEDO-10527, Supplement 2, January 1973.
22. Letter, FVY 83-100, dated September 15, 1983, W. P. Murphy to T. E. Murley, Regional Administrator, "Cycle X Startup Test Report".
23. Loss-of-Coolant Accident Analysis for Vermont Yankee Nuclear Power Station, NEDO-21697, August 1977, as amended.